

8-2016

Production of Acetic Acid in Kraft Pulp Mill Biorefinery Using Bi-Polar Membrane Electrodialysis

Ravikant Amogisidha Patil
University of Maine

Follow this and additional works at: <http://digitalcommons.library.umaine.edu/etd>

 Part of the [Membrane Science Commons](#), and the [Wood Science and Pulp, Paper Technology Commons](#)

Recommended Citation

Patil, Ravikant Amogisidha, "Production of Acetic Acid in Kraft Pulp Mill Biorefinery Using Bi-Polar Membrane Electrodialysis" (2016). *Electronic Theses and Dissertations*. 2597.
<http://digitalcommons.library.umaine.edu/etd/2597>

This Open-Access Dissertation is brought to you for free and open access by DigitalCommons@UMaine. It has been accepted for inclusion in Electronic Theses and Dissertations by an authorized administrator of DigitalCommons@UMaine.

**PRODUCTION OF ACETIC ACID IN KRAFT PULP MILL BIOREFINERY USING
BI-POLAR MEMBRANE ELECTRODIALYSIS**

By

Ravikant Amogisidha Patil

B. Tech Institute of Chemical Technology, Mumbai, India, 2007

M. Tech Indian Institute of Technology, Kharagpur, India, 2010

M.S. University of Maine, Orono, ME, 2012

A DISSERTATION

Submitted in Partial Fulfillment of the

Requirements for the Degree of

Doctor of Philosophy

(Chemical Engineering)

The Graduate School

The University of Maine

August 2016

Advisory Committee:

Joseph M. Genco, Professor of Chemical and Biological Engineering, Advisor

Hemant P. Pendse, Professor of Chemical and Biological Engineering, Co-Advisor

Adriaan R.P. van Heiningen, Professor of Chemical and Biological Engineering

Raymond C. Fort, Jr. Professor of Chemistry

Barbara J. W. Cole, Professor of Chemistry

David J. Neivandt, Professor of Chemical and Biological Engineering

**PRODUCTION OF ACETIC ACID IN KRAFT PULP MILL BIOREFINERY USING
BI-POLAR MEMBRANE ELECTRODIALYSIS**

By Ravikant Amogisidha Patil

Thesis Advisor: Dr. Joseph M. Genco

An Abstract of the Dissertation Presented
in Partial Fulfillment of the Requirements for the
Degree of Doctor of Philosophy
(in Chemical Engineering)
August 2016

The objective of this dissertation was to develop a process for the production of acetic acid in kraft mills. Acetyl groups in hardwood can be hydrolyzed using alkali at 50 °C. The product from this process contains about 15 g/L of sodium acetate and was determined to be suitable for the production of acetic acid.

Experiments performed using aqueous sodium acetate to evaluate the ability of electrodialysis (ED) to separate and concentrate sodium acetate showed that sodium acetate can be concentrated up to 275 g/L starting with an initial concentration of 17 g/L. The transport of water with sodium and acetate ions through ED membranes limited the maximum obtainable concentration.

To avoid the deleterious effects of white liquor on ED, selectivity experiments were performed using synthetic oxidized white liquor extract. These experiments showed a decrease in the efficiency of ED process due to the presence of sodium carbonate and sodium sulphate in the extract. Hence, it was concluded that caustic should be used as the extraction solvent.

Bi-polar electrodialysis (BPMED) experiments performed using sodium acetate showed that up to 200-280 g/L of acetic acid can be produced using BPMED. Although higher concentrations of sodium hydroxide can also be produced using BPMED, 30 g/L concentration was considered to be sufficient for recycle to the extraction process.

Feed and bleed mode BPMED experiments were performed to determine the current efficiencies and the suitable inlet concentration of sodium acetate for the production of up to 200 g/L of acetic acid. Both feed and bleed mode and batch experiments showed that the current density was the major driving force for BPMED.

Two types of concentrated wood extracts; namely (1) clarified and (2) unclarified were prepared with and without the lignin removal pre-treatment, respectively. The results of the ED and BPMED experiments performed using these extracts were similar to those of the synthetic sodium acetate. A major difference involved an increase of about 15% in electric energy consumption arising from the transport of formate, lactate and glycolate salts. The color of the anionic membranes slightly changed after processing unclarified extract through ED and BPMED.

ACKNOWLEDGEMENTS

I am thankful to Prof. Genco for his support and mentorship. I appreciate his efforts in making sure that I am learning as a whole besides working on my dissertation project. Many thanks go to all committee members for contributing their time, energy and expertise for the benefit of my dissertation. I wish to thank Prof. Pendse and Prof. van Heiningen for their suggestions about the process development work. I very much appreciate the constructive feedback received from Prof. Fort and Prof. Cole during the weekly group meetings. I am very grateful to Prof. Neivandt for agreeing to review my dissertation.

I would like to recognize Michael Paleologou of FP Innovations Inc., Daniel Bar of Ameridia Inc., Dennis Chai of Electrosynthesis Inc. and Jean Cloutier of Hydro-Québec for their guidance and suggestions about electro dialysis process. Special thanks go to Peter Hart of WestRock Inc. for his suggestions about the pulping conditions. Many thanks go to Amos Cline for troubleshooting the electro dialysis equipment used in this work and helping me to collect reproducible data using this equipment. I would also like to thank Haixuan Zou for training me for the pulping and providing me pre-treated hardwood extract. I am thankful to Amy Luce for supplying the wood chips and training me for the electro dialysis equipment. I am grateful to thank Christa Muelenberg, Yurui Zhen and Seong Park for their assistance with the analytical work. Many thanks go to Chi Truong for her assistance in performing the electro dialysis experiments. I appreciate the funding received from the University of Maine Pulp and Paper Foundation, Louis Calder Professorship, Forest Bio-Products Research Institute, J. Larcom Ober Research Chair and Graduate School's Chase Distinguished Research Assistantship. Lastly, I wish to acknowledge my parents, siblings and extended family for their loving support. All experiments and the related analytical work listed in this dissertation except the analysis of

physical and optical properties pulp samples and ICP analysis of selected samples was performed by the author of this dissertation.

TABLE OF CONTENTS

ACKNOWLEDGEMENTS.....	iv
LIST OF TABLES.....	x
LIST OF FIGURES.....	xiii
LIST OF ABBREVIATIONS	xviii
1. INTRODUCTION.....	1
1.1 OBJECTIVES	1
1.2 INTRODUCTION OF THE PROBLEM.....	1
1.3 CHEMICAL COMPOSITION OF WOOD	2
1.4 INTEGRATING THE EXTRACTION PROCESS INTO AN EXISTING KRAFT PULP MILL	4
1.5 METHOD FOR THE SEPARATION AND FURTHER PROCESSING OF SODIUM ACETATE	6
1.6 KRAFT PULPING, TWO-STAGE PULPING AND PROPERTIES OF PULP.....	10
1.7 SCOPE OF THE DISSERTATION.....	14
2. THEORY OF ELECTRODIALYSIS.....	16
2.1 ION EXCHANGE MEMBRANES AND SPACERS.....	16
2.2 TWO-COMPARTMENT ELECTRODIALYSIS SYSTEM	22
2.2.1 Arrangement of cation and anion exchange membranes in the stack.....	22
2.2.2 Working Principle.....	23
2.3 BIPOLAR MEMBRANE ELECTRODIALYSIS - INTRODUCTION AND WORKING PRINCIPLE	25
2.3.1 General Process Guidelines for Bi-Polar Membrane Electrodialysis	28
2.4 MASS TRANSFER IN ELECTRODIALYSIS	28
2.4.1 Donnan Exclusion Phenomenon	30
2.5 PARAMETERS AFFECTING THE PERFORMANCE OF ELECTRODIALYSIS EQUIPMENT	32
2.5.1 Current Density and Voltage.....	32
2.5.2 Current Efficiency.....	33
2.5.3 Flow Velocity.....	34
2.5.4 Concentration Polarization	34
2.5.5 Limiting Current Density	37
2.5.6 Water Transport across Membranes.....	39
2.5.7 Feed and Product Compositions.....	40

2.6	ELECTRODIALYSIS PROCESS COSTS	40
2.6.1	Fixed Investment Costs	40
2.6.2	Operating Costs.....	41
2.7	OPTIMIZATION OF ELECTRODIALYSIS PROCESS	43
2.7.1	Optimization of Feed Composition	43
2.7.2	Optimization of Product Composition and Solubility Limits	44
2.7.3	Controlling Flow Rate	46
2.7.4	Preventing Scaling and Fouling of Membranes.....	46
2.8	ELECTRODIALYSIS PROCESS PERFORMANCE INDICES.....	47
2.8.1	Separation Factor	47
2.8.2	Selectivity and Relative Number Moles of Salt Transported	47
2.8.3	Flux	48
2.8.4	Specific Electrical Energy.....	48
2.8.5	Current Efficiency	49
2.8.6	Overall Water Transport Index	49
2.9	LITERATURE DATA - SEPARATION & SPLITTING OF SODIUM ACETATE USING ELECTRODIALYSIS	49
3.	LOW TEMPERATURE EXTRACTION AND TWO-STAGE PULPING EXPERIMENTS.....	54
3.1	LOW TEMPERATURE EXTRACTION EXPERIMENTS USING LOW WHITE LIQUOR CHARGE	54
3.2	LOW TEMPERATURE EXTRACTION EXPERIMENTS USING LOW CAUSTIC CHARGE	57
3.3	TWO STAGE PULPING EXPERIMENTS WITH WHITE LIQUOR PRE-EXTRACTION.....	57
3.3.1	Physical Properties of Unbleached Control and Pre-Extracted Pulp	59
4.	SEPARATION AND CONCENTRATION OF SODIUM ACETATE USING ELECTRODIALYSIS.....	64
4.1	INTRODUCTION	65
4.2	EXPERIMENTAL METHODS.....	66
4.2.1	Experimental Apparatus.....	66
4.2.2	Experimental Procedure	68
4.2.2.1	Procedure for the Determination of Limiting Current Density	69

4.2.3	Experimental Design	70
4.2.3.1	Experiments to Study the Separation of Sodium Acetate from Water.....	70
4.2.3.2	Effect of Tramp Ions of Oxidized White Liquor on Selectivity of Electrodialysis	71
4.2.3.3	Electrodialysis Experiments using Pre-Treated Extracts	73
4.3	RESULTS AND DISCUSSION.....	76
4.3.1	Determination of Limiting Current Density.....	76
4.3.2	Separation of Sodium Acetate from Water	77
4.3.2.1	Effect of Feed Concentration	81
4.3.2.2	Effect of Current Density.....	82
4.3.2.3	Maximum Attainable Product Concentration.....	83
4.3.3	Effect of Tramp Ions of Oxidized White Liquor Extract on Selectivity of Electrodialysis.....	84
4.3.4	Electrodialysis Experiments Using Pre-Treated Extracts.....	89
5.	SPLITTING OF SODIUM ACETATE USING BI-POLAR MEMEBRANE ELECTRODIALYSIS.....	95
5.1	INTRODUCTION	95
5.2	EXPERIMENTAL METHODS.....	96
5.2.1	Experimental Apparatus.....	96
5.2.2	Experimental Procedure	98
5.2.3	Experimental Design	99
5.2.3.1	Determination of Limiting Current Density.....	100
5.2.3.2	Preliminary Scoping Experiments using Sodium Acetate	100
5.2.3.3	Study of Effect of Feed Concentration using Feed and Bleed Mode Experiments	101
5.2.3.4	Experiments using Pre-Treated Extracts	102
5.3	RESULTS AND DISCUSSION.....	104
5.3.1	Determination Limiting Current Density.....	104
5.3.2	Preliminary Scoping Experiments using Sodium Acetate	104
5.3.3	Study of Effect of Feed Concentration using Feed and Bleed Mode Experiments.....	113
5.3.4	Experiments Using Pre-Treated Extracts.....	126

6.	CONCLUSIONS AND RECOMMENDATIONS FOR FUTURE WORK	132
6.1	CONCLUSIONS.....	132
6.1.1	Low Temperature Extraction and Two-Stage Pulping Experiments	132
6.1.2	Separation and Concentration of Sodium Acetate Using Electrodialysis	133
6.1.3	Splitting of Sodium Acetate using Bi-Polar Membrane Electrodialysis.....	134
6.2	RECOMMENDATIONS FOR FUTURE WORK.....	136
	REFERENCES	138
	APPENDIX A: ESTIMATION OF THE ERRORS ASSOCIATED WITH THE ELECTRODIALYSIS EXPERIMENTS.....	142
	APPENDIX B: ESTIMATION OF THE ERRORS ASSOCIATED WITH THE BI-POLAR MEMBRANE ELECTRODIALYSIS EXPERIMENTS.....	146
	APPENDIX C: STANDARD METHODS FOR EVALUATING PULP PROPERTIES	150
	APPENDIX D: OPERATING PROCEDURE FOR ELECTRODIALYSIS EQUIPMENT.....	157
	BIOGRAPHY OF THE AUTHOR.....	169

LIST OF TABLES

Table 1.1 Characterization of Liquor Streams in Kraft Pulp Mills	13
Table 2.1 General Process Guidelines for BPMED Process	28
Table 2.2 Literature Data on Separation of Sodium Acetate and Acetic Acid using Electrodialysis	51
Table 2.3 Literature Data on Separation of Sodium Acetate and Acetic Acid using Electrodialysis	52
Table 2.4 Literature Data on Splitting of Sodium Acetate using Electrodialysis.....	53
Table 3.1 Compositions of Extracts obtained under Different Conditions	56
Table 3.2 Experimental Conditions for Control and Two-Stage Pulping Experiments	59
Table 3.3 Physical and Optical Properties of the Control and Pre-Extracted Pulp Samples.....	61
Table 4.1 Maximum Allowed Voltage Drop for Different Components of the ED Cell.....	67
Table 4.2 Experiments for Studying Separation of Sodium Acetate from Water	70
Table 4.3 Experiments to Study the Effect of Tramp Ions of White Liquor on Selectivity of ED	72
Table 4.4 Composition of Pre-Treated Extracts (4% EA, 0% S, 80 C) used in Electrodialysis	75
Table 4.5 Results of ED Experiments for Separating Sodium Acetate from Water	81
Table 4.6 Properties of the Feed Solutions Used in Experiments F-2 and F-4.....	87
Table 4.7 Concentration of Feed and Product Solutions for the ED Experiment Performed using Clarified Extract	93
Table 4.8 Concentration of Feed and Product Solutions for the ED Experiment Performed using Unclarified Extract.....	93

Table 4.9 Comparisons of the ED Experiments Performed Using Pre-Treated Extracts.....	94
Table 5.1 Maximum Allowed Voltage Drop for Different Components of the BPMED	
Cell	97
Table 5.2 Circulation Rates of the Salt Solution.....	99
Table 5.3 Batch Experiments using Bi-Polar Membrane Electrodialysis.....	100
Table 5.4 Feed and Bleed Mode Experiments using Bi-Polar Membrane Electrodialysis	102
Table 5.5 Composition of Pre-Treated Hardwood Extracts (4% EA, 0% S, and 80 °C)	103
Table 5.6 Overall Water Transport Indices and Maximum Achievable Product	
Concentrations	110
Table 5.7 Specific Electric Energy Consumption for Batch Experiments Performed using	
BPMED	111
Table 5.8 Average Concentrations of the Base Product and Residual Salt Solutions in Feed	
and Bleed Mode Experiments	117
Table 5.9 Summary of Results of Feed and Bleed Mode Experiments.....	126
Table 5.10 Concentration of Salt and Base Solutions for the BPMED Experiment Performed	
using Clarified Extract	129
Table 5.11 Concentration of Acid Solution for the BPMED Experiment Performed using	
Clarified Extract.....	129
Table 5.12 Concentration of Salt and Base Solutions for the BPMED Experiment Performed	
using Unclarified Extract	129
Table 5.13 Concentration of Acid Solution for the BPMED Experiment Performed using	
Unclarified Extract	129
Table 5.14 Summary of the BPMED Experiments Performed Using Pre-Treated	
Extracts	131

Table A.1 Experimental Conditions for Error Analysis Experiments for Electrodialysis	142
Table A.2 Error Analysis Data for Electrodialysis Experiments	145
Table B.1 Experimental Conditions for Error Analysis Experiments for BPMED	146
Table B.2 Error Analysis Data for Bi-Polar Membrane Electrodialysis.....	149
Table C.1 Typical Brightness Values for Different Grades of Paper.....	154
Table D.1 Properties of Ion Exchange Membranes used in this Study.....	167

LIST OF FIGURES

Figure 1.1 Structure of Glucuronoxylan.....	3
Figure 1.2 Effect of pH on Ionization of Acetic acid.....	6
Figure 1.3 Desalination Costs as a Function of Feed Concentration for Various Processes.....	7
Figure 1.4 Process for the Manufacture of Sodium Acetate from Wood Extract.....	9
Figure 1.5 Process for the Manufacture of Acetic Acid from Wood Extract	9
Figure 1.6 Simplified Diagram of the Kraft Pulping Process	11
Figure 1.7 Formation of Formic and Glycolic Acid During Alkaline Cook.....	12
Figure 1.8 Formation of Lactic Acid During Alkaline Cook.....	13
Figure 2.1 Molecular Structure of Ion Exchange Membrane.....	18
Figure 2.2 Photo of Neosepta CMX Cation Exchange Membrane	19
Figure 2.3 Comparison of Ion Exchange Resin and Ion Exchange Membrane.....	20
Figure 2.4 Baffled Flow Pattern Created by Spacer	20
Figure 2.5 Photo of PCCell ED 64-004 Spacer	21
Figure 2.6 Possible Configuration of Membranes for Two-Compartment ED Cell.....	23
Figure 2.7 Working Principle for a Two-Compartment Electrodialysis System Applied to Sodium Acetate Solution	24
Figure 2.8 Structure of Bipolar Membrane.....	26
Figure 2.9 Working Principle of the Three-Compartment Bipolar Membrane Cell.....	27
Figure 2.10 Donnan Equilibrium in a Cation Exchange Membrane for Sodium Chloride.....	32
Figure 2.11 Velocity and Concentration Profiles in Electrodialysis Cell.....	34
Figure 2.12 Fluxes and Concentration Profiles across a Cation Exchange Membrane.....	36
Figure 2.13 Water Dissociation at the Surface of the Ion Exchange Membrane at the Limiting Current Density for Sodium Chloride	38

Figure 2.14 Limiting Current (A) and Current Density vs Feed Concentration (B).....	39
Figure 2.15 Major costs in Electrodialysis as a Function of Applied Current Density.....	42
Figure 2.16 Back Diffusion of Ions and Molecules in Bi-Polar Membrane Electrodialysis.....	45
Figure 3.1 Effect of White Liquor Charge and Temperature on Sodium Acetate Concentration in Extract	55
Figure 3.2 Kraft Control Pulping Process	58
Figure 3.3 Two Stage Cooking Process.....	59
Figure 3.4 Effect of Degree of Refining on Pulp Freeness and Internal Bond Strength.....	62
Figure 3.5 Effect of Degree of Refining on Tensile and Tear Indices	63
Figure 3.6 Effect of Degree of Refining on Brightness and Bulk Density	63
Figure 4.1 Two-Compartment Electrodialysis Cell.....	67
Figure 4.2 Two-Compartment Electrodialysis Apparatus	68
Figure 4.3 Pre-treatment of Hardwood Extract Prior to Use in the Electrodialysis Experiments	73
Figure 4.4 Effect of Extraction Temperature on Sodium Formate Concentration in Extract.....	74
Figure 4.5 Limiting Current Density for Neosepta AMX/CMX Membranes.....	76
Figure 4.6 Concentrations and Volumes of Feed and Product Solutions for Experiment C-3	78
Figure 4.7 Current, Voltage and Cumulative Energy for Experiment C-3	79
Figure 4.8 Effect of Feed Concentration on Sodium Acetate and Water Fluxes and Specific Energy	82
Figure 4.9 Effect of Current Density on Sodium Acetate and Water Fluxes and Specific Energy	83

Figure 4.10 Calculation of Overall Water Transport Index	84
Figure 4.11 Concentrations of Feed and Product, Current and Voltage in Experiment F-1.....	85
Figure 4.12 Concentrations of Feed and Product Solutions in Experiment F-2.....	86
Figure 4.13 Concentrations of Feed and Product Solutions in Experiment F-3.....	87
Figure 4.14 Concentrations of Feed and Product Solutions in Experiment F-4.....	88
Figure 4.15 Variation in Feed Concentration for Separation Experiments.....	89
Figure 4.16 Photos of clarified and unclarified wood extracts	90
Figure 4.17 Concentration Profiles for ED Experiment Performed Using Clarified Extract	91
Figure 4.18 Concentration Profiles for ED Experiment Performed Using Unclarified Extract	91
Figure 5.1 Configuration of a Three-Compartment Bi-Polar Membrane Electrodialysis Cell	97
Figure 5.2 Schematic Diagram of BPMED Apparatus Operated in the Batch Mode	98
Figure 5.3 Costs in Electrodialysis as a Function of the Applied Current Density.....	99
Figure 5.4 Limiting Current Density for Neosepta AHA/CMB Membranes	104
Figure 5.5 Concentration of Sodium Acetate in Salt Solution during Batch Experiments.....	105
Figure 5.6 Concentration of Acetic Acid in Acid Solution during Batch Experiments.....	106
Figure 5.7 Concentration of Sodium Hydroxide in Base Solution during Batch Experiments	106
Figure 5.8 Volumes of Salt Solutions during Batch Experiments.....	107
Figure 5.9 Volumes of Acid Solutions during Batch Experiments.....	108
Figure 5.10 Volumes of Base Solutions during Batch Experiments	108

Figure 5.11 Pathways for Diffusion in Bi-Polar Membrane Electrodialysis Process	109
Figure 5.12 Current, Voltage and Energy Consumption for Batch Experiment No. 2	111
Figure 5.13 Current Efficiencies for Batch Experiments Performed using BPMED	112
Figure 5.14 Concentration of Acetic Acid in the Acid Solution for Feed and Bleed Mode Experiments.....	113
Figure 5.15 Volume of the Acid Solution for Feed and Bleed Mode Experiments	114
Figure 5.16 Sodium Hydroxide and Sodium Acetate Concentrations in Base and Salt Solutions (respectively) for Experiment FB-1	115
Figure 5.17 Variation in Volumes of Acid and Base Solutions for Experiment FB-1.....	116
Figure 5.18 Concentrations of Minor Components in Salt, Acid and Base Solutions for Experiment FB-1	118
Figure 5.19 Cumulative Current Efficiencies for the Production of Acetic Acid in Feed and Bleed Mode Experiments.....	120
Figure 5.20 Cumulative Current Efficiencies for the Production of Sodium Hydroxide in Feed and Bleed Mode Experiments.....	121
Figure 5.21 Energy Consumption for Feed and Bleed Mode Experiment	122
Figure 5.22 Specific Average Energy Consumption	123
Figure 5.23 Normalized Rate of Production of Acetic Acid.....	123
Figure 5.24 Volumes and Concentrations of Acids in Feed and Bleed Mode Experiments	125
Figure 5.25 Concentration Profiles for the BPMED Experiment Performed using Clarified Extract.....	127
Figure 5.26 Concentration Profiles for the BPMED Experiment Performed using Unclearified Extract.....	127

Figure A.1 Reproducibility of the sodium acetate concentration measurement for Electrodialysis	142
Figure A.2 Reproducibility of the cell voltage measurement for Electrodialysis.....	143
Figure A.3 Reproducibility of the volume measurement for Electrodialysis	143
Figure B.1 Reproducibility of the concentration measurements for Bi-Polar Electrodialysis	146
Figure B.2 Reproducibility of the volume measurements for Bi-Polar Electrodialysis.....	147
Figure B.3 Reproducibility of the voltage measurements for Bi-Polar Electrodialysis.....	147
Figure C.1 Mechanism of Tear Testing	153
Figure C.2 Experimental Set-up for Measuring Internal Bond Strength.....	155
Figure D.1 Photo of PCCell ED 64-004 Electrodialysis cell	157
Figure D.2 Detailed Flow Patterns within Electrodialysis Cell	158
Figure D.3 Detailed Schematic of Laboratory Scale Electrodialysis Equipment	159
Figure D.4 Arrangement of Anode for Stacking the Cell.....	160
Figure D.5 Arrangement of Membranes and Spacers for Two-Compartment Electrodialysis Cell.....	161
Figure D.6 Arrangement of Membranes and Spacers for Three-Compartment Bi-Polar Membrane Electrodialysis cell	161
Figure D.7 Experimental Setup for Leak Test for Electrodialysis Cell	162
Figure D.8 Limiting Current.....	163

LIST of ABBREVIATIONS

AEM: Anion exchange membrane

BPM: Bi-polar membrane

BPMED: Bi-polar membrane electrodialysis

CEM: Cation exchange membrane

CFD: Computational fluid dynamics

CSA: Crude sodium acetate

DC: Direct current

EA: Effective alkali, on percentage basis

ED: Electrodialysis

RHS: Right hand side

RO: Reverse osmosis

AEM: Anion exchange membrane

BPM: Bi-polar membrane

CHAPTER 1

INTRODUCTION

This chapter contains the objectives, background information and organization of the dissertation.

1.1 Objectives

The primary objective of this dissertation was to develop a process for the production of acetic acid for application in Kraft pulp mills. Electrodialysis (ED) was evaluated for its ability to separate, concentrate and split sodium acetate, a pre-cursor of acetic acid, from alkaline hardwood extract obtained by low temperature extraction of industrial hardwood chips. Bi-polar membrane electrodialysis (BPMED), electro-dialytic splitting process, can convert sodium acetate into acetic acid and sodium hydroxide. Two-stage pulping experiments were performed to determine the suitability of the pre-extracted wood as a feedstock for producing marketable hardwood pulp.

The current work complements the work performed for my M.S. thesis where I evaluated the conditions suitable for the cleavage of acetyl groups from hardwood chips during a caustic (white liquor) pre-treatment step in the kraft pulping process [Patil, 2012]. The raw extract from the extraction step serves as the starting material for separation and subsequent conversion of sodium acetate into acetic acid, which represents a potential by-product in kraft pulp mills. Sodium hydroxide is a by-product of the salt splitting process and can be reused in the extraction process.

1.2 Introduction of the Problem

Due to the environmental, economic and supply issues associated with the use of fossil fuels, there is a need to manufacture fuels and chemicals from renewable materials. Lignocellulosic biomass such as woody plants represent an abundant and sustainable source of carbon and thus, it is a potential feedstock for the production of fuels and chemicals.

Wood contains about 3-4% acetyl groups on a dry weight basis. Currently, acetyl groups end up in the black liquor (spent liquor) stream in the kraft process and are burned as fuel. There are several advantages to recovering acetyl groups in wood as either sodium acetate or acetic acid. Benefits include: (1) increased revenue from the sale of a commodity chemical, (2) facilitation of the downstream fermentation process due to separation of acetic acid which is sometimes a fermentation inhibitor in the recovery of sugars, (3) reduction in the amount of shives, (4) increased pulp yield due to increased liquor penetration in the wood and (5) the increased competitiveness for Kraft pulp mills [van Heiningen, 2006].

Pulp and paper mills have used crude sodium acetate (CSA, 30% on weight basis) for sodium makeup to the process and for energy recovery (energy value = 3000 BTU/wet lb) for many years. Since CSA does not contain sulfur, it can improve mill operations in situations where high sulfidity is a concern. Acetic acid is an important commodity chemical used in the manufacture of food, pharmaceuticals, paint and synthetic fibers and fabrics.

1.3 Chemical Composition of Wood

The term 'Lignocellulose' is used to describe the three-dimensional polymeric composites formed by plants as a structural material. Lignocellulosic feedstock is composed primarily of carbohydrate polymers (cellulose and hemicelluloses) and phenolic polymers (lignin). There are also small amounts of various other compounds such as proteins, acids, salts and minerals that are present. However, the relative distribution of these components varies depending upon the type of species. Hardwoods, for example, contain about 45 wt% cellulose, 28-35 wt% hemicelluloses, 18-22 wt% lignin and small quantities of extractives and ash. The acetyl groups are present as side chains on the hemicellulose in hardwoods.

Cellulose is a linear homogenous polysaccharide consisting of β -D-glucopyranose units linked to each other through (1 \rightarrow 4)-glycosidic bonds [Sjöström, 1993]. Cellulose in woody plants has a degree of polymerization (DP) ranging from 7,000 to 15,000.

Hemicelluloses are heterogeneous polysaccharides. In most cases they are extensively branched and have a low degree of polymerization of around 200 or about 1/10th of the DP of cellulose [Sjöström, 1993]. These side chains inhibit crystallization and result in amorphous hemicellulose polymers. The irregular structure of the hemicellulose molecules minimizes the number of hydrogen bonds that can be formed between hemicellulose molecules and results in a less compact macro structure than that of cellulose. The chemical reactions of hemicelluloses are similar to those of cellulose except that their reactivity is greater. The fundamental components of hemicelluloses are D-glucose, D-mannose, 4-O-methyl-D-glucuronic acid, D-galactose, D-xylose, L-arabinose and L-rhamnose. The major hemicellulose in hardwoods is O-acetyl-4-O-methylglucurono- β -D-xylan, also known as glucuronoxylan. The content of xylan in hardwood varies from 15 to 30 wt% of the dry wood depending on the hardwood species. Besides xylans, hardwoods also contain 2-5 wt% glucomannan. Glucuronoxylan has a backbone consisting of β -D-xylopyranose units. The monomeric sugars are linked by (1 \rightarrow 4) glycosidic bonds. The O-acetyl groups are mostly located at the C-2 and/or C-3 position. There are approximately seven (7) O-acetyl groups per ten (10) xylose units as shown in Figure 1.1 [Sjöström, 1993].

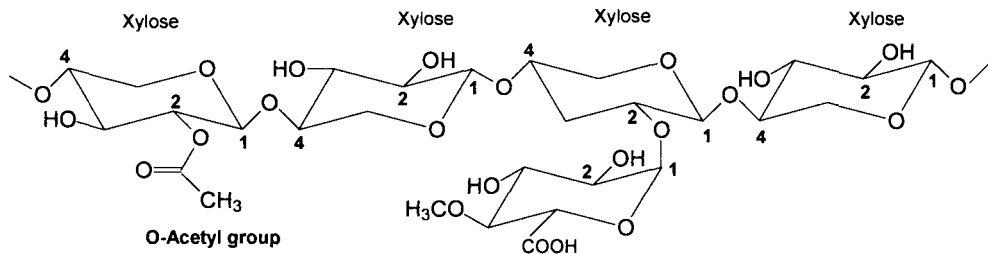


Figure 1.1 Structure of Glucuronoxylan

Lignin is comprised of phenylpropane units that may be oxygenated on any of the side chain positions. The ring contains one or two methoxy groups at C-3 or C-4 positions and the C-4 position is linked to either an ether or free hydroxide group. The phenylpropane units are randomly cross-linked to each other by a variety of different chemical bonds. These linkages

include both C-O-C (ether) and C-C (carbon carbon) linkages. The ether types of linkages represent two thirds or more of the total; while the rest are of the carbon to carbon type.

1.4 Integrating the Extraction Process into an Existing Kraft Pulp Mill

Production of acetic acid or any other new chemicals from hemicelluloses or lignin in a biorefinery setting is thought to be economic only if the new process is integrated into an existing wood product facility such as a kraft pulp mill. This occurs because of the high capital and operating costs associated with the wood handling and preparation systems and complexity in the processing. Stand-alone facilities have proven to be presently uneconomic [Woolley, 1999 and Mitchell, 2006]. When integrating a new product into an existing wood products facility, it is necessary to minimize the changes in the principal products from that facility. For example, integration of a hemicellulose pre-extraction process into a kraft pulp mill requires minimal change in the final properties of the pulp which is the main product, and minimal disruption to the normal operation of the facilities.

Mao and coworkers (2010) evaluated the "Near Neutral Extraction Process" which involves production of both ethanol and acetic acid in a kraft pulp mill by using green liquor as the extraction liquor. Green liquor in Kraft pulping parlances is an intermediate stream consisting principally of Na_2CO_3 and Na_2S in the Kraft recovery cycle; that is, the cycle that produces the pulping liquor in the kraft process. The Near Neutral Extraction process involves extraction of hemicelluloses using green liquor prior to kraft pulping. In Mao's process design study, the pre-extraction reactor was integrated into an existing northeast hardwood Kraft pulp mill. Ancillary unit operations include hydrolysis of the extracted carbohydrates using sulfuric acid, removal of the extracted lignin, liquid-liquid extraction of acetic acid, liming of the residual extract followed by separation of gypsum, fermentation of C-5 and C-6 sugars to ethanol, and upgrading the acetic acid and ethanol products by distillation. The results of Mao's techno-economic study showed that the overall process had a low rate of return on investment due to high capital investment associated with the

complexity of the process. Furthermore the bulk of the revenue generated by the process arose from the sale of acetic acid, as opposed to sale of ethanol arising from the conversion of C-5 and C-6 sugars into ethanol. The only circumstance where the process was deemed financially viable as originally conceived was for the case of very large pulp mills that have an existing pressure vessel which could be modified to perform the extraction, and where additional waste treatment and low cost steam were available to accommodate the new processes.

Patil and co-workers (2012) modified the near-neutral extraction process to recover acetic acid as the only by-product in the Kraft pulp mills. They substituted white-liquor, a readily-available inexpensive source of alkali, in place of the green liquor in the extraction step of the process. This was done in an effort to reduce the capital and operating cost and to improve the rate of return on investment for the process. Experimental data was reported on the rate of cleavage of acetyl groups from industrial hardwood chips using various alkali streams such as caustic, green liquor and white liquor. The effects of soaking temperature and extraction temperature were also evaluated. Eight percent (8%) white liquor, calculated on an effective alkali (EA) basis, was found to be effective for deacetylation due to the high initial concentration of hydroxide ions in the cooking liquor. Using 8% white liquor (EA), most of the acetyl groups can be cleaved off from industrial hardwood chips at an extraction temperature as low as 50 °C. The use of low extraction temperature reduces the pressure inside the digester, thus avoiding the use of a pressure vessel. Consequently, the cost of the extraction equipment is greatly reduced. The low extraction temperature also helps to reduce the energy requirements of the process. In addition, it reduces the amount of lignin and sugar extracted and thus, simplifies the downstream separation process.

1.5 Method for the Separation and Further Processing of Sodium Acetate

Figure 1.2 shows the effect of pH on ionization of acetate ion at 25 °C. Most acetate groups are present as acetate ions when the pH of the solution is above 10 or as acetic acid when the pH is below about 2. The pKa of acetic acid is about 4.8, and it represents the pH at which 50% of the acid exists in the acetate form. Thus, sodium acetate can be separated under either alkaline or acidic conditions.

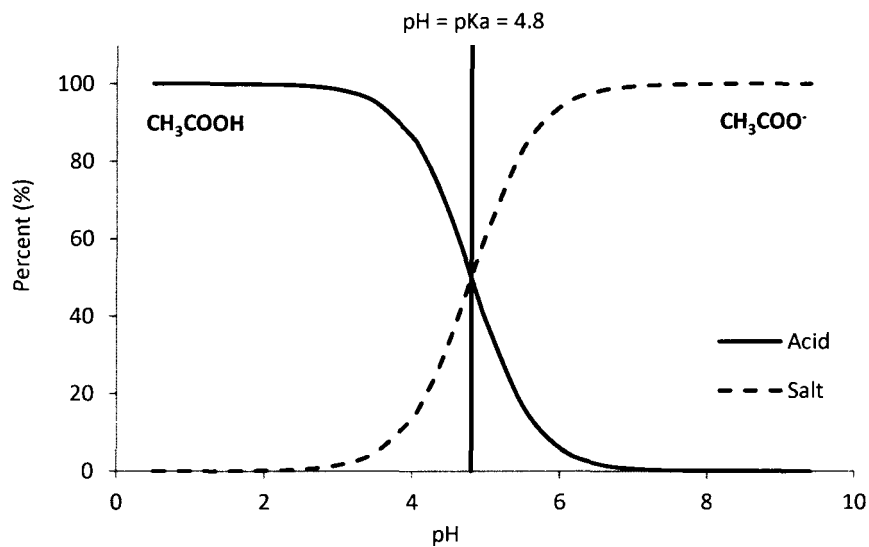


Figure 1.2 Effect of pH on Ionization of Acetic acid

For the present problem, recovery of acetyl groups using alkaline extract is most desirable since it does not involve neutralization of the extract, downstream salt processing and avoids disposal of waste products such as calcium sulfite. Also, the residual alkaline extract remaining after the separation of acetyl groups can be further used in the downstream pulping operations, which reduces alkali and water requirement for the overall process.

Acetate ions, being electrically charged, can be separated using ion exchange resins and/or electrodialysis (ED). In ED, an electric field is applied to separate ions from salt solution. ED is particularly promising and has been studied extensively for the desalination of

sea water. It is particularly effective in the desalination of brackish and sea waters at low solids concentration. For the desalination of sea water at high concentrations, ED is less effective.

Figure 1.3 shows the specific cost for separation of sodium chloride as a function of feed solution concentration using different separation process [Strathmann, 2003]. Since steam is expensive, distillation is not economically feasible if the salt concentration is less than about 10%. This results because the cost of evaporation of water is more than the selling price of the final product, clean water. ED requires electric energy and periodic replacement of membranes, both of which are expensive. But, if the salt concentration is low, ED is economically feasible when compared to distillation provided the proper membranes are used. Ion exchange resins don't require a lot of energy but they consume large quantities of acids and alkalis during regeneration. Thus, the use of ion exchange resin is expensive even when the concentration of salt is low.

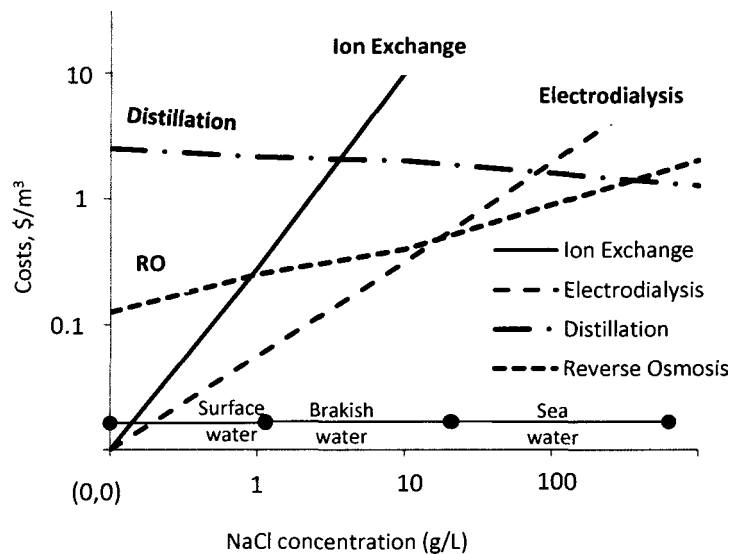


Figure 1.3 Desalination Costs as a Function of Feed Concentration for Various Processes

It is clear that ED and Reverse Osmosis (RO) can be cost effective methods for the present case, where the concentration of the salt to be separated is about 15-17 g/L.

However, RO is not currently feasible for the present problem due to the inability of membranes to operate at the high pH of the alkaline hardwood extract.

ED was selected as the method to be investigated in the separation of sodium acetate because it has been used for more than five decades for desalination of brackish water [Walker, 2010]. ED pushes ions through an ion exchange membrane against a concentration gradient using an electric voltage as the driving force. ED technology shows promise as a feasible process because of two primary reasons [Neosepta, 2013]. First, unlike the use of ion exchange resins, ED does not require large quantities of regeneration chemicals. Secondly, ED is more robust than RO in terms of operating over a greater pH range.

Bi-polar membrane electrodialysis (BPMED) is an electro-membrane process which can convert aqueous sodium acetate into acetic acid and caustic. BPMED is a promising method for the recovery of acetyl groups from alkaline hardwood extract because of the following reasons. First, the demand for acetic acid is higher than that of sodium acetate and a significantly higher selling price can be achieved if acetic acid is concentrated to about 99% by weight. Secondly, the use of BPMED allows the recovery of about two third of the caustic used in the extraction process at no additional cost.

Figure 1.4 and 1.5 show block flow diagrams of the two potential processes for the processing of sodium acetate from alkaline hardwood extract. Figure 1.4 illustrates the manufacture of sodium acetate while figure 1.5 demonstrates a process for producing acetic acid.

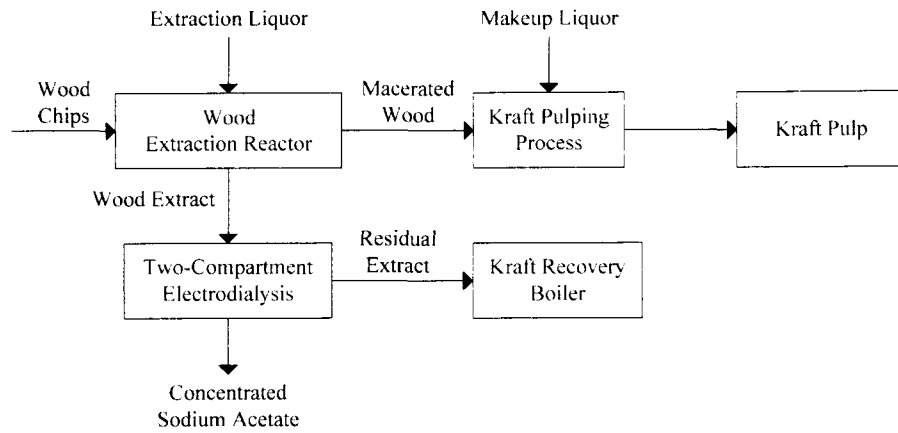


Figure 1.4 Process for the Manufacture of Sodium Acetate from Wood Extract

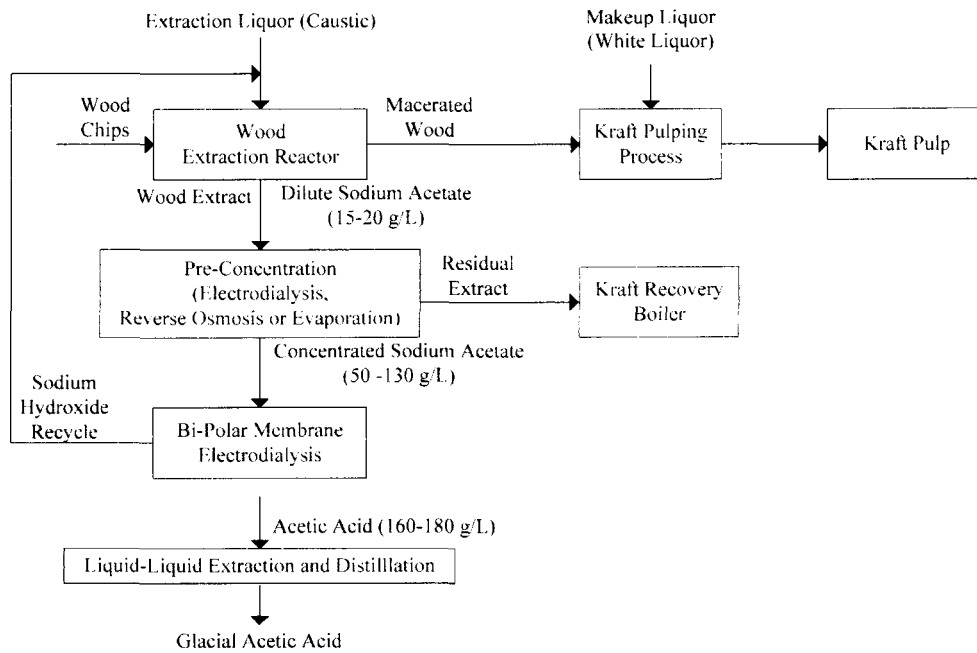


Figure 1.5 Process for the Manufacture of Acetic Acid from Wood Extract

An overview of the Kraft pulping process is provided in the remainder of this chapter.

Finally, the organization of this dissertation is briefly discussed.

1.6 Kraft Pulping, Two-Stage Pulping and Properties of Pulp

Wood pulp is used predominantly for papermaking in either a bleached or unbleached form, while high purity alpha cellulose pulp is an intermediate material used in the manufacture of chemical products based on cellulose. The major objective of wood pulping is to generate cellulose based fibers and it is usually accomplished by either a chemical method or a mechanical method, or a combination of both. Chemical pulping accounts for 70% of North American production of wood pulp. Approximately 90% of pulp production is manufactured by the dominant Kraft process because of advantages in chemical recovery and pulp strength [Smook, 2002].

In Kraft pulping, wood chips are cooked with a solution of sodium hydroxide (NaOH) and sodium sulfide (Na₂S). This causes the breakdown of lignin into smaller segments whose sodium salts are soluble in the cooking liquor. The residual cooking liquor containing dissolved lignin and hemicellulose is called 'black liquor'; and it is evaporated and then burned in a recovery furnace. The resulting smelt consisting of sodium carbonate and sodium sulfite is dissolved in water to form 'Green Liquor' and then causticized by calcium hydroxide addition to form sodium hydroxide and calcium carbonate [Sjöström, 1993]. Figure 1.6 illustrates the Kraft process showing the makeup chemicals to account for sodium and sulfur losses in the system [Smook, 2002].

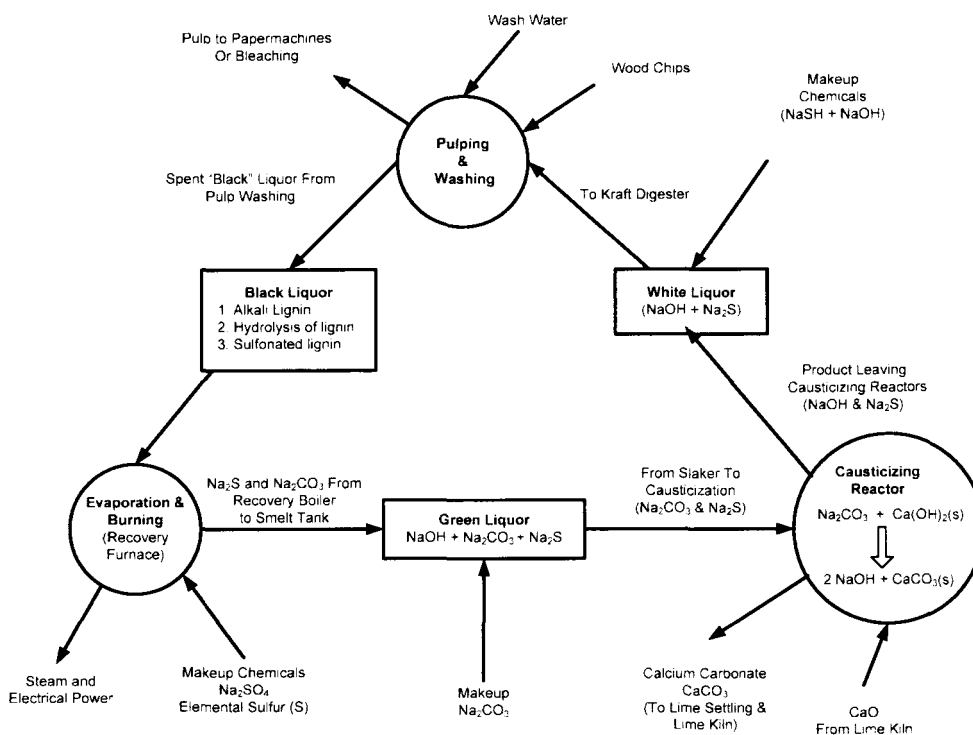


Figure 1.6 Simplified Diagram of the Kraft Pulping Process

The carbohydrate chemistry of kraft pulping involves a number of complicated reactions such as swelling, dissolution without chemical degradation, adsorption of dissolved carbohydrates on pulp, hydrolysis of acetyl groups, peeling and stopping reactions and hydrolysis of β -glycosidic bonds. The peeling reactions involve enolization and hydrolysis of β -alkoxycarbonyl bonds and further degradation of the products of hydrolysis, including isomerizations, as well as hydrolysis, to hydroxyl acids. The stopping reactions involve dehydration and fragmentation or intramolecular rearrangements to alkali-stable configurations. Formic and glycolic acids are formed during the stopping reaction (Figure 1.7). Whereas, lactic acid is formed during the fragmentation of a peeled monomer (Figure 1.8).

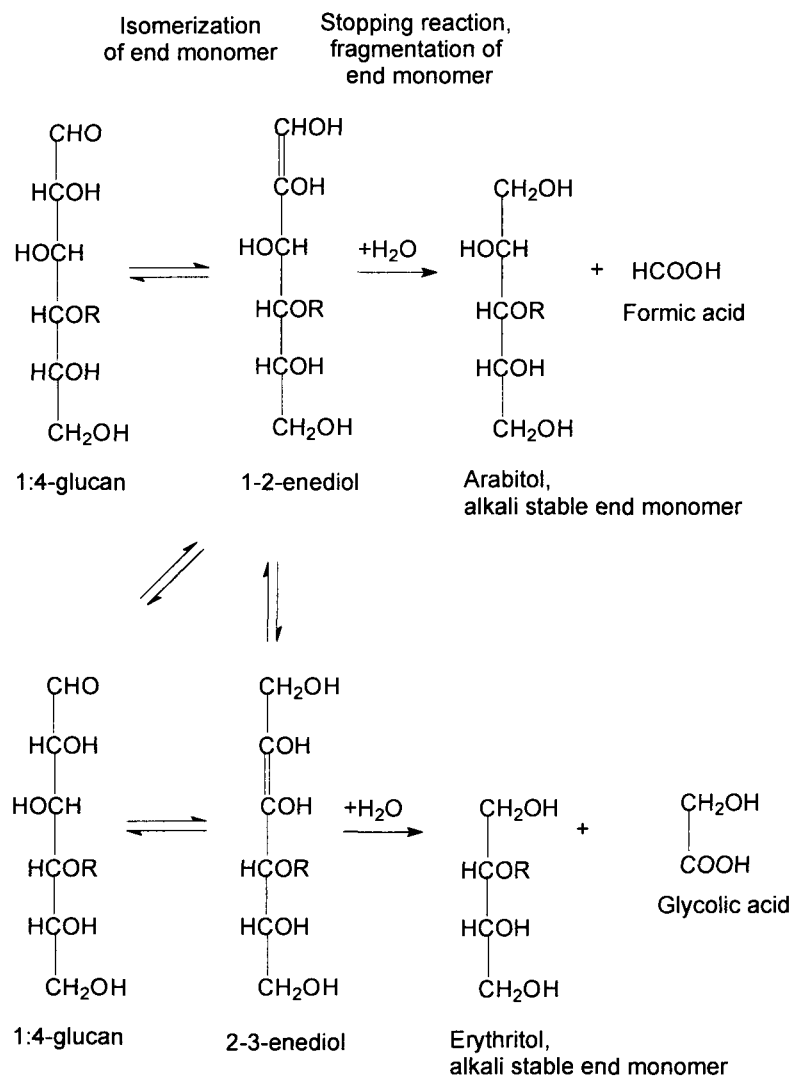


Figure 1.7 Formation of Formic and Glycolic Acid During Alkaline Cook

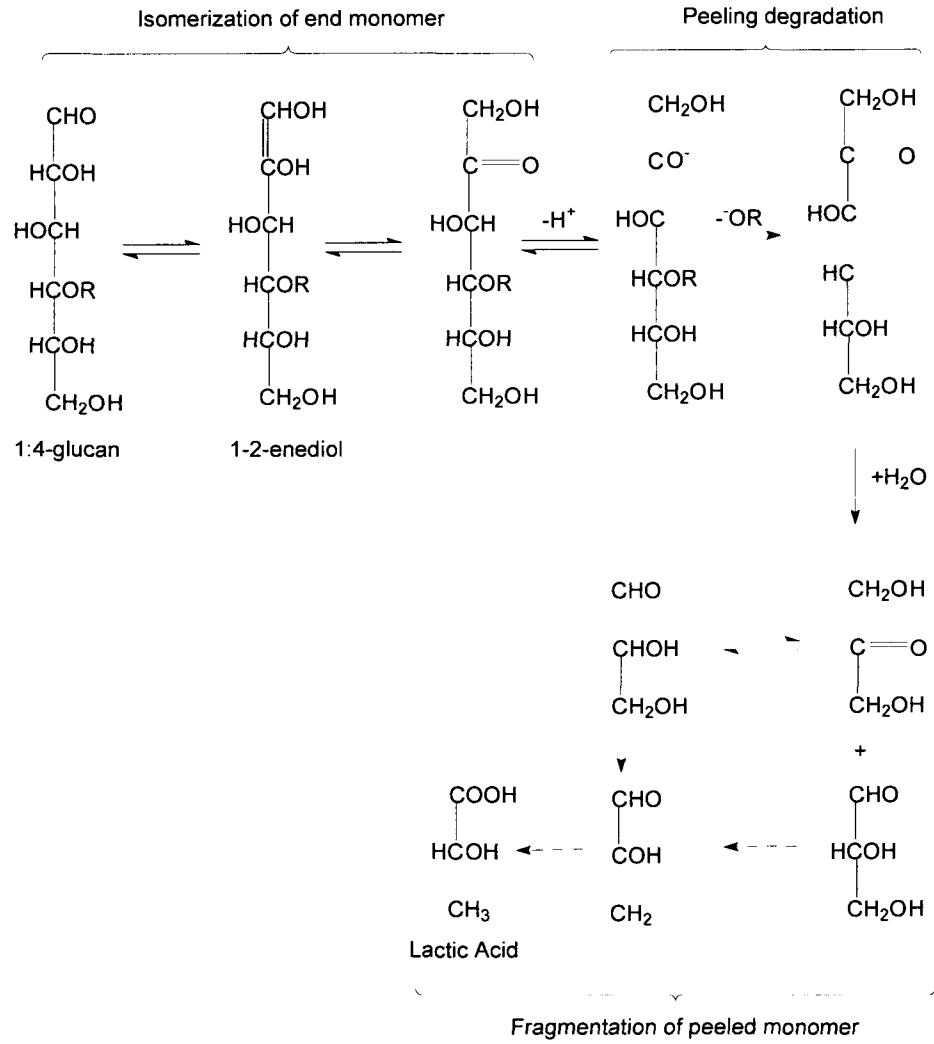


Figure 1.8 Formation of Lactic Acid During Alkaline Cook

Table 1.1 shows the major terminology used to chemically characterize different liquor streams in kraft pulp mills [Sjöström, 1993].

Table 1.1 Characterization of Liquor Streams in Kraft Pulp Mills

Term	Definition	Units
Total Titratable Alkali (TTA)	NaOH + Na ₂ S + Na ₂ CO ₃	g/L as Na ₂ O
Active Alkali (AA)	NaOH + Na ₂ S	g/L as Na ₂ O or % of Wood
Effective Alkali (EA)	NaOH + 0.5×Na ₂ S	g/L as Na ₂ O or % of Wood
Sulfidity (S)	Na ₂ S/ (NaOH + Na ₂ S)	%

The charge of 'Effective Alkali' for a typical hardwood kraft pulping is about 12.5-15.5% of the total dry wood [Sjöström, 1993]. Hardwood kraft pulping is typically performed at 170 °C with a digester residence time of 60-120 minutes. This process has pulp a yield of 40-50% based on dry wood [Smook, 2002]. Kraft pulp retains approximately 90% of the initial cellulose, 50% of the hemicellulose, and only 20% of the lignin [Smook, 2002]. Black liquor contains the remainder of the lignin, cellulose and hemicellulose in the form of carbohydrate degradation products such as aliphatic carboxylic acids, predominantly as hydroxyl monocarboxylic acids [Sjöström, 1993].

'Two-Stage Pulping' is a method for the production of kraft pulp by modifying the conventional kraft cooking process so that the changes in the chemical concentration and lignin concentration profiles during the cook leads to beneficial results such as additional by-products, extended delignification and improved selectivity. However, this must be done without sacrificing the conventional pulp yield and strength [Li, 1996].

Since the proposed processes (Figures 1.4 and 1.5) for the processing of sodium acetate from alkaline hardwood extract involve pulping of pre-extracted hardwood chips as opposed to the use of fresh chips to produce marketable hardwood kraft pulp, 'Two-Stage Pulping' experiments must be performed to determine the suitability of the macerated wood chips for the production of marketable hardwood kraft pulp.

A number of standard test methods are used to characterize pulps with respect to their quality, processability and suitability for various end uses [Smook, 2002]. A brief introduction to some of the test methods is given in Appendix C.

1.7 Scope of the Dissertation

As previously stated, the primary objective of this dissertation is to develop a process for the production of acetic acid suitable for use in Kraft pulp mills. The second chapter of this dissertation presents an overview of both the two-compartment electro dialysis and bi-polar membrane electro dialysis processes. Parameters affecting

performance of ED, cost, optimization strategies and process performance indices are also discussed. Finally, a review of literature data on separation and splitting of sodium acetate using electrodialysis is provided.

The third chapter contains experimental data on the pre-extraction of northeastern hardwood chips using white liquor and caustic at low alkali charge levels and low temperature. It also contains results of the two-stage pulping experiments performed to determine the suitability of the pre-extracted wood as a feedstock for producing marketable hardwood pulp.

The fourth chapter contains experimental data on separation of sodium acetate from dilute sodium acetate solution, synthetic oxidized white liquor extract and pre-treated alkaline hardwood extract using ED.

The fifth chapter contains experimental data on conversion of synthetic solution of sodium acetate into acetic acid and sodium hydroxide using batch and feed and bleed mode BPMED system. In addition, some batch experiments were performed using pre-treated alkaline hardwood extracts.

CHAPTER 2

THEORY of ELECTRODIALYSIS

Electrodialysis (ED) was invented in the early 1900s as a modification of the dialysis process. This was accomplished by adding electrodes causing direct current to increase the rate of flow of ions in electrolyte solutions. Since the 1940s, electrodialysis has evolved into a membrane based separation process for separating electrolyte feed solution into a product and a residual feed solution using an electric field and ion exchange membranes. Thus, electrodialysis involves coupling of mass transport with an electric current through ion exchange membranes [Strathmann, 2010].

2.1 Ion Exchange Membranes and Spacers

The ion exchange membrane is the key component of the Electrodialysis process. It is a sheet-shaped polymeric material. There are three different types of ion exchange membranes.

1] Cation exchange membrane (CEM): Cation exchange membranes contain negatively charged groups fixed to a hydrophobic polymer matrix. Mobile cations present for electrical neutrality with the fixed negatively charged groups can be exchanged with other cations present in the external liquid phase in contact with the membrane. Anions are almost excluded from the membrane depending upon the electrolyte concentration.

2] Anion exchange membrane (AEM): Anion exchange membranes contain positively charged groups fixed to a hydrophobic polymer matrix. Mobile anions present for electrical neutrality with the fixed positively charged groups can be exchanged with other anions present in the external liquid phase in contact with the membrane. Cations are almost excluded from the membrane depending upon the electrolyte concentration.

3] Bi-polar membrane (BPM): Bi-polar membranes are composed of an anion exchange and a cation exchange membrane laminated together by maintaining a thin liquid interphase of a

few nanometers between both layers. When an electric potential difference is applied across a BPM placed in an electrolyte solution and if the anion-side of the BPM is facing towards the positive electrode (anode), BPM can increase the rate of dissociation of water molecules present within the space between the membranes at the interphase. The OH^- and H^+ ions generated from the dissociation of water molecules move through the BPM into the adjacent electrolyte solutions (Figure 2.8). When the free hydroxyl (OH^-) and hydrogen (H^+) ions combine with the other ions formed from the dissociation of salt molecules, corresponding acids and bases are formed.

In ion exchange membranes, the fixed ions are in electrical equilibrium with the mobile ions bearing an electric charge opposite to that of the fixed ions (Figure 2.1). These mobile ions are termed **counter-ions**. Accordingly, cations are considered as counter ions in cation exchange membranes. Whereas, the ions which carry similar charge as that of fixed groups, are called **co-ions**. Most ion exchange membranes are impermeable to co-ions provided the concentration of salts in the solution is less than that of the ion exchange groups in the ion exchange membrane. Therefore, counter-ions will carry most of the current through the membrane. When the concentration of co-ions present in solution exceeds the concentration of the fixed groups, then the co-ions displace the counter-ions and the selectivity of the membrane is reduced. This phenomenon is called the Donnan Exclusion Phenomenon and it is discussed later in this chapter.

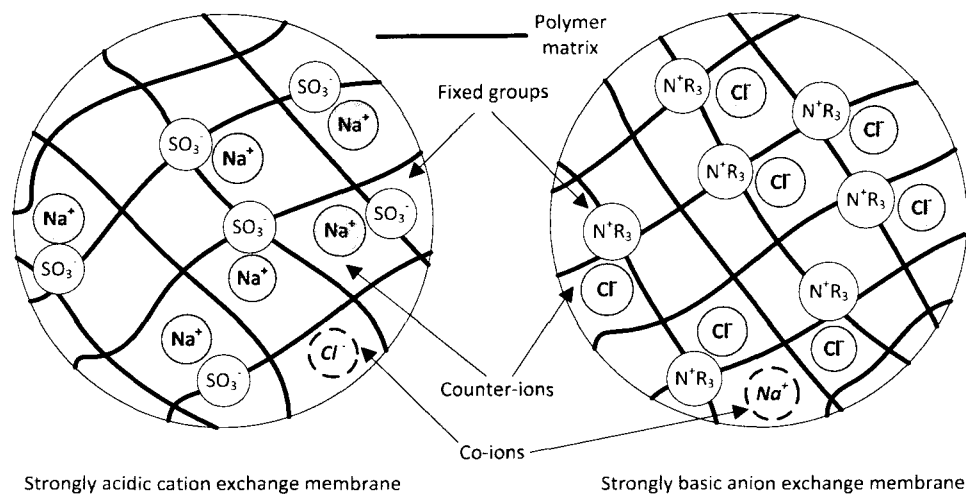


Figure 2.1 Molecular Structure of Ion Exchange Membrane

The most desired properties of ion exchange membranes are: (1) selectivity to a specific ion, (2) low electric resistance, and (3) high chemical, mechanical and thermal stability. Most of today's commercially available membranes meet these requirements.

Characteristics of Ion Exchange Membranes: The properties of ion exchange membranes are derived from two parameters: (1) the polymer matrix and (2) composition of fixed ionic groups. The polymer matrix determines the thermal, electric and mechanical stability of the membrane. The type and concentration of fixed groups determine its selectivity, electrical resistance, degree of swelling and mechanical properties, to a lesser extent. Cation and anion exchange membranes consist of polymers with substituent groups such as $-\text{SO}_3^-$, $-\text{COO}^-$ and $-\text{N}^+\text{H}_2\text{R}$, $-\text{N}^+\text{HR}_2$, $-\text{N}^+\text{R}_3$, respectively. These groups provide the surface charge to the membranes. The sulfonic acid ($-\text{SO}_3^-$) group is completely dissociated over nearly the entire pH range, while the carboxylic acid ($-\text{COO}^-$) group is hardly dissociated in the pH range <3 . The quaternary ammonium group ($-\text{N}^+\text{R}_3$) again is completely dissociated over the entire pH range, while the secondary ammonium group ($-\text{N}^+\text{HR}_2$) is only weakly dissociated. Accordingly, ion-exchange membranes are referred to as being weakly or strongly acidic or basic in character.

The ion exchange capacity is typically in the range 0.5 to 3.0 equivalents per kilogram of dry polymer. Since the typical polymers have densities almost equal to that of water, the fixed charge density is approximately 0.5 to 3.0 equivalents per liter. The typical thickness of an ion exchange membrane ranges from 0.1 to 1.0 mm. Typical AEM and CEM membranes are flat with a smooth surface, similar to a plastic sheet (Figure 2.2).

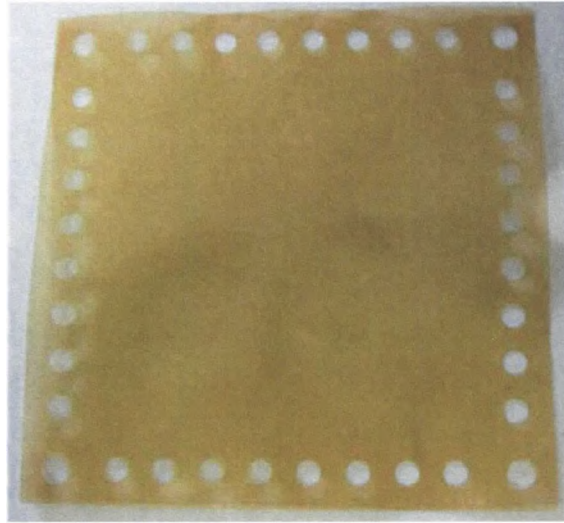


Figure 2.2 Photo of Neosepta CMX Cation Exchange Membrane

Difference between ion exchange resins and ion exchange membranes: Ion exchange resins are in granular form and function by pore diffusion and adsorptive exchange of ions (Figure 2.3). But, the major shortcoming of ion exchange resins is that it is a slow process and it requires regeneration when the adsorptive capacity is consumed. On the other hand, as the ion exchange membrane allows ions to permeate by DC electric current, no regeneration is required and it can be continuously used for a prolonged period [Neosepta, 2013]. The electrolytic flux of ions under the action of direct current is much higher than the diffusion flux through the membrane; 1 to 40 moles per m² per hour for ED compared to 0.1 to 2.3 moles per m² per hour for molecular diffusion.

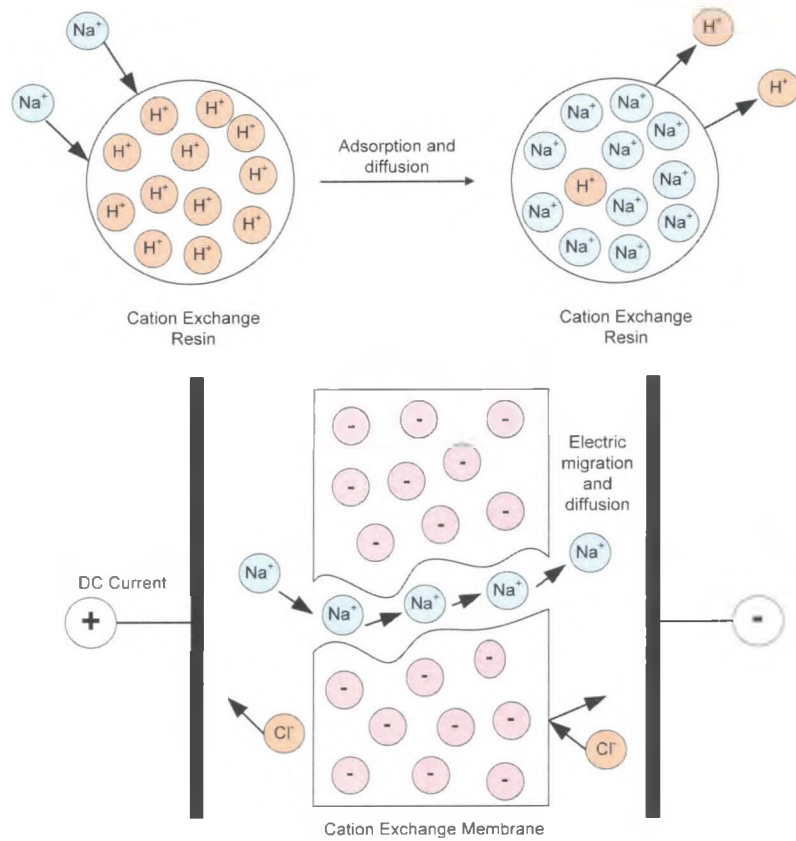


Figure 2.3 Comparison of Ion Exchange Resin and Ion Exchange Membrane

A spacer must be placed in between any two adjacent membranes as shown in Figure 2.4. The function of a spacer is to provide structural support to the membranes, which are fragile, and keep them separated from each other. The spacers also create flow paths for the electrolyte streams and ensure moderate turbulence in the volume between the spacers as shown in Figure 2.4.

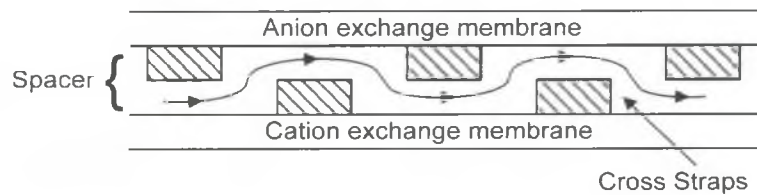


Figure 2.4 Baffled Flow Pattern Created by Spacer

Figure 2.5 shows a photograph of a typical spacer.

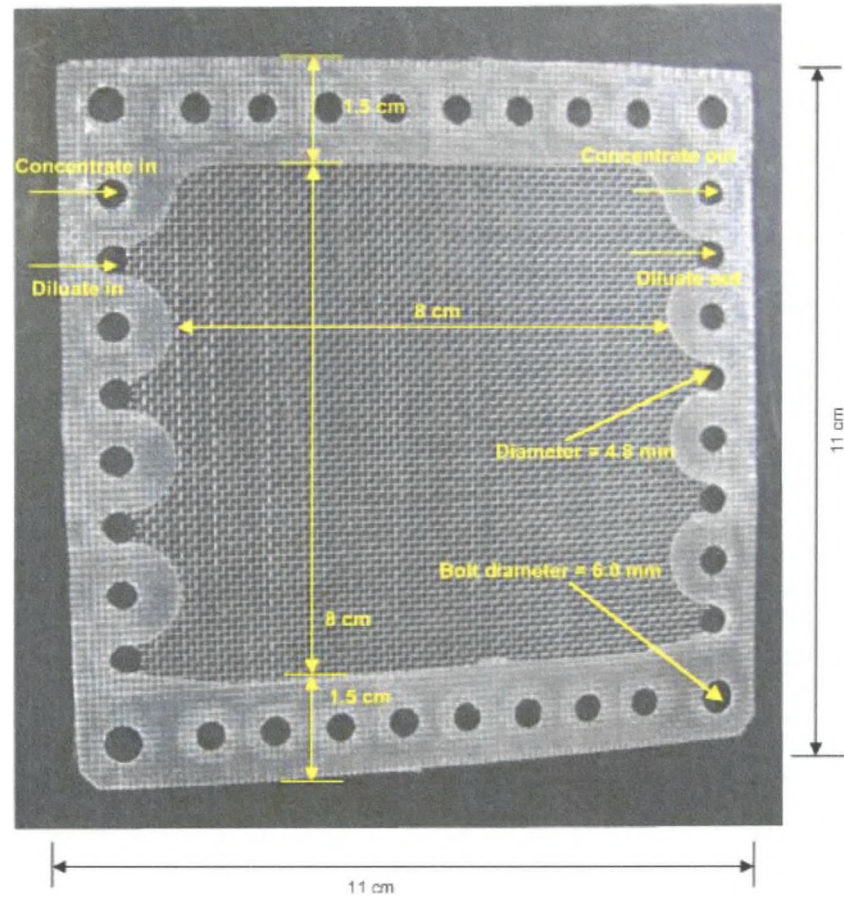


Figure 2.5 Photo of PCCell ED 64-004 Spacer

When an electro dialysis cell is tightened with a sufficient force, spacers form a flow channel that is leak free for the fluid flowing in the channel. The typical thickness of a spacer ranges from 0.3-2.0 mm, which fixes the thickness of the electrolyte streams in the cell. The thickness of the electrolyte streams controls their resistance. Different models and sizes of spacers are available for specific applications. The main difference in all models is volume of the flow path, which decides the electrolyte velocity.

2.2 Two-Compartment Electrodialysis System

This section covers information about the arrangement of membranes and working principle for two-compartment electrodialysis system which is used to separate and concentrate salts from their aqueous solutions.

2.2.1 Arrangement of cation and anion exchange membranes in the stack

For a two-compartment ED cell, membranes can be arranged in four different ways as shown in Figure 2.6 [Walker, 2010]. Configurations 1 and 3 consist of the same type of membrane on either ends of the stack. In this type of configuration, the stack continuously loses ions to one electrode rinse compartment and gains ions with similar charge from the other compartment. Therefore, the pH of the electrode rinse solution will remain within a reasonable limit if both rinse and electrolyte solutions contain similar types of ions. Configuration 1 is preferred over Configuration 3 to avoid transfer of corrosive chloride ions into the electrode compartments in the case of desalination. In configuration 2, the electrode rinse continuously loses both cations and anions to the neighboring compartments. Thus, the electrode rinse solution needs to be replaced periodically. The transfer of ions from electrode rinse solution into feed or product solutions needs to be taken into account while performing mass balance calculations, and it further increases the complexity of the analysis of results. In a similar manner, the electrode rise solution in configuration 4 continuously gains ions from the neighboring compartments and it would increase the complexity of the process. Thus, configuration 1 was found to be the most suitable for use in the present work.

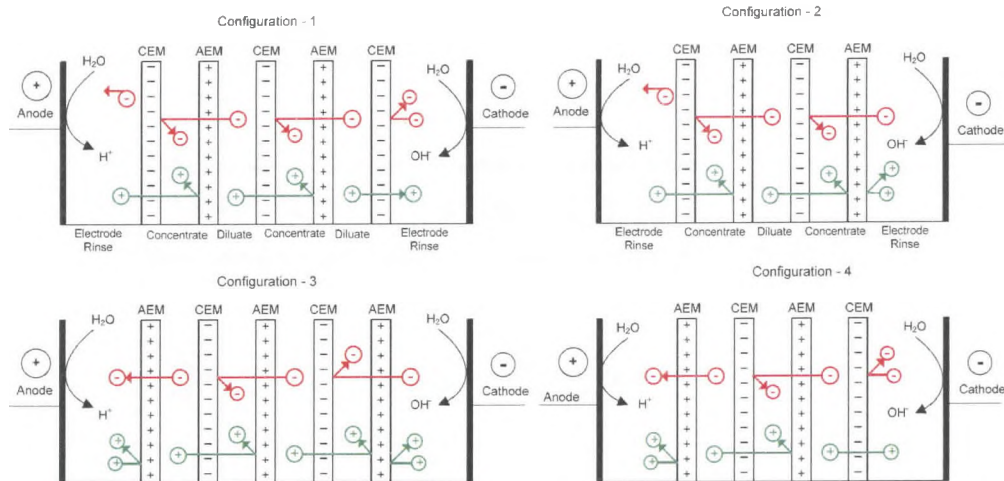


Figure 2.6 Possible Configuration of Membranes for Two-Compartment ED Cell

2.2.2 Working Principle

Typical ED equipment consists of an ED cell, a DC power supply and recirculation pumps. The ED cell consists of a series of anion and cation exchange membranes (Figure 2.7). Detailed schematics are available in the Appendix D. Depending upon the number of repeating electrolyte compartments excluding the electrode rinse compartments, the ED cells are termed as a two, three or four-compartment cell. The cell shown in Figure 2.7 is called a 'Two-Compartment Cell' because it has only two repeating electrolyte streams excluding the electrode rinse solutions: 1) feed and 2) product. If an electrolyte solution is circulated through the cell and a direct current is applied across it, cations and anions migrate towards cathode and anode, respectively. This leads to an increase in the concentration of ions in the product compartments, while feed compartments simultaneously become depleted of ions. Since the reactions at anode and cathode produce equivalent amounts of protons and hydroxide ions, the rinse solutions of both the electrodes are often combined to maintain a uniform concentration of electrode rinse solution.

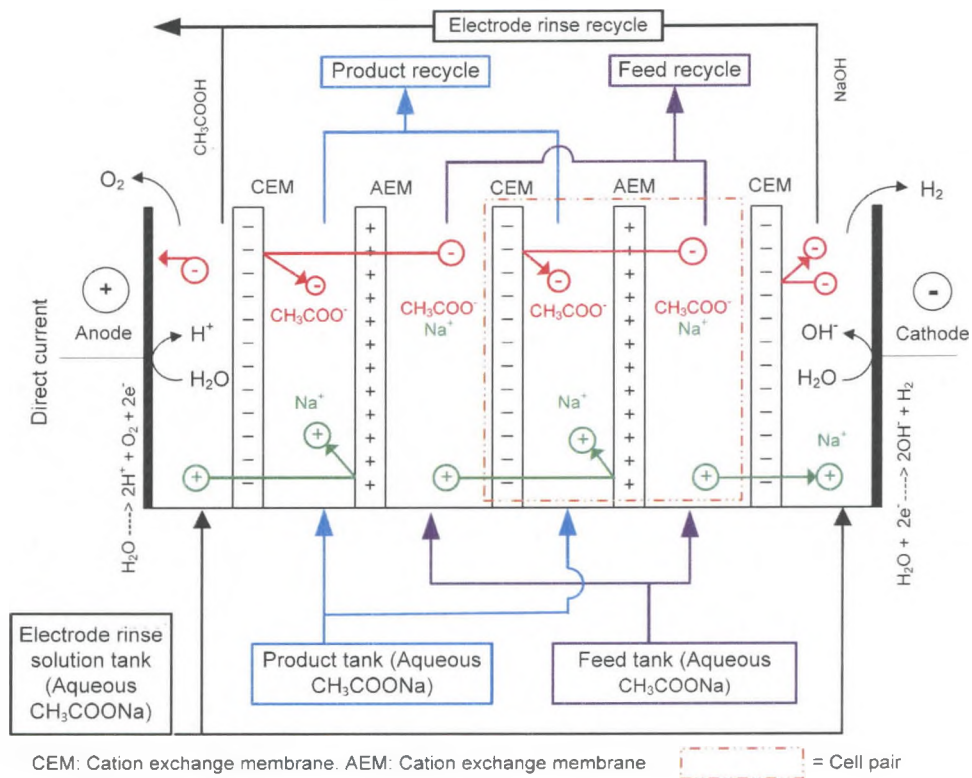


Figure 2.7 Working Principle for a Two-Compartment Electrodiolysis System Applied to Sodium Acetate Solution

The total space occupied by one feed compartment, one product compartment and the contiguous anion and cation-exchange membranes make up a cell pair. The cell pair is a repeating unit in an ED stack. An actual ED unit, which is also referred to as a stack, may have 1 to 600 cell pairs, depending upon the type of application. A typical ED stack containing “n” cell pairs is formed by “n+1” cation exchange membranes and “n” anion exchange membranes. The ED cell shown in Figure 2.7 contains two cell pairs applied to the concentration of aqueous sodium acetate solution. Although there are many different components necessary for the proper and efficient operation of an electrodiolysis plant such as the electrical power supply, pumps, and control and monitoring devices; the stack is the key element. Electrodiolysis system can be operated in either a feed and bleed mode, or alternatively in a batch or single pass recirculation mode.

The ED process is governed by Faraday’s law of electrolysis. According to this law, one Faraday (96,250 coulombs) of electricity reduces, or oxidizes, one equivalent of oxidizing agent at the cathode and one equivalent of reducing agent at the anode, respectively. This reaction corresponds to the transfer of Avogadro’s number (6.023×10^{23}) of electrons through wiring from the anode to the cathode. The electric current is:

$$I = \frac{Z_i \cdot F (V_F(0) \cdot C_{F,i}(0) - V_F(t) \cdot C_{F,i}(t))}{\eta \cdot t} \dots\dots\dots \text{Equation 2.1}$$

Where,

- I = Electric current (A)
- Z_i = Charge number of an ion “i”
- F = Faraday’s constant (A·s·equivalent⁻¹)
- C_{F,i} = Concentration of an ion “i” in feed solution (mol·m⁻³)
- V_F = Volume of feed solution (m³)
- η = Current efficiency (%)
- t = Time(s)

Alternatively, the electric current (I) can be obtained from the current density (i) and the surface area of the cell (A_{cell}).

$$I = A_{\text{Cell}} \cdot i \dots\dots\dots \text{Equation 2.2}$$

Where,

- A_{cell} = Total surface area of “n” number of membranes (m²)
- i = Current density (A·m⁻²)

2.3 Bipolar Membrane Electrodialysis - Introduction and Working Principle

A bi-polar membrane increases the rate of dissociation of water molecules and is used to convert salts into their corresponding acids and bases. BPMED is an electro-membrane process which converts aqueous salts into their corresponding acids and bases using electric energy [Strathmann, 2010]. The structure of a BPM is shown in Figure 2.8.

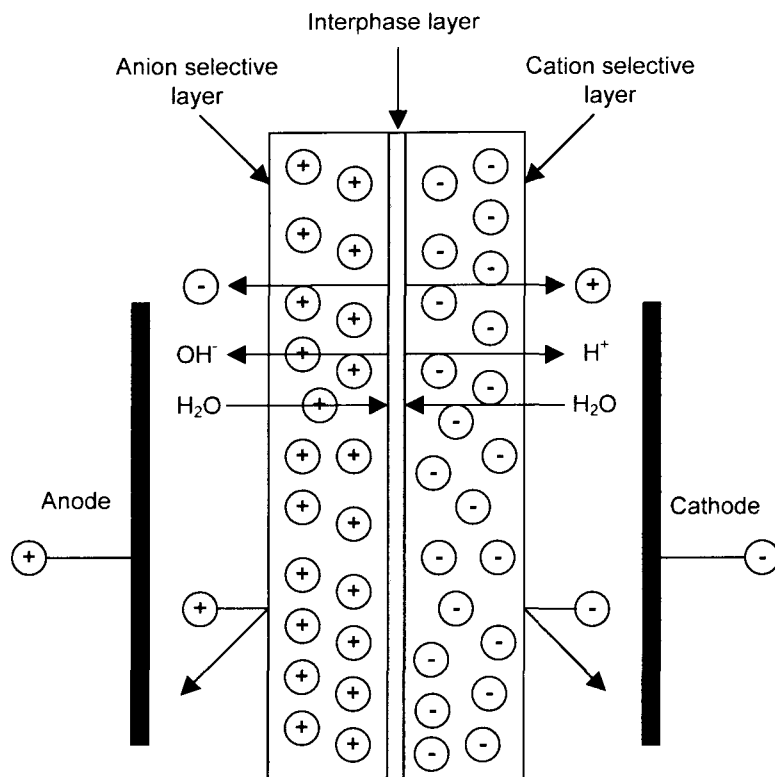


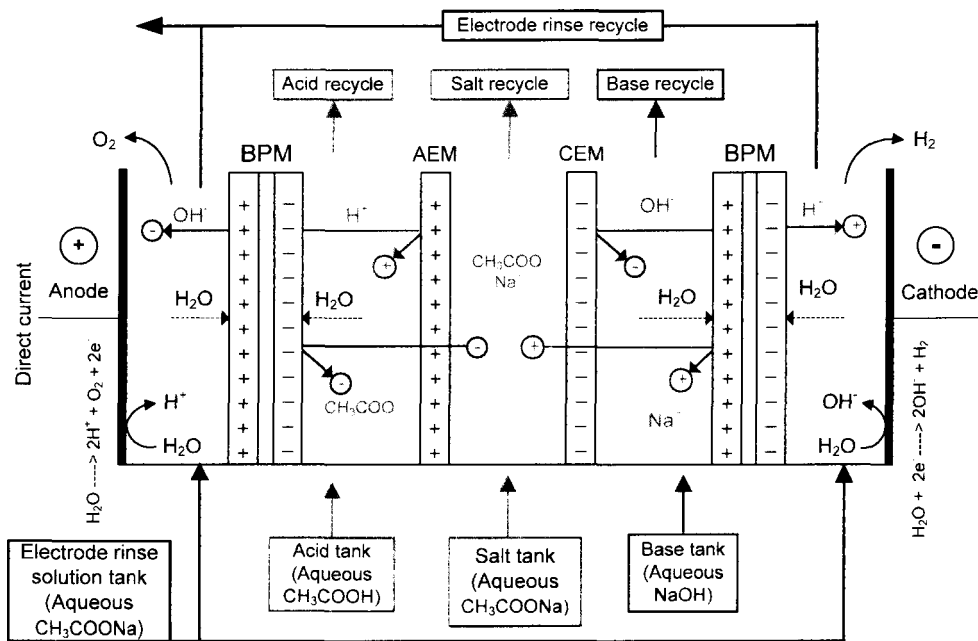
Figure 2.8 Structure of Bipolar Membrane

When an electric potential difference is applied across a BPM placed in an electrolyte solution and if the anion-selective layer of the BPM is facing towards the anode, most of the ions present in the interphase are quickly removed and only water will be left. The water in or at the membrane surface begins to dissociate when a critical current density is reached. Further transport of electrical current is accomplished by the flow of H^+ and OH^- ions generated due to the dissociation of water molecules present at the interphase. When these ions migrate across the BPM and combine with the corresponding ions of salt in the neighboring compartments, conjugate acids and bases are formed in different compartments. The rate of transport of H^+ and OH^- ions from the interphase into the outer phases depends upon the rate of diffusion of water into the interphase and also on the rate of formation of H^+ and OH^- ions, which is higher in a BPM as compared to the normal water.

Very high production rates of acids and bases can be achieved by using BPMED [Strathmann, 2000].

BPMED cells use BPM in combination with either CEM or AEM, or both (Figure 2.9). The salt solution is recirculated between the cation and anion exchange membranes. Under the action of the electric field, the water molecules present in the interphase of BPM dissociate into H^+ and OH^- ions and migrate into the compartments adjacent to the BPM. In addition, cations present in the salt compartment move across the cation exchange membranes and combine with the OH^- ions present in the base compartment to form the base. Similarly, anions present in the salt compartment move across the anion exchange membranes and combine with the H^+ ions present in the acid compartment to form the acid.

Three-compartment BPMED cells consist of three different fluid compartments: salt, acid and base. However, BPMED can be used to regenerate only acids, only base or both by using appropriate combinations of membranes.



CEM: Cation exchange membrane, AEM: Anion exchange membrane, BPM: Bipolar membrane

Figure 2.9 Working Principle of the Three-Compartment Bipolar Membrane Cell

2.3.1 General Process Guidelines for Bi-Polar Membrane Electrodialysis

Table 2.1 shows general process guidelines for the BPMED process [Mani, 1991]. The current density for the BPMED process is higher than that for conventional two-compartment ED (50-100 mA/cm² vs 20-40 mA/cm²) because of the current efficiency considerations. Therefore, in order to minimize the voltage drop across the cell, the minimum required conductivity of feed solution is higher for BPMED process.

Table 2.1 General Process Guidelines for BPMED Process

<p>Feed Salt Solutions Soluble salts Clear solution Conductivity > 35 mS/cm Multivalent Metals < 2 ppm Minimize high molecular weight products</p>
<p>Acid Products Caution with poor solubility acids Typical acid concentrations: 1-2 N for strong acids, up to 5 N for weak acids</p>
<p>Base Products Typical Concentrations: 2-5 N</p>
<p>General Conditions Temperature: up to 40 °C No oxidizing chemicals, organic solvents Current density: 50-100 mA/cm² Unit cell pair voltage: 1.3-1.9V (Two-compartment BPMED), 1.6-2.5V (Three-compartment BPMED) Expected membrane life: 1 year +</p>

2.4 Mass Transfer in Electrodialysis

The electrochemical flux of an ion is the sum of its diffusion flux, electrical migration flux and convection flux [Strathmann, 2010]. Equation 2.3 shows an expression for the electrochemical flux (J_i). Mass transport in ED is explained by using the extended Nernst-Planck equation.

$$J_i = -D_i \frac{dC_i}{dx} - D_i \cdot C_i \frac{Z_i \cdot F}{R \cdot T} \frac{d\Phi}{dx} + V_i \cdot C_i \dots \dots \dots \text{Equation 2.3}$$

Where

J_i = flux of an ion or molecule "i" through membrane (mol·m⁻²·s⁻¹)

D_i = Diffusion coefficient of an ion or molecule "i" (m²·s⁻¹)

- C_i = Concentration of ion or molecule "i" ($\text{mol}\cdot\text{m}^{-3}$)
- x = Directional co-ordinate (m)
- Z_i = Charge number of an ion "i"
- F = Faraday's constant ($\text{A}\cdot\text{s}\cdot\text{equivalent}^{-1}$)
- R = Gas constant ($\text{J}\cdot\text{mol}^{-1}\cdot\text{K}^{-1}$)
- T = Absolute Temperature (K)
- ϕ = Electric potential (V)
- V_i = Superficial velocity in "i" direction ($\text{m}\cdot\text{s}^{-1}$)

The first term on the right hand side (RHS) of Equation 2.3 represents mass transfer due to diffusion, the second term on the RHS represents migration due to electric potential gradient and the last term represents convection due to a pressure gradient, which is negligible in electrodialysis. The ionic mobility (u_i) of ionic species "i" is given by equation 2.4.

$$u_i = \frac{D_i \cdot Z_i \cdot F}{R \cdot T} \dots\dots\dots \text{Equation 2.4}$$

Where
 u_i = Ionic mobility ($\text{m}^2\cdot\text{s}^{-1}\cdot\text{V}^{-1}$)

Combining Equations 2.3 and 2.4 and neglecting the convection term from Equation 2.3 yields the basic differential equation governing ED:

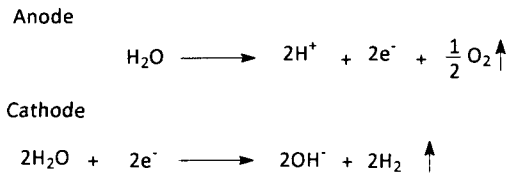
$$J_i = -D_i \frac{dC_i}{dx} - u_i \cdot C_i \frac{d\Phi}{dx} \dots\dots\dots \text{Equation 2.5}$$

Equation 2.5 illustrates that the flux of an ionic species in an ED cell as it moves across a semi-permeable membrane results from both diffusion and movement of the ion in an applied electric field. Often the flux due to the electric field predominates and pushes the ionic species up a concentration gradient from a low concentration to a high concentration.

In order to apply an electrical potential across an electrolyte solution, it must be in contact with two anode and cathode on either sides. At the surfaces of both electrodes, electrical conductance is converted into ionic conductance by an electrochemical reaction. Under the action of an electric potential, migration of cations and anions constitutes the electric current. When anions move towards the anode, they become oxidized at its surface

and release electrons to the electrode. Similarly, cations move towards the cathode and receive electrons from the electrode. At the anode, water is oxidized into proton (H⁺) and oxygen gas; while at the cathode, water is reduced to give hydrogen gas and hydroxyl ion (OH⁻).

Electrode Reactions



Since the reactions at anode and cathode produce equivalent amounts of H⁺ and OH⁻ ions, the electrode rinse streams for both electrodes are often combined to maintain a uniform concentration in the electrode rinse compartment.

In electro dialysis, current is carried by the flow of ions. The current density (i) is the amount of current flowing per unit surface area of the membrane [Strathmann, 2010].

$$I = A_{\text{membrane}} \cdot i = \frac{V_{\text{stack}}}{R_{\text{stack}}} = F \sum_i Z_i \cdot J_i \cdot A_{\text{membrane}} \dots\dots\dots \text{Equation 2.6}$$

- Where
 A_{membrane} = Surface area of one membrane (m²)
 V_{stack} = Voltage drop across an electro dialysis cell (V)
 R_{stack} = Resistance of an electro dialysis cell (ohms)

Inserting Equation 2.3 into Equation 2.6 gives

$$I = F \cdot A_{\text{membrane}} \sum_i \left[Z_i \cdot \left(-D_i \frac{dC_i}{dx} - D_i \cdot C_i \frac{Z_i \cdot F}{R \cdot T} \frac{d\Phi}{dx} + V_i \cdot C_i \right) \right] \dots\dots\dots \text{Equation 2.7}$$

2.4.1 Donnan Exclusion Phenomenon

In order to improve the efficiency of the electro dialysis process, ion exchange membranes must be impermeable to co-ions. Although, most of today’s commercially

available membranes meet this requirement, the impermeability to co-ions can also be affected by the concentrations of electrolyte solutions in contact with these membranes. The effect of electrolyte concentration on the permeability of co-ions into the ion exchange membranes (or the concentration of co-ion in an ion exchange membrane) is governed by the Donnan equilibrium.

According to the Donnan equilibrium, as the concentration of electrolytic solution becomes higher than that of ion exchange groups in the membrane, an electrochemical gradient is established between the solution and the membrane. This gradient results in an increased flow of all types of ions towards the surface of membrane. If the magnitude of the gradient increases significantly, the membrane can no longer prevent co-ions from entering into it. Thus, the concentration of co-ions in an ion exchange membrane is governed by the concentration of the electrolyte solutions in contact with it.

The mathematical expression for the Donnan equilibrium is derived from Equation 2.3, the extended Nernst Planck equation [Tanaka, 2010]. In Equation 2.8, X and Y represent the cation and anion of salt molecules, respectively.

$$C_X^{u_X} \cdot C_Y^{u_Y} = C_{M,X}^{u_X} \cdot C_{M,Y}^{u_Y} \dots\dots\dots \text{Equation 2.8}$$

Where

C_i = Concentration of ion "i" in an electrolyte solution or a membrane (mol·m⁻³)

u_i = Number of moles of ions in one molar solution of an electrolyte "i"

X, Y = Cations and anions of a salt molecule

M = Membrane

Figure 2.10 shows the effect of concentration of electrolyte on the ratio of concentrations of co-ion and counter ion in a cation exchange membrane for two different ion exchange membranes with fixed group concentrations of 4 and 8 equivalents per liter, respectively. When the electrolyte concentration is lower than that of fixed groups in the membrane, most co-ions are excluded from the membrane and it is perfectly selective

towards counter-ions. This phenomenon is called the Donnan exclusion principal. However, as the concentration of the electrolyte solution becomes higher than the concentration of fixed groups in the membrane, a greater amount of co-ions migrate into the membrane and the selectivity towards counter-ions is rapidly reduced.

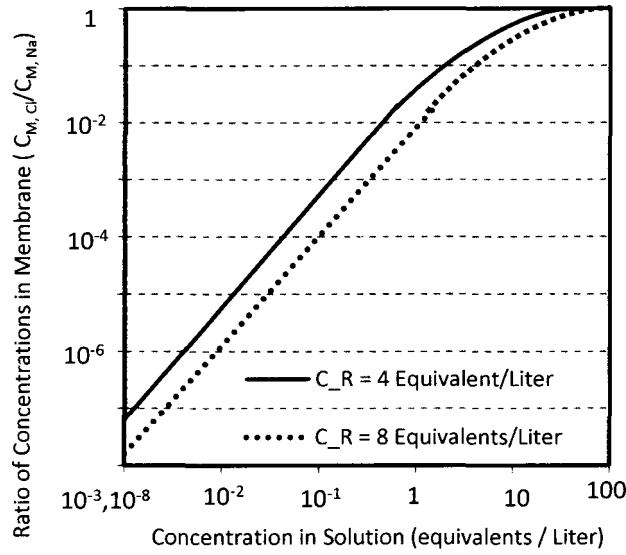


Figure 2.10 Donnan Equilibrium in a Cation Exchange Membrane for Sodium Chloride

2.5 Parameters Affecting the Performance of Electrodialysis Equipment

The performance of electrodialysis equipment is affected by several factors, such as the chemical nature of the membranes, concentrations of feed and product, current, voltage and flow velocities.

2.5.1 Current Density and Voltage

Current density is the major driving force in ED because it determines the quantity of equivalents of salt transported across the membranes. For a given separation process, the use of high current density requires less membrane area and processing time, thus potentially making the process economically more attractive. However, at higher current density, the specific energy consumption increases because of an increase in the

thermodynamic irreversibility of the process [Walker, 2010]. So, there is a trade-off between electric energy cost and membrane cost.

Most electrodialysis equipment is operated using constant voltage or constant current or a combination of both these modes. In constant voltage mode, a constant voltage drop is maintained across the stack and the current varies with time; whereas in constant current mode, a fixed current density (usually, up to 80% of limiting current density) is applied and the voltage is allowed to vary to maintain the fixed current density.

2.5.2 Current Efficiency

In ED, current can be lost because of several factors such as: (1) non-perfect permselectivity or the transfer of undesirable ions, (2) the passage of current through non-active surfaces of the spacer, which do not come into contact with electrolyte solutions and (3) diffusion and back-diffusion of ions/molecules. Thus, the overall current efficiency is always less than 100%.

The current efficiency (η) for forming (or transferring or splitting) a given mass of an electrolyte (M) is the ratio of the theoretical ($C_{Theoretical}$) and the actual (C_{Actual}) charges required to form the same mass of the electrolyte.

$$\eta = \frac{C_{theoretical}}{C_{actual}} = \frac{M \cdot F}{E \cdot N \cdot C_{actual}} \cdot 100 \dots\dots\dots \text{Equation 2.9}$$

Where,
 E = Molecular weight (gm)
 N = Number of cell pairs

$$C_{actual} = \int_0^t I \cdot dt \dots\dots\dots \text{Equation 2.10}$$

Where,
 t = time (sec)

2.5.3 Flow Velocity

The flow conditions can significantly affect the performance of an ED system. Figure 2.11 shows the approximate inter-membrane velocity and concentration profile in an ED cell pair [Walker, 2010].

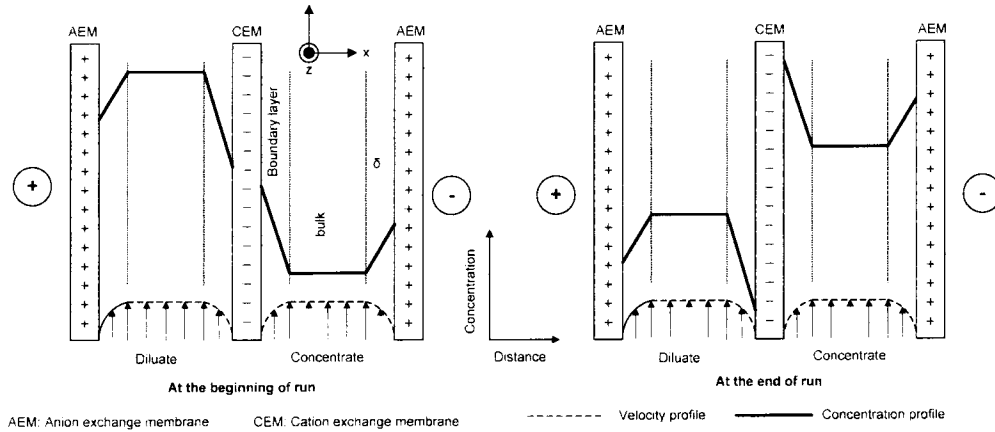


Figure 2.11 Velocity and Concentration Profiles in Electrodesialysis Cell

Superficial velocities (v_i) in the feed and product streams are calculated according to the following formula.

$$v_i = \frac{Q_i}{N_{CP} \cdot t_{\text{spacer}} \cdot w_{\text{spacer}}} \dots\dots\dots \text{Equation 2.11}$$

Where,
 t_{spacer} = Thickness of a spacer (m)
 w_{spacer} = Width of a spacer (m)
 Q_i = volumetric flow rate ($\text{m}^3 \cdot \text{s}^{-1}$)
 i = F, P, ED (F: Feed, P: Product, ED: Rinse solution)

2.5.4 Concentration Polarization

In ED, electrolytes are continuously removed from the feed compartment through neighboring membranes. Thus, the salt concentration in the bulk of the feed compartment is always higher than that of the membrane surfaces in contact with feed solution (Figure 2.12).

Similarly, the salt concentration in the bulk of the product compartment is lower than that of membrane surfaces in contact with it. Accordingly, the electrolyte concentration profile (x-direction) is assumed to be a constant concentration within the well mixed bulk and linear within the boundary layer. A concentration difference between the two sides of the membrane is called "concentration polarization". The x-directional concentration gradient in the diffusion boundary layer is approximately proportional to the applied current density in x-direction [Walker, 2010].

$$\frac{\Delta C_{BL}}{\delta} \propto i \dots\dots\dots \text{Equation 2.12}$$

Where,
 ΔC_{BL} = Concentration difference across boundary layer (mol·m⁻³)
 δ = Thickness of the boundary layer (m)

Figure 2.12 shows the fluxes and concentration profile across a cation exchange membrane [Strathmann, 2010]. The symbols J and C represent the flux and concentrations, respectively. The superscripts F, P, Mig, Diff, B and M denote feed, product, electro-migration, diffusion, bulk phase and membrane surface, respectively. The subscripts "-", "+", and S represent anion, cation and salt, respectively.

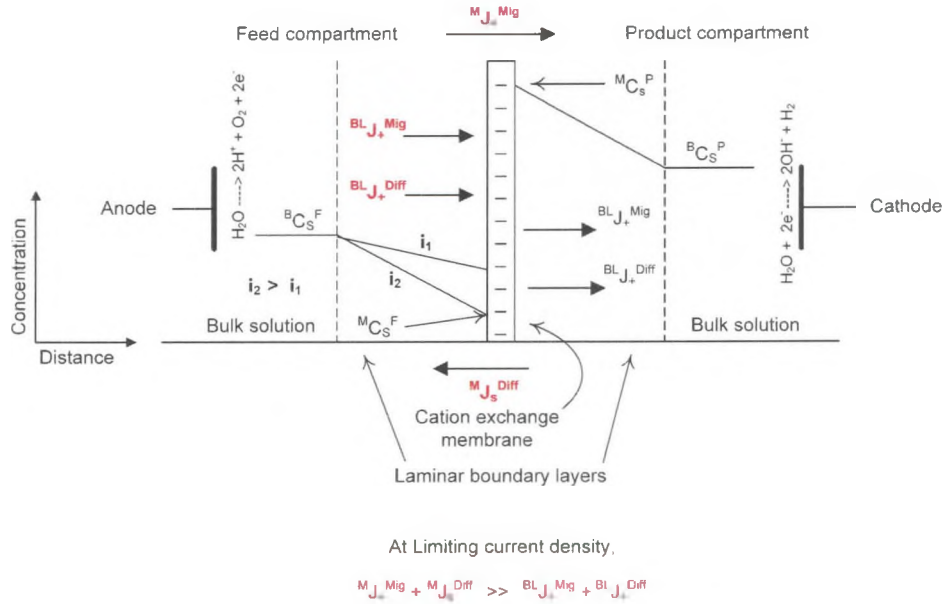


Figure 2.12 Fluxes and Concentration Profiles across a Cation Exchange Membrane

Near the surface of the cation exchange membrane which is in contact with the boundary layer of the feed compartment, cations migrate into the membrane; and thus, their concentration in the solution gets reduced. Since anions migrate in the opposite direction, their concentration in the feed solution near the surface of the membrane is also reduced and a concentration gradient is established between the bulk phase and the membrane surface.

This concentration gradient then leads to the diffusive transport of cations towards the membrane surface. The overall cation concentration in the boundary layer is a function of the migration and diffusion fluxes. A steady state is reached when the sum of diffusive and migrational transport of cations through the boundary layer ($BL_{J_+}^{Mig} + BL_{J_+}^{Diff}$) is balanced by the sum of the migration and diffusion fluxes of cations through the membrane ($M_{J_+}^{Mig} + M_{J_+}^{Diff}$) due to the applied current density.

Because of the presence of ion exchange groups in the membrane, the migration flux through the membrane ($M_{J_+}^{Mig}$) is higher than that through the boundary layer ($BL_{J_+}^{Mig}$). Both types of migration fluxes increase with the applied current density; and at certain

current density, the net mass transfer through membrane ($M_{J+}^{Mig} + M_{J-}^{Diff}$) becomes higher than the net mass transfer through boundary layer ($^{BL}J_{+}^{Mig} + ^{BL}J_{+}^{Diff}$).

Thus, the feed concentration on the surface of membrane ($^{M}C_{s}^F$) starts to drop. If the current density increases beyond a specific limiting value, $^{M}C_{s}^F$ instantaneously reduces to zero. This value of current density is called the limiting current density for the given electrolyte concentration and the velocity.

2.5.5 Limiting Current Density

The limiting current density is the maximum current that can be sent through an ED cell without any adverse effects. If the applied current is higher than the limiting current density, then the feed boundary layer in contact with the membrane and the corresponding membrane surfaces become depleted of electrolyte and it in turn leads to an increase in the resistance of the feed compartment, an increase in the energy consumption, the dissociation of water at the membrane surface and a change in the pH of the feed. As shown in Figure 2.13, water dissociation in the feed compartment leads to the formation of OH^{-} and H^{+} ions on the surfaces of cation and anion exchange membranes in contact with feed solutions, respectively [Krol, 1997]. If the OH^{-} ion concentration on the surface of membrane exceeds the maximum allowed limit, it can damage the membrane.

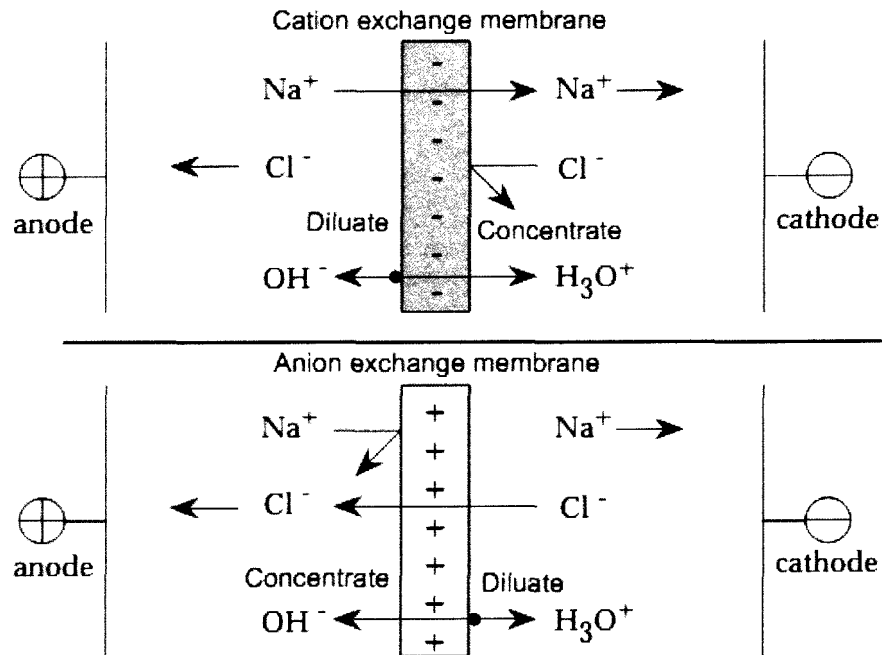


Figure 2.13 Water Dissociation at the Surface of the Ion Exchange Membrane at the Limiting Current Density for Sodium Chloride

The limiting current density is a function of electrolyte concentration, solution velocity and membrane properties. The limiting current is reached when the salt (or counter-ion) concentration at the surface of a membrane becomes 0; that is when $M C_s^F$ in Figure 2.12 becomes 0.

For practical applications, limiting current is determined by measuring current as a function of the applied voltage across a single membrane or an ED stack for different feed concentrations (Figure 2.14). The limiting current density is reached when the slope of this line changes.

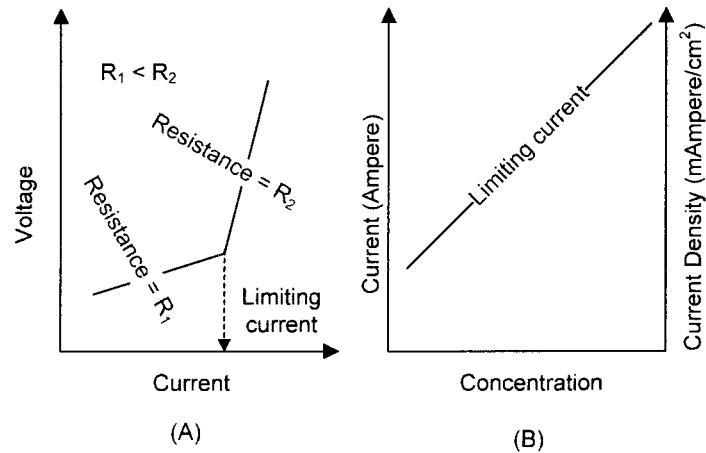


Figure 2.14 Limiting Current (A) and Current Density vs Feed Concentration (B)

Measurements with multi stack usually do not show a clear change in the resistance when the limiting current is reached [Strathmann, 2004]. Therefore, Cowan and Brown (1959) determined the limiting current density by plotting the overall resistance versus the reciprocal of the current density. Additionally, a change in the pH of the feed solution can be used to determine the limiting current density.

2.5.6 Water Transport across Membranes

Water transport can occur across any membrane by three mechanisms: 1] a convective flux due to the pressure gradient across the membrane, 2] an osmotic flux due to the concentration gradient across the membrane and 3] an electro-osmotic flux due to coupling of water molecules along with the ions transported through the membranes. Each of these mechanisms can be the dominant mechanism depending upon the type of membrane, concentration difference across the membrane and the applied current density.

Electro-osmosis is predominant at higher current densities and the flux of water is proportional to the flux of ions being transferred. It also depends upon membrane and

electrolyte size, valence and ion concentration. Usually, 4 to 10 moles of water are transported for each mole of the salt being separated [Strathmann, 2010].

Osmosis is more evident at lower current densities where the rate of separation of salt is very low, and also when the electrolyte concentration difference across the membrane is high [Walker, 2010].

Since inter membrane pressure in ED is zero, water transport by convection is negligible. The amount of water transported by osmosis and electro-osmosis can be calculated by performing a regression analysis on the rates of water transported at different voltages and different concentrations [Walker, 2010].

Water transport across the membrane is not beneficial for the two reasons. Firstly, it limits the maximum achievable product concentration. Secondly, it decreases the amount of purified water produced during the desalination process.

2.5.7 Feed and Product Compositions

Feed and product compositions (or conductivity) must be maintained within pre-determined limits. Any concentration outside these limits can decrease the efficiency of the process. Criteria for optimization of these concentrations are discussed in next section.

2.6 Electrodialysis Process Costs

The total cost of an ED system is the sum of fixed costs and operating costs. Both of these costs are affected by feed and product concentrations, plant capacity and overall process design.

2.6.1 Fixed Investment Costs

The investment costs are mainly estimated by using the required membrane area for the desired plant capacity. The capital costs of the remaining items such as pumps and process control equipment are considered as being proportional to the required membrane area. The required membrane area for a particular process will depend upon total current

necessary for the removal of a fixed number of ions and the applied current density. Membrane area is estimated using Faraday's law. The total current is estimated using the inlet and outlet concentrations of feed and its volumetric flow rate. As discussed earlier, the applied current density is calculated using the limiting current density, which can be either obtained from the manufacturer or estimated manually. The fixed cost of the equipment is converted to a yearly operating cost from the depreciation.

2.6.2 Operating Costs

In addition to the fixed charges associated with the capital investment (i.e. depreciation, interest and taxes), the major operating costs are the cost of energy and maintenance costs. Maintenance costs are proportional to the size of the process and are estimated as a certain percentage of the investment-related costs. The energy required in an ED system occurs in two forms: 1) electrical energy required for transferring and splitting salts and 2) the hydraulic energy required for circulating solutions through the cell. Since more than 200 cell pairs are commonly present between two electrodes, the energy loss due to electrode reactions can be neglected. The energy required for operating the control systems can also be neglected [Strathmann, 2010].

The electric energy can be calculated from the equation below,

$$E_{elec} = \int V_{stack} \cdot I \cdot dt = \int R_{stack} \cdot I^2 \cdot dt \dots\dots\dots \text{Equation 2.13}$$

Where,
 E_{elec} = Electrical energy (A·V·s)
 t = Time (s)

The hydraulic energy required to pump electrolytic solutions through stack can be calculated as,

$$E_{hyd} = \int \rho \cdot g \cdot (Q_F \cdot \Delta H_F + Q_P \cdot \Delta H_P + Q_{ED} \cdot \Delta H_{ED}) dt \dots\dots\dots \text{Equation 2.14}$$

Where,
 E_{Hyd} = Hydraulic energy (A·V·s)
 ρ = Density (kg·m⁻³)

- g = Gravitational constant ($m \cdot s^{-2}$)
- Q_F = Volumetric flow rate of feed solution ($m^3 \cdot s^{-1}$)
- Q_P = Volumetric flow rate of feed solution ($m^3 \cdot s^{-1}$)
- Q_{ED} = Volumetric flow rate of feed solution ($m^3 \cdot s^{-1}$)
- ΔH_F = Head loss for feed solution (m)
- ΔH_P = Head loss for product solution (m)
- ΔH_{ED} = Head loss for ED rinse solution (m)

Electrical energy consumption is directly proportional to the square of current. Whereas, the amount of salt transferred is directly proportional to the current. Hence, for a given processing rate, the energy requirement exponentially increases with increase in the current density. The electric migration flux of ions and the rate of dissociation of water in bipolar membranes increase with an increase in the current density and thus, less membrane area is required for a given process. Similarly, as current density is lowered, the electric energy cost decreases and more membrane area is required.

Thus, for a fixed processing rate, there is a trade-off between membrane cost and the energy costs as a function of current density. At a certain current density, the total cost reaches a minimum value (Figure 2.15).

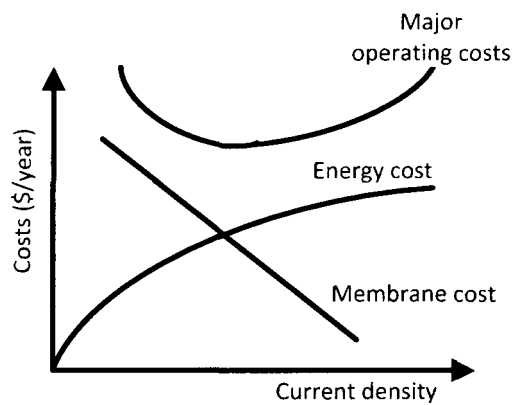


Figure 2.15 Major costs in Electrodialysis as a Function of Applied Current Density

2.7 Optimization of Electrodialysis Process

The efficiency of the ED process can be improved by decreasing the resistance of the stack. This can be done by; (1) by using membranes with lower electric resistances and electrolyte solutions with high conductivity and (2) by increasing the velocity to decrease the boundary layer thickness.

The total resistance of the stack is the summation of the resistances of all cell pairs and the electrode rinse solutions. As shown in Figure 2.11, each cell pair is composed of eight electrically independent resistances: 1) the feed diffusion boundary layer next to the CEM, 2) the CEM, 3) the product diffusion boundary layer next to the CEM, 4) the bulk product, 5) the product diffusion boundary layer next to the AEM, 6) the AEM, 7) the feed diffusion boundary layer next to the AEM and 8) the bulk feed.

The area resistances of most ion exchange membranes are available in the literature [Xu, 2005 and Strathmann, 2010]. Typical values are in the range of 1-10 $\Omega\text{-cm}^2$. Resistances of electrolytes are function of their conductivities;

$$R_{\text{electrolyte}} = \frac{w_{\text{spacer}}}{k_{\text{electrolyte}}} \dots\dots\dots \text{Equation 2.15}$$

Where,

$R_{\text{electrolyte}}$ = Resistance of an electrolyte compartment (Ω)

$k_{\text{electrolyte}}$ = Electrical conductivity of an electrolyte solution ($\Omega^{-1}\text{m}^{-1}$)

2.7.1 Optimization of Feed Composition

According to the Donnan exchange equilibrium, if the concentration of the feed or product becomes higher than the concentration of ion exchange groups in the membrane, then the co-ion concentration in membrane increases and the membrane will lose its selectivity towards counter-ions [Tanaka, 2010]. Therefore, the concentration of electrolyte should always be slightly less than that of ion exchange groups in the membrane. Although, the Donnan equilibrium fixes the upper limit for feed and product compositions, the

electrolyte compositions are also affected by other parameters. These parameters need to be optimized to improve mass transfer in electrodialysis.

For most processes, the inlet feed composition is fixed. However, this composition may not be optimum for ED processes.

If the inlet feed composition is very low, it limits the maximum current that can be applied to the membranes. With a decrease in the applied current density, the rate of transfer of ions across the membranes and the specific electrical energy are also reduced. Thus, in order to achieve an acceptable rate of separation of salt, more membrane area is required.

Whereas, if the concentration of inlet feed is high or feed is pre-concentrated prior to the ED process, a higher current density can be applied. This in turn increases the rate of transfer of salts across membranes and the specific electrical energy consumption. Thus, the membrane area requirement decreases.

Therefore, as explained previously, there is a trade-off between membrane area and electric energy consumption. The optimum conditions can be determined by evaluating the total operating costs as a function of current density or inlet feed concentration (Figure 2.15)

2.7.2 Optimization of Product Composition and Solubility Limits

The maximum obtainable concentration of the product stream is limited by the current efficiency and precipitation of salt.

Some electrolytes, such as divalent salts, have very low solubility in water; for example CaSO_4 and Ca(OH)_2 . Since ED systems must be free of suspended solids, divalent salts can be concentrated only up to their solubility limits.

As an ED process progresses, the concentrations of product and feed solutions start to increase and decrease, respectively. Because of an increase in the concentration difference between two compartments, ions and molecules from the product compartment start to diffuse back into the feed compartment. This phenomenon is called 'back-diffusion'

and it decreases the current efficiency because of the additional current required to transfer the back-diffused ions again into the product compartment [Luo, 2004]. This effect is illustrated in Figure 2.16 where MX, HX and MOH are salt, acid and base, respectively. As shown in the figure, both ionized and unionized species can diffuse in any direction depending upon the concentration gradient. Some of these diffusion pathways result in the transfer of product back into feed and other compartment and thus, the efficiency of electrodialysis is reduced because additional charge is needed to transfer these species into the product compartment once again.

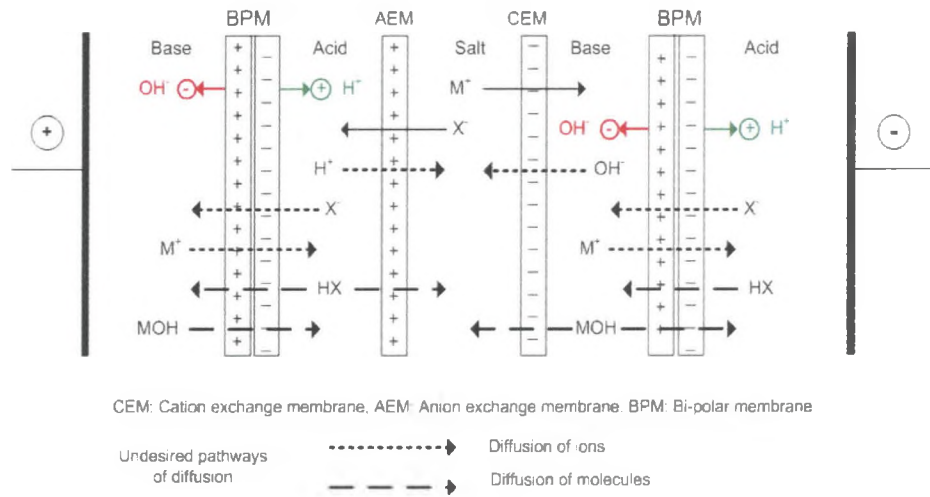


Figure 2.16 Back Diffusion of Ions and Molecules in Bi-Polar Membrane Electrodes

In some cases, where the solubility of the product streams is high and back diffusion is low, the product concentration can be up to 20 times the feed concentration. This concentration factor is much higher than that for reverse osmosis and thus, ED is used to concentrate and produce table salts.

In ED, high product concentrations can be achieved by recycling the product back into the system until the limiting concentration ratio is reached or visible salt precipitation occurs [Walker, 2010]. An increase in concentration of the product stream reduces its electrical resistance and thus, helps to increase the current density.

2.7.3 Controlling Flow Rate

Since ED spacers have complicated structures, it is difficult to estimate the true velocity in the volume between the spacers and thus, the superficial velocity is used in most calculations. Operating at low velocities results in lower pressure drops across the cells and decreased pumping cost.

Pumping costs increase with increased velocity. Higher velocities improve mass transfer through ion exchange membranes by reducing the thickness (δ_i) of the diffusion boundary layer (see Figure 2.12). Reduction in the boundary layer thickness in turn decreases the electrical resistance of the stack, increases current density, and improves current efficiency.

It has been shown that, for a laboratory scale ED apparatus similar to that being used in this study, the pumping cost was only 6% of total specific energy even at a high superficial velocity of 4.8 cm/s [Walker, 2010]. The same effect can be expected in the present work regardless of the type and the concentration of electrolyte being used. Hence, all experiments in the present work were carried out at high superficial velocity.

2.7.4 Preventing Scaling and Fouling of Membranes

In applications with clean feed and low current densities, membrane life can reach several years. For example, membrane life can be as high as ten years for removal of nitrate ion from drinking water. For a given current density, the voltage drop across the cell increases over time as membranes become chemically affected or fouled by the contaminants in the solution. Even with 'clean' solutions, membranes will eventually lose active sites through their polymeric structure.

Membrane fouling can be caused by many impurities in feed solutions such as organic matter, microorganisms and colloidal substance which can be either soluble or insoluble in the feed. Pre-treatment using micro-filtration, ultra-filtration or ion exchange can be helpful to remove some of these impurities.

Scaling and fouling can also be reduced by: 1) adding acid or alkali to control the pH to prevent precipitation in the electrolyte compartments, 2) reversing polarity of electrodes and thus, interchanging feed and product compartments, which in turn re-dissolves salts deposited on the surface of membranes, and 3) by the use of anti-scaling agents which function by forming water soluble chemical complexes with the salts.

2.8 Electrodialysis Process Performance Indices

By contrast with BPMED which is involved in salt splitting, ED involves increasing the concentration of the salt and in some cases, separating impurities from a product.

2.8.1 Separation Factor

The technical feasibility of the ED process depends upon its ability to remove a given ion from the feed solution. The extent to which an ion is removed from the feed is quantified by the ‘Separation Factor (SF)’, which is a measure of the chemical efficiency of the system and is dimensionless.

$$SF_i = \frac{V_f(0) \cdot C_{F,i}(0) - V_f(t) \cdot C_{F,i}(t)}{V_f(0) \cdot C_{F,i}(0)} \dots\dots\dots \text{Equation 2.16}$$

Where,
 SF_i = Separation factor for an ion “i”

2.8.2 Selectivity and Relative Number of Moles of Salt Transported

The degree to which a desired ion is selectively removed from the feed solution is also a measure of the efficiency of the ED system. Conventional selectivity (S) is defined as the ratio of the molar flow rate of the desired product to that of an undesired product.

$$S = \frac{\text{Exit molar flow rate of desired product}}{\text{Exit molar flow rate of undesired product}} = \frac{V_p(t) \cdot C_{P,i}(t)}{V_p(t) \cdot C_{P,j}(t)} \dots\dots\dots \text{Equation 2.17 a}$$

However, selectivity is not useful when a reaction system leads to the formation of more than one undesired product. In such cases, ‘relative number of moles of each species

transported (or split)' is more useful and it is defined as the ratio of the number of moles of a given salt transported across the membranes to the total moles of all salts transported in the same direction (Equation 2.17 b).

$$RM_i = \frac{V_F(0) \cdot C_{F,i}(0) - V_F(t) \cdot C_{F,i}(t)}{V_F(0) \cdot C_F(0) - V_F(t) \cdot C_F(t)} \dots\dots\dots \text{Equation 2.17 b}$$

Where,

RM_i = Relative number of moles of a given salt transported across membranes or split

C_F = Total concentration of all ions present in feed solution (mol·m⁻³)

2.8.3 Flux

The flux (J_i) of an ion or a molecule through an ion exchange membrane indicates the amount of a particular ion or molecule transferred from feed to product per unit time per unit surface area of the membranes.

$$J_i = \frac{V_F(0) \cdot C_{F,i}(0) - V_F(t) \cdot C_{F,i}(t)}{A_{\text{membrane}} \cdot N_{CP} \cdot t} \dots\dots\dots \text{Equation 2.18}$$

where,

J_i = Flux of an ion or molecule "i" through membrane (mol·m⁻²·s⁻¹)

N_{CP} = Number of cell pairs in an electrodialysis cell

2.8.4 Specific Electrical Energy

Specific electrical energy (E_{Elec, spec}) represents the amount of energy required for transferring a unit equivalent of a desired electrolyte "i" from the feed to the product compartment.

$$E_{\text{elec, spec}} = \frac{E_{\text{elec}}}{V_F(0) \cdot C_{F,i}(0) \cdot SF_i} \dots\dots\dots \text{Equation 2.19}$$

Where,

E_{elec, spec} = Specific electrical energy (A·V·s·mol⁻¹)

2.8.5 Current Efficiency

The electrical current efficiency (η) is discussed in section 2.5.2.

2.8.6 Overall Water Transport Index

The "Overall Water Transport Index" (OWTI) refers to the moles of water transferred into the product compartment per equivalent of salt transferred or acid or base formed in the same compartment.

$$OWTI_i = \frac{\rho_{\text{solution}} \cdot (V_F(0) - V_F(t)) - (V_F(0) \cdot C_F(0) - V_F(t) \cdot C_F(t)) \cdot MW_{\text{Na-Acetate}}}{(V_F(0) \cdot C_F(0) - V_F(t) \cdot C_F(t)) \cdot 18} \dots\dots\dots \text{Equation 2.20}$$

Where,

OWTI_i = Overall water transport index of an ion i

MW_{Na-Acetate} = Molecular weight of sodium acetate

2.9 Literature Data - Separation & Splitting of Sodium Acetate using Electrodialysis

Table 2.2 and 2.3 summarize literature data on separation of sodium acetate and acetic acid using two-compartment electrodialysis systems.

Narebska (2001) determined the diffusion flux of 0.2M to 1.2M acetic acid, lactic acid and propionic acid solution into water, which was an approximate representation of experimental conditions. Acetic acid was the most permeable compared to the other acids, probably because of its smaller size. The diffusion flux of acetic acid was about 0.1 to 1 moles per m² of membrane area per hour, depending upon the type of membrane and the solution concentration. The diffusion flux of acetic acid was comparable with Chukwu's (1999) experimental data. The diffusion of acetic acid was lowest (0.25 mol/m²/hour) for Neosepta AMX membranes as compared to other Neosepta membranes. Narebska also determined the osmotic flux for water into 0.75 to 1M acetic acid solution through different types of Neosepta membranes. Neosepta AMX was the most resistive against osmotic permeation of water with a flux of 2 moles of water/m²/hour.

Table 2.4 presents literature data on the splitting of sodium acetate using bi-polar membranes. Kassotis and co-workers (1984) converted about 6 wt% solution of sodium

acetate solution into 35 wt% acetic acid and about 8 wt% sodium hydroxide using a three-compartment BPMED cell at a current density of 109 mA/cm². In another lab-scale study using a three-compartment cell, about 4 to 12 wt% solution of sodium acetate was converted into 8 to 12 wt% acetic acid solution [Trivedi, 1997]. The membranes used in this study were synthesized using ion exchange resins. Eurodia Industry commissioned a two-compartment pilot scale BPMED unit which converted a by-product stream of 22 wt% sodium acetate into 18 wt% acetic acid and 6 wt% sodium hydroxide. The current efficiency was optimum and the payback period was of less than two years [Bar, 2006]. No studies were located on the decomposition of significantly high quantity of alkaline hardwood extract with a low concentration of sodium acetate.

Table 2.2. Literature Data on Separation of Sodium Acetate and Acetic Acid using Electrodialysis

Author (year)	Superficial velocity (cm/s)	Membrane		Variation in concentrations*		Number of cell pairs	Current/ Voltage		Energy (A·V·hr·mol ⁻¹)	Flux (mol·m ⁻² ·hr)	Current efficiency (%)	OWTI	Comments
		Type	Area cm ²	Feed	Product		Mode	Value					
Kassotis (1984)	--	CMV, AMV (Aashi glass)	--	48 g/L CH ₃ COOH	48 - 198 g/L CH ₃ COOH	1	Constant current	17.3 mA/cm ²	--	--	96 To 53	--	Although Aashi glass membranes were better than IONAC, the extent of back diffusion of acetic acid was substantial. The flux due to back diffusion was equivalent to the current density of 15 mA/cm ² , which was very close to the applied current density
	--	Ionac	--	48 g/L CH ₃ COOH	6 - 49 g/L CH ₃ COOH	1	Constant current	20 mA/cm ²	--	--	27	--	
Nomura (1988)	---	ACH-45 T, CH-45 T	200	0 - 24 g/L CH ₃ COOH pH:3.8 or higher	0 - 57 g/L CH ₃ COOH	1	Constant current	5 mA/cm ²	---	0.9	---	3.4	Used electrodialysis for in-situ removal of CH ₃ COOH at the pH of 3.8 or higher for 72 hours.
Nomura (1989)	----	(Neosepta)	410	0 - 24 g/L CH ₃ COOH pH:3.8 or higher	0-150 g/L CH ₃ COOH	2	Constant current	3.7 mA/cm ²	---	1.18	--	---	Used electrodialysis for in-situ removal of CH ₃ COOH at the pH of 3.8 or higher for 30 days.
Zhang (1994)	13.9	A-201, K-101 (Aashi glass)	150	12 - 24 g/L CH ₃ COOH pH:2 - 10	20 - 60 g/L CH ₃ COOH	1	Constant voltage	15 V 27-86 mA/cm ²	--	36-32	100-75	---	Studied ED transfer of mixture of CH ₃ COOH and KH ₂ PO ₄ (1% mole) over the pH range of 2-10. Used NaOH to adjust pH. Current efficiency and flux was highest for pH 4.5-5.5, near the pKa of CH ₃ COOH.

*: Variations in the concentrations include maximum and minimum concentration during the experiment.

Table 2.3. Literature Data on Separation of Sodium Acetate and Acetic Acid using Electrodialysis

Author (year)	Superficial velocity (cm/s)	Membrane		Variation in concentrations*		Number of cell pairs	Current/ Voltage		Energy (A·V·hr·mol ⁻¹)	Flux (mol·m ⁻² ·hr)	Current efficiency (%)	OWTI	Comments
		Type	Area cm ²	Feed	Product		Mode	Value					
Zhang (1994)	13.9	A-201, K-101 (Aashi glass)	150	12 - 24 g/L CH ₃ COOH pH:2 - 10	20 - 60 g/L acetic acid	1	Constant voltage	15 V 27-86 mA/cm ²	--	36-32	100-75	---	Studied ED transfer of mixture of CH ₃ COOH and KH ₂ PO ₄ (1% mole) over the pH range of 2-10. Used NaOH to adjust pH. Current efficiency and flux was highest for pH 4.5-5.5, near the pKa of CH ₃ COOH.
Chukwu (1996)	-	CR61 CAL-386, AR103 QZL-386 (Ionics Inc.)	4600	91 - 5 g/L CH ₃ COOH pH:2.5	90-120 g/L CH ₃ COOH	20	Constant current	4.3 - 17.4 mA/cm ²	30-60	2.75-12.6	--		Shown that with increase in feed concentrations, water flux and specific energy reduces; and with increase in current density, specific energy and water flux increases. Used multistage stages to product acetic acid to 308 g/L. Use of multiple stacks reduce water transport and increases concentration.
Chukwu (1999)	---			69 - 0 g/L CH ₃ COONa, pH:6.8	69 to 97 g/L CH ₃ COONa, pH:6.8				12-30	1.9-9.2	----	16-24	Experimentally determined the diffusion flux (0.3-2.3 moles/m ² /hr) of CH ₃ COONa solution (0-300 g/L) into pure water. Osmotic flux of water was about 30 moles/m ² hr
Fidelao (2005)	4 -- 5	CMV-AMV (Aashi glass Inc.)	72	45 - 0 g/L CH ₃ COONa, pH: 6.8	45 -75 g/L CH ₃ COONa	9	Constant current	11 - 33 mA/cm ²	12 -- 26	44	93	15	Modeled 2-compartment separation of Na- acetate. Results were in agreement with experimental data. Maximum theoretical product concentration was 286 g/L.

Table 2.4. Literature Data on Splitting of Sodium Acetate using Electrodialysis

Author (year)	Membrane		Variation in concentrations			Number of cell pairs	Current/Voltage	Energy (A·V·hr·mol ⁻¹)	Flux (mol·m ⁻² ·hr)	Current efficiency (%)	OWTI	Comments
	Type	Area	Acid	Salt	Base		Mode, Value					
Kassotis (1984)	CMV, AMV (Aashi glass), ACBM-3	11 cm ²	0-270 g/L CH ₃ COOH + 3-5% CH ₃ COONa	6% CH ₃ COONa	20-32 g/L NaOH	1	Constant current 109 mA/cm ²	60 to 91 Based on HAc	25-12	90 to 38 (for 366 g/L of CH ₃ COOH)	28	For steady state runs (not listed in the table), 70-280 g/L solution of CH ₃ COONa could be split into 400 g/L CH ₃ COOH and NaOH. For IONAC membranes, current efficiency fell to 27% when 5% CH ₃ COOH was obtained.
Trivedi (1997)	In house synthesis using ion exchange resin	80 cm ²	Up to 90 g/L CH ₃ COOH	4 to 123 g/L CH ₃ COONa	Up to 40-80 g/L NaOH	5	Constant voltage 4-6 V/Cell pair	106-164 Based on Na-Ac	----	98 to 90	---	High power consumption can be because of in-house synthesis of membranes.
Bar (2006)	-----	255 m ²	220g/L CH ₃ COONa to 180 g/L CH ₃ COOH		Up to 60 g/L NaOH	--	Constant current 85 mA/cm ²	---	19.1	---	---	This is an industrial unit installed by Eurodia Industry in Germany. Because of very low conductivity of acetic acid, salt was in situ converted to acetic acid. Economic analysis shows a payback period of less than two years.

CHAPTER 3

LOW TEMPERATURE EXTRACTION AND TWO-STAGE PULPING EXPERIMENTS

This chapter summarizes experimental data on the pre-extraction of northeastern hardwood chips using low alkali charge and the results of pulping experiments.

Extraction experiments were performed previously as a part of the author's MS thesis [Patil, 2012]. Experimental conditions and results have been previously reported [Patil 2012 and Patil, 2013]. These experiments showed that the concentration of residual sodium hydroxide in the extract was about 8 g/L when the white liquor charge was 8% EA based on wood. These early experiments illustrated the possibility of further reducing the white liquor charge used in the extraction experiments thus minimizing unreacted caustic, which unduly raises the pH of the extract to about 13.6 and could damage the membranes used in the electro dialysis (ED) cell. Therefore, additional extraction experiments were performed using white liquor charges of 6% and 4% EA. These experiments were undertaken to evaluate the minimum alkali charge required to achieve essentially complete deacetylation.

3.1 Low Temperature Extraction Experiments using Low White Liquor Charge

Extraction experiments were performed at 50 °C and 80 °C using low white liquor charges of 6% and 4% EA. These experiments were conducted by following the experimental protocol reported by Patil (2013). Figure 3.1 illustrates the concentration of sodium acetate as a function of time in the extracts obtained for four different extraction experiments. The maximum obtainable concentration of sodium acetate in the extract was approximately 17 g/L when the liquor to wood ratio was 4 grams liquor per gram of bone dry wood (Figure 3.1). The maximum obtainable concentration represents the condition when all acetyl groups have been cleaved off the xylan hemicelluloses. The sodium acetate concentration in the hardwood extract was found to vary between 14 and the maximum 17 g/L depending upon the extraction conditions.

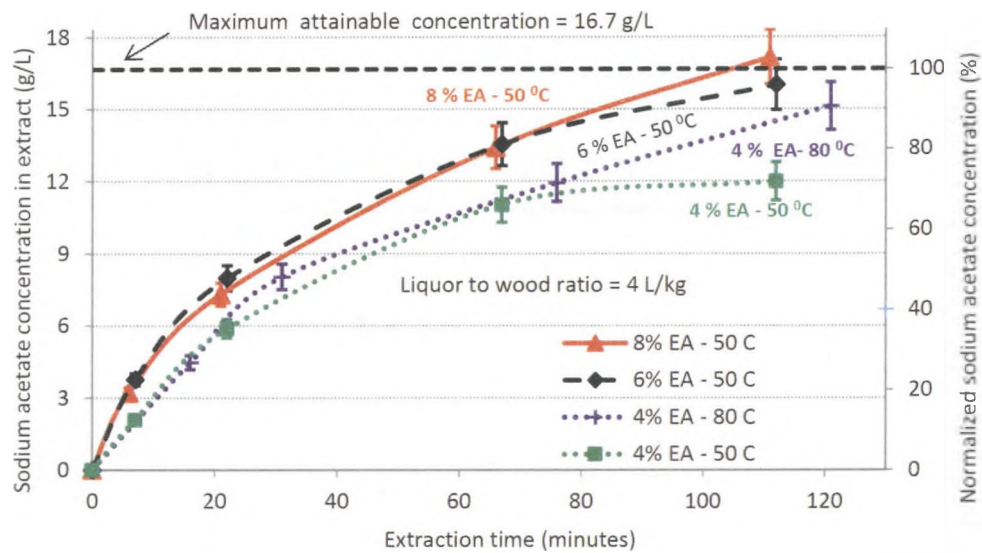


Figure 3.1. Effect of White Liquor Charge and Temperature on Sodium Acetate Concentration in Extract

The compositions of the final extracts obtained for the four extraction conditions are shown in Table 3.1. Lignin and sugar concentrations were found to vary between 2 to 7 g/L and 0.4 to 1.3 g/L, respectively. In these experiments, no chip washing was performed and the final liquor was simply drained from the digester. The amount of acetyl groups recovered in the drained liquor was about 2/3rd of the total acetyl groups in the raw wood [Patil, 2012]. The remaining acetyl groups were present in the liquor present within the extracted chips. For the extraction conditions mentioned in the present work, if chips were washed using the same quantity of water as that of drained liquor, additional liquor with sodium acetate concentration of about 5 g/L would be obtained. Washing could increase the recovery of acetyl groups to about 90%.

The alkali charges of 6% EA (at 50 °C) and 4% EA (at 80 °C) were thought to be the optimum for the extraction of acetyl groups at a liquor-to-wood ratio of 4-to-1. In addition, the concentrations of residual sodium hydroxide in these extracts were lower when compared to the other extracts. However in a commercial process, if chip washing was

included to remove additional sodium acetate, then under these conditions it is felt that extraction using 5% EA alkali at both 50 °C and 80 °C would need to be evaluated.

Table 3.1 Compositions of Extracts obtained under Different Conditions

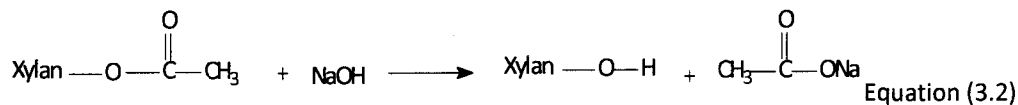
	White Liquor Extracts						Caustic Extract
	8			4			
Effective alkali (%)	8	6	4	8	4		4
Sulfidity (%)	34			34			0
Extraction temperature (°C)	50			80			80
Liquor-to-wood ratio(L/kg)	4			4			4
pH of the extract	13.8	13.0	12.3	13.6	11.9		11.8
Dissolved solids (% w/w)	5.8	4.3	3.2	6.8	3.7		3.9
Dissolved organics (% w/w)	1.7	1.4	0.9	2.2	1.1		1.9
CH ₃ COONa (g/L)	17.4	17.1	13.9	16.2	15.5		15.1
Total lignin (g/L)	3.9	3.0	2.7	7.5	5.3		4.5
Total sugars (g/L)	0.9	0.7	0.4	1.2	0.5		1.3
NaOH (g/L)	7.2	4.0	2.6	8.0	1.6		0.7
Na ₂ S (g/L)	10.8	3.9	2.0	5.8	3.0		-
Na ₂ CO ₃ (g/L)	7.1	5.1	3.4	7.0	3.0		-
Estimated Flow rate (m ³ /day) for 1000 tons of pulp per day	5039						5039

The reaction scheme shown below occurs when acetyl groups on the hemicelluloses are hydrolyzed in the presence of white liquor.

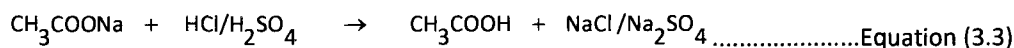
A) Reaction of Na₂S with H₂O



B) Deacetylation of xylan



C) Neutralization of Acetyl Groups During pH Adjustment before HPLC Analysis



3.2 Low Temperature Extraction Experiments using Low Caustic Charge

Although the use of ordinary or oxidized white liquor seems complementary for kraft pulp mill operations, these liquors contain several extraneous compounds other than sodium acetate and sodium hydroxide. Materials present include sodium sulfide, sodium carbonate and sodium sulfate. Since these additional compounds are ionic in nature, the efficiency of ED will be reduced. In addition, the presence of sodium sulfide can lead to safety issues during the operation of the ED cell. A detailed discussion about the disadvantages of processing white liquor extract in ED is available in the fourth chapter.

Therefore, it was proposed to use caustic (4% Effective alkali, 0% Sulfidity) for the extraction of hardwood chips and limit the final pH of the extract to a value of approximately 10.5 to 12. pH values of 12 or less are thought not to be detrimental to the membranes in the ED cell. The composition of the caustic extract obtained under these conditions is shown in Table 3.1 and is similar to the composition of the 4% EA white liquor extract except for the presence of sodium sulfide and sodium carbonate.

3.3 Two Stage Pulping Experiments with White Liquor Pre-Extraction

Initial work was performed to determine the pulping characteristics of pre-extracted wood following extraction of acetyl groups. The objective of these experiments was to determine the suitability of the pre-extracted wood as a feedstock for producing marketable hardwood pulp relative to a control pulp. The pulping conditions used in these experiments were similar to those used at Mead-Westvaco in Covington, Virginia, USA.

Control pulp was obtained by extracting wood chips with 14.9% EA white liquor to a target H-factor of 780 hours. The H-factor is a severity factor used to estimate the extent of delignification. The liquor-to-wood ratio was 3.5 in both the pulping and extraction experiments. The objective of the control pulping experiments was to determine a base line for comparing the physical properties of the pre-extracted pulp to those of the control.

Figure 3.2 shows a schematic diagram of the Kraft cooking process followed in the present work. Wood chips and alkali were cooked in a laboratory scale digester. A detailed description of the digester is available in the literature [Patil, 2013]. As shown in Figure 3.2, green wood chips and 14.9% EA white liquor were cooked at 170 °C for 41 minutes to reach the target H-factor of 780 hours.

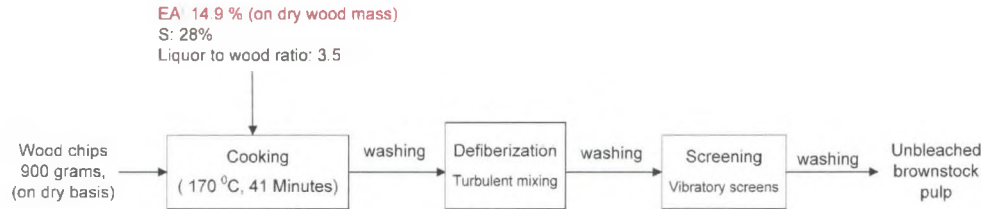


Figure 3.2 Kraft Control Pulping Process

Figure 3.3 shows a block diagram for the two stage pulping process. In the first stage, green wood chips were extracted at 50 °C for 110 minutes using 6% EA white liquor. At the end of the extraction process, the extract was drained from the digester and its weight was noted. Fresh make-up liquor was then prepared by using additional alkali such that the total alkali charge was 14.9% EA. Sufficient water was added to the make-up white liquor to maintain the same liquor to wood ratio in the pulping process. The macerated wood chips were then pulped using the make-up liquor to reach the target kappa number of 15 to 17 by varying the H-factor, starting with 780 hours.

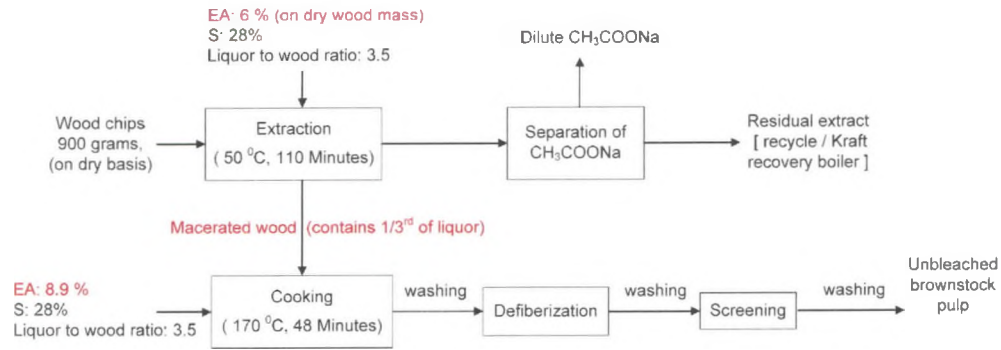


Figure 3.3 Two Stage Cooking Process

Table 3.2 summarizes the experimental conditions for both control and two-stage pulping experiments. The total H-factor for the two-stage pulping process (extraction and pulping) was 880 hours.

Table 3.2. Experimental Conditions for Control and Two-Stage Pulping Experiments

	Control pulping	Two stage cooking	
		Extraction	Pulping
Effective alkali (% on dry wood basis)	14.9	6	8.9
Sulfidity (%)	28		
Causticizing efficiency (%)	80		
Liquor to wood ratio	3.5		
Cooking temperature (°C)	170	50	170
Cooking time (excluding ramp, minutes)	41	90	48
Target H-factor (hours)	780	880 (to meet target kappa number)	
Temperature ramp = 45 minutes to 170 °C			

3.3.1 Physical Properties of Unbleached Control and Pre-Extracted Pulp

The samples of unbleached brownstock pulp were analyzed for kappa number, screened yield and shives. A plot of physical properties as a function of degree of refining or freeness is called a “beater or refining curve” and is obtained by processing the pulp in a PFI mill. In a PFI mill, mechanical processing is achieved by having an inner roll and outer casing rotate under constant load, in the same direction, but with different peripheral speeds. The Kraft control and the pre-extracted Kraft pulps were processed in the PFI mill for 0, 1,000, 2,000, 4,000 and 6,000 revolutions [TAPPI Standard T-248, 2008].

The purpose of processing the pulp in the PFI mill was to simulate pulp refining and obtain samples of the pulps at several freeness values. Samples of both the unrefined and refined pulp were evaluated for physical and optical properties (opacity and brightness). Following each pulp processing level, the freeness was determined and standard TAPPI handsheets (60 gram/square meter) were prepared. The handsheets were conditioned in a constant humidity room. The conditioned handsheets were then tested for caliper, bulk, tensile strength, tear strength, Scott internal bond and wet zero-span breaking length. In all tests, standard TAPPI methods were used. A detailed discussion of these methods is available in the Appendix C.

Refining physically modifies the pulp fibers by imparting mechanical energy to the pulp in the form of mechanical pulses. The mechanical pulses imparted to the pulp increased its surface area by fibrillation, or unraveling of the fibrils comprising the wall of the pulp, and force water into the body of the pulp. These physical changes improve the ability of the pulp to hold water, improve its flexibility and increase the bonding between adjacent fibers. The result of the pulp processing was to increase the tensile and burst strength of the pulp. With increased fiber-to-fiber bonding there is a concomitant decrease in the tear strength and porosity of the pulp.

Table 3.3 summarizes the physical and optical properties of the two types of the brownstock pulps produced in the two-stage pulping process.

Table 3.3 Physical and Optical Properties of the Control and Pre-Extracted Pulp Samples

Pulp Type	Total H-factor (hrs)	% EA (Extraction, Pulping)	PFI Revolutions	kappa number (after screening)	CSF (mL)	Bulk (cm ³ /g)	Tensile Index (N·m/g)	Tear Index (mN·m ² /g)	Wet zero span breaking length (Km)	ISO Brightness (%)	Internal Bond Strength (Kg.cm/ in ²)	Yield	Shives
												(on % OD wood basis)	
Control	773	0, 14.9	0	15.8	598	1.65	48.8	6.79	13.17	34.5	0.87	50.3	0.33
			1000	---	492	1.40	65.1	9.07	14.30	31.9	1.89		
			2000	---	444	1.33	71.0	9.42	14.00	30.6	2.36		
			4000	---	353	1.25	83.8	9.37	13.69	29.1	3.59		
			6000	---	287	1.22	88.3	9.46	13.48	28.0	4.27		
Pre-extracted	880	6, 8.9	0	15.8	575	1.64	43.7	6.57	13.90	33.8	0.90	49.5	0.25
			1000	---	474	1.42	65.1	8.64	14.30	31.4	2.02		
			2000	---	440	1.33	74.3	9.43	13.59	30.3	2.55		
			4000	---	357	1.26	83.3	9.31	13.92	28.5	3.54		
			6000	---	292	1.23	85.5	9.44	13.23	27.5	4.42		

Figures 3.4 to 3.6 illustrate the effect of degree of refining on various pulp properties as a function of the revolutions of the PFI mill. Figure 3.4 compares the Canadian Standard Freeness and the internal bond strength of the control and the pre-extracted pulps. Similarly Figures 3.5 and 3.6 illustrate the tear and tensile strength (Figure 3.5) and the bulk and pulp brightness (Figure 3.6). It can be concluded from these graphs that the pulp properties do not appreciably change after the extraction of the acetyl groups and pulping to equal kappa numbers using alkali equivalent to a conventional kraft cook; i.e. splitting the alkali into an extraction stage and a pulping stage (two-stage pulping).

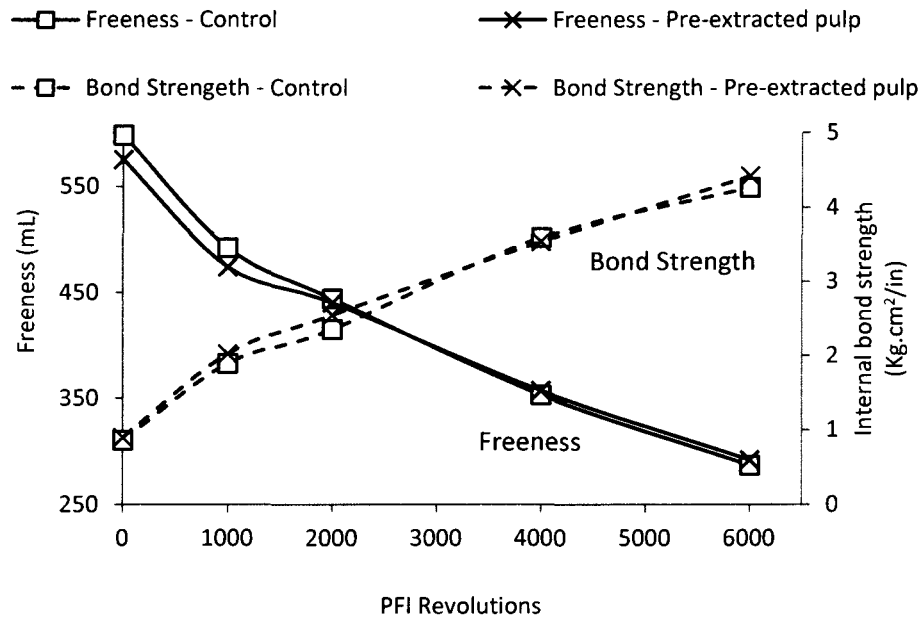


Figure 3.4 Effect of Degree of Refining on Pulp Freeness and Internal Bond Strength

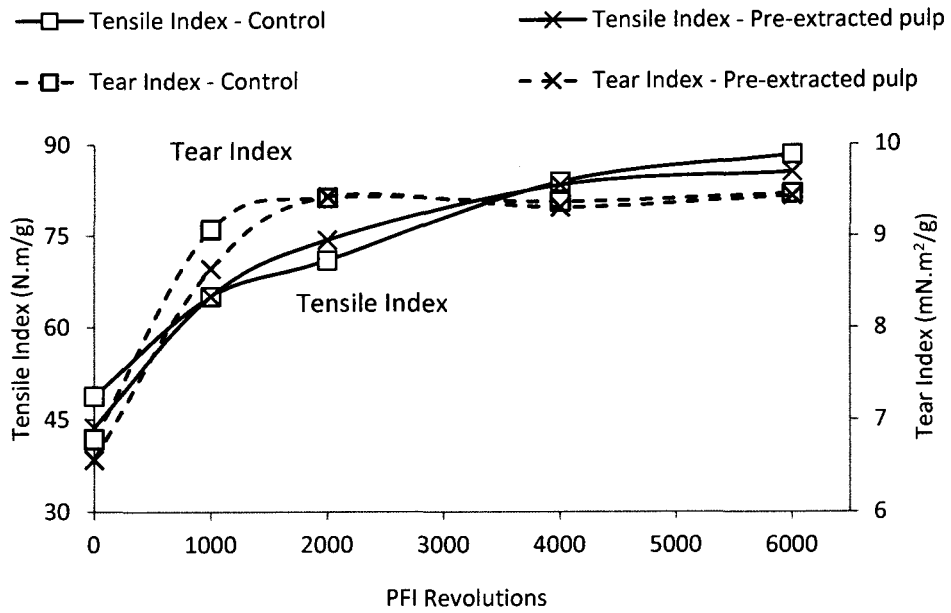


Figure 3.5 Effect of Degree of Refining on Tensile and Tear Indices

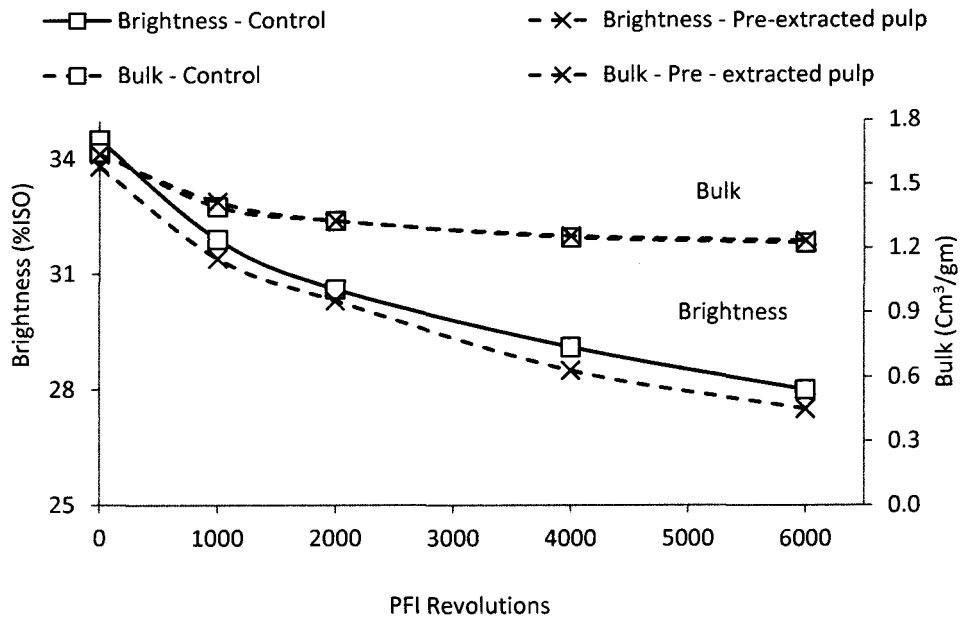


Figure 3.6 Effect of Degree of Refining on Brightness and Bulk Density

CHAPTER 4

SEPARATION AND CONCENTRATION OF SODIUM ACETATE USING ELECTRODIALYSIS

The present chapter summarizes experimental data on the separation and concentration of aqueous sodium acetate using electrodialysis (ED). Experiments were performed using dilute sodium acetate and synthetic and pre-treated extracts. Three types of experiments were performed:

Preliminary Concentration Experiments to Study Separation of Sodium Acetate from Water:

Preliminary separation experiments were performed using dilute sodium acetate to gain an understanding of the effects of current density, feed concentration and electro-osmosis.

Effect of Tramp Ions of Oxidized White Liquor Extract on Selectivity of ED: Secondly, ED experiments were performed to study the effect of various tramp ions present in the oxidized white liquor extract on the selectivity of the ED process. In these experiments, it was assumed that fully oxidized synthetic white liquor would be used as the solvent in the extraction process. Thus, carbonate, sulfate and other sulfur bearing ions would be present in the extract.

ED Experiments Using Pre-Treated Extracts: Pre-treated wood extract was processed through the ED apparatus to estimate the electric energy consumption and current efficiency. Two types of pre-treated wood extracts were evaluated as feed in the ED apparatus. These were designated as (1) Clarified and (2) Unclarified wood extracts. Information obtained using wood extract was required for the design and scale up of ED systems. The clarified extract was obtained after treating the hardwood extract with activated charcoal to partially remove lignin and then concentrating the clarified solution. For comparison, the unclarified extract was obtained after concentration of the raw hardwood extract without the activated charcoal pre-treatment.

As a practical matter, three reactants are possible for cleaving acetyl groups off of the hemicelluloses in the wood; caustic (NaOH), white liquor (NaOH and Na₂S) and oxidized white liquor (NaOH and Na₂SO₄).

4.1 Introduction

Current density and feed concentration are the major parameters that affect the ED process. Therefore, these parameters were studied to determine the optimum conditions for the separation of sodium acetate using ED. Preliminary experiments were performed using dilute sodium acetate solution to establish a baseline for the separation process. Experiments of this type were helpful in estimating capital and operating costs for concentrating sodium acetate to different concentration levels using ED.

The wood extract contains extraneous materials other than sodium acetate depending upon the solvent used in the extraction process. If white liquor is used as the solvent, then unreacted sodium hydroxide, sodium sulfide and sodium carbonate would also be present in the wood extract in addition to sodium acetate. Since these compounds are ionic in nature, they will reduce the selectivity of the ED process.

Sodium sulfide can be present in the form of either HS⁻ or S²⁻ depending upon the pH of the extract. In both the ED and the BPMED processes, the HS⁻ ions will be transferred along with the acetate ions. In the case of the BPMED process, both the HS⁻ and acetate ions will become acidified by hydrogen ions (H⁺) migrating from the other side of the compartment. Consequently, hydrogen sulfide would be formed in addition to acetic acid. In addition, S²⁻ ions can diffuse through the membranes towards the anode where it is oxidized to form elemental sulfur (S⁰). Since sulfur is insoluble in water, it can decrease the current efficiency or damage the membranes. Therefore, in order to avoid the deleterious effects of hydrogen sulfide, fully oxidized synthetic white liquor was used in the selectivity experiments. In all likelihood, either

makeup caustic or oxidized white liquor would be used in the extraction process in a commercial system rather than white liquor. Using white liquor has the potential advantage of raising the pulp yield due to two stage-pulping, but suffers the disadvantage of possibly forming H_2S in the ED cell. Oxidized white liquor is sometimes used in pulp mills, for example in oxygen delignification, where a source of alkali is required but the sulfide ion is undesirable [Magnotta et al, 1996]. Oxidized white liquor can be obtained by the complete or partial oxidation of Na_2S to Na_2SO_4 or $Na_2S_2O_3$, respectively. In the experiments described here, sodium sulfate (Na_2SO_4) was assumed to be present in the oxidized synthetic white liquor extract. The concentration of the sodium sulfate was assumed to be equivalent to the Na_2S concentration in the white liquor extract obtained in the extraction experiments.

However, the separation of sodium acetate from oxidized white liquor extract resulted in a significant decrease in the efficiency of the ED process. The detailed results are discussed in section 4.3.3. Therefore, it was proposed to use pure sodium hydroxide solution for the cleavage of acetyl groups from hardwood in the extraction process. Accordingly, pre-treated extracts were prepared using caustic extract (4% EA, 0% S, 80 °C).

4.2 Experimental Methods

This section contains information about the equipment used in this work and methodology used for the selection of experimental conditions.

4.2.1 Experimental Apparatus

The experimental ED cell was manufactured by PCCell/PCA GmbH, Heusweiler, Germany (Figure 4.1). For the purpose of simplification, Figure 4.1 contains only two cell pairs. However, the experimental cell consisted of five cell pairs of cation and anion exchange membranes (Neosepta AMX/CMX, Tokuyama America; Arlington Heights, IL, USA). The surface area of each membrane was 64 cm². Spacers were placed between adjacent membranes which allow the

flow of solution between the membranes. The procedure for the stacking of ED cell is available in Appendix D.

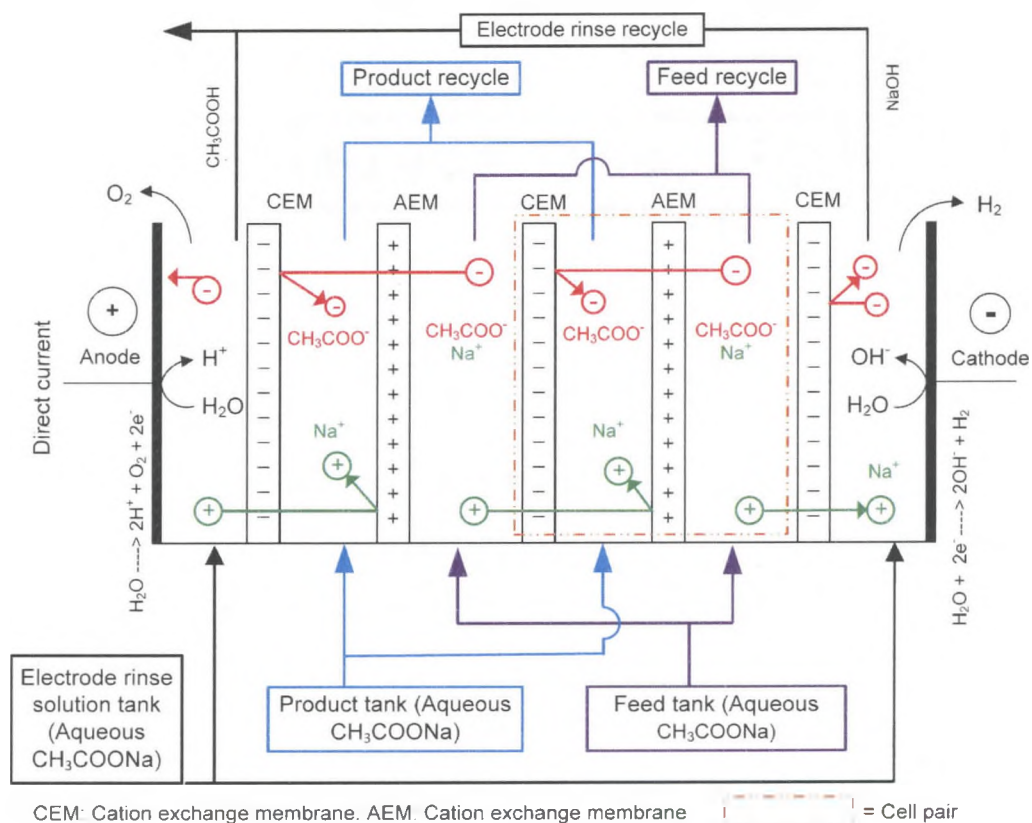


Figure 4.1 Two-Compartment Electrodialysis Cell

The maximum allowable voltage drop for the various components of the ED cell are shown in Table 4.1. The maximum allowed voltage for the ED cell used in this study was 10.4 volts.

Table 4.1 Maximum Allowed Voltage Drop for Different Components of the ED Cell

Component	Maximum Voltage (V)	Quantity	Total Voltage (V)
Cation Exchange Membrane	0.4	6	2.4
Anion Exchange Membrane	0.4	5	2.0
Electrodes (Anode and Cathode)	6	1	6.0
Maximum allowed voltage for the ED cell used in this work (V)			10.4

A schematic diagram of the ED apparatus is presented in Figure 4.2 and shows the circulation of the feed, product and electrode rinse flow streams. The equipment also consisted of a heat exchanger (not shown) which maintained the temperatures of all solutions below 25 °C. The function of the heat exchanger was to protect the membranes from damage due to an excessive temperature rise caused by resistance heating of the liquors in the ED apparatus.

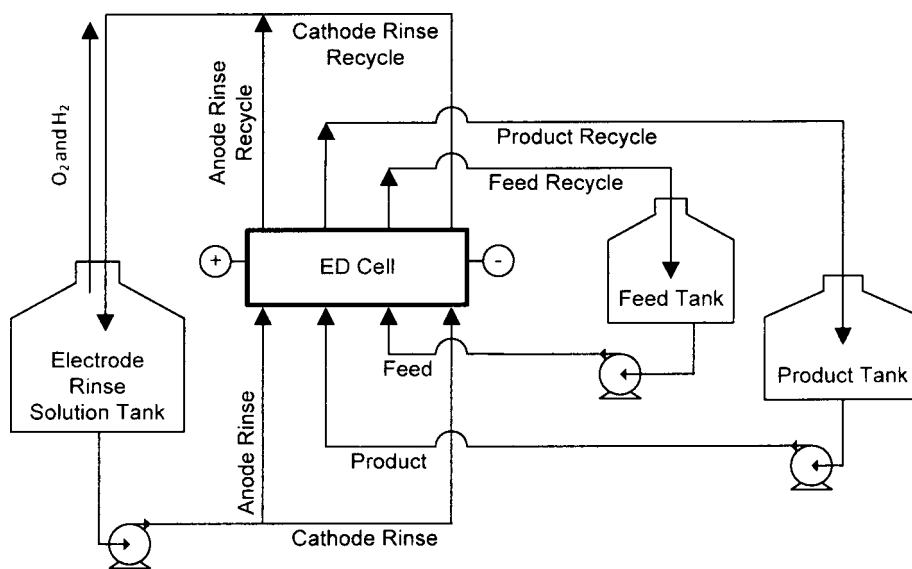


Figure 4.2 Two-Compartment Electrodialysis Apparatus

Conductivity and pH probes were used to monitor the real-time concentration of sodium acetate and pH, respectively. The sodium acetate concentration was assumed to follow the conductivity. The voltage and current were recorded in real-time with a computer.

4.2.2 Experimental Procedure

An ED process can be operated at constant current, constant voltage or a combination of both. The constant current mode was chosen for this study because it maintains a constant

rate of separation and production. All experiments were conducted in the batch recycle mode illustrated in Figure 4.2.

The electrolyte solutions were fed from the bottom of the ED cell to avoid carryover of any air into the cell. Initially, water was charged into all tanks and recirculation pumps were simultaneously turned on to check for leaks in the equipment. If there was no leakage, electrolyte solution were charged into the respective tanks. If air bubbles were formed in any of the solutions, then all recirculation pumps were turned off for few minutes until the bubbles vanished.

The feed solution was recirculated at a constant flow rate of 550 mL/minute, which corresponded to a superficial velocity of 5.1 cm/s. The recirculation rates of the product and the electrode rinse solutions were then adjusted to maintain a constant pressure at the inlet to the ED cell. The direct current (DC) was then turned on. At the end of each experimental run, the current was first turned off and subsequently recirculation of the solutions was stopped.

4.2.2.1 Procedure for the Determination of Limiting Current Density

It is necessary to maintain the applied current density below its limiting value to avoid the loss of electric energy resulting from the decomposition of water at overlimiting currents. The procedure for the determination of limiting current density is described by Cowan and Brown (1959).

4.2.3 Experimental Design

This section contains detailed discussion about the experimental conditions for the three types of separation experiments.

4.2.3.1 Experiments to Study the Separation of Sodium Acetate from Water

Table 4.2 summarizes the experiments performed to evaluate ED for its ability to separate sodium acetate from water. The feed concentration used in the initial experiment (designated Experiment A-1) corresponded to the composition of the hardwood extract obtained using 6% EA white liquor at 50 °C and a liquor-to-wood ratio of 4-to-1. Under these experimental conditions, the hardwood extract contained about 17 g/L of sodium acetate. In order to estimate the effect of feed concentration over a broader range, additional experiments were conducted using 34, 85, 150 and 200 g/L sodium acetate solutions.

The initial concentration of product solution was 17 g/L of sodium acetate in all experiments. The presence of a small quantity of salt in the initial product solution was necessary to give the product solution some minimum level of conductivity and reduce its electric resistance. The initial concentration of the electrode rinse solution was the same as the initial concentration of the feed solution in the respective experiment. The initial volumes of liquid in the product and electrode rinse compartments of the ED cell were 1 L each.

Table 4.2 Experiments for Studying Separation of Sodium Acetate from Water

Initial Concentration and Volume of Feed Solution	Major Current Density		
	25 mA/cm ²	45 mA/cm ²	60 mA/cm ²
17 g/L, 2 Liters	Experiment A-1	-----	-----
34 g/L, 2 Liters	Experiment B-1	Experiment B-2	-----
85 g/L, 2 Liters	Experiment C-1	Experiment C-2	Experiment C-3
150 g/L, 2 Liters	-----	Experiment D-2	-----
200 g/L, 2 Liters	-----	Experiment E-2	-----

4.2.3.2 Effect of Tramp Ions of Oxidized White Liquor on Selectivity of Electrodialysis

Experiments for studying selectivity were performed using a synthetic feed solution containing 31 g/L of sodium acetate and the equivalent amount of other components in the white liquor extract, except for sugars and lignin. This concentration represents twice the concentration of the extract obtained using 4% EA white liquor at 80 °C. The use of 31 g/L sodium acetate in the feed solution allowed the estimation of selectivity at a mid-level current density of 45 mA/cm². The lignin and sugars were not considered in the selectivity experiments because they are not ionic in nature, and hence should not have any direct effect on the selectivity during the separation of sodium acetate using ED. However, lignin and sugars can foul the ion exchange membranes in the long run. The determination of the effect of lignin and sugars on the separation of sodium acetate would be the next logical step in this study if the inorganic compounds in the synthetic oxidized white liquor extract do not appreciably affect the selectivity.

Table 4.3 summarizes the concentrations of feed solutions used in the selectivity experiments. The initial concentrations of product and electrode rinse solutions were 15.5 and 31 g/L of sodium acetate, respectively. The initial volumes of feed, product and electrode rinse solutions were 2.1, 1 and 1 L, respectively.

In order to establish a baseline for comparing the extent of separation of sodium acetate in different experiments, a constant electric energy input of 29.5 W-hours was supplied in all experiments.

It was necessary to maintain the pH of the feed to the ED system below 12 to avoid damaging the Neosepta AMX/CMX ion exchange membranes. This was done by using a 2 N solution of sulfuric acid to control the final pH of the feed solution.

Table 4.3 Experiments to Study the Effect of Tramp Ions of White Liquor on Selectivity of ED

Experiment No. / Concentration		F-1	F-2	F-3	F-4
Desired composition of initial feed solution (g/L)	CH ₃ COONa	31	31	31	31
	NaOH	--	3.2	3.2	3.2
	Na ₂ CO ₃	--	--	6	6
	Na ₂ SO ₄	---	--	--	11
pH of feed solution before pH adjustment		8.5	12.4	12.7	12.7
Amount of 2N H ₂ SO ₄ solution used for pH adjustment (mL)		---	66	98	100
pH of feed solution after pH adjustment		--	10.2	10.5	10.5
Volume of the feed solution after pH adjustment (L)		2.1	2.1	2.1	2.1
Actual composition of initial feed solution (g/L)	CH ₃ COONa	31	31	31	31
	NaOH ^(a)	--	--	--	--
	Na ₂ CO ₃	--	--	4	4
	NaHCO ₃	--	--	2.1	2.1
	Na ₂ SO ₄	---	4.5	6.6	17.5
(a): pH = 10.5					

In order to achieve the desired initial feed concentration of the different components shown in Table 4.3, the required amounts of chemicals corresponding to a final volume of 2.1 L were put into a volumetric flask and the volume of the solution was adjusted to 1.9 L. The pH of the solution was noted and it was adjusted to about 10.5 by adding sulfuric acid (2 N). Finally, the volume of the acidified solution was adjusted to 2.1 L. During the pH adjustment, most of the sodium hydroxide was converted into sodium sulfate. Since the final pH of the feed was about 10.5 in most of the experiments, approximately 40% of the carbonate ions were present in the form of sodium bi-carbonate.

The pH adjustment represents a decrease in the efficiency due to the presence of sodium hydroxide because the sodium sulfate formed during the pH adjustment is also transferred into the product stream along with the sodium acetate.

4.2.3.3 Electrodialysis Experiments using Pre-Treated Extracts

The hardwood extract was processed in the ED system by using two types of feed solutions: 1) Clarified and 2) Unclarified extracts. Figure 4.3 illustrates the procedure used to prepare these solutions.

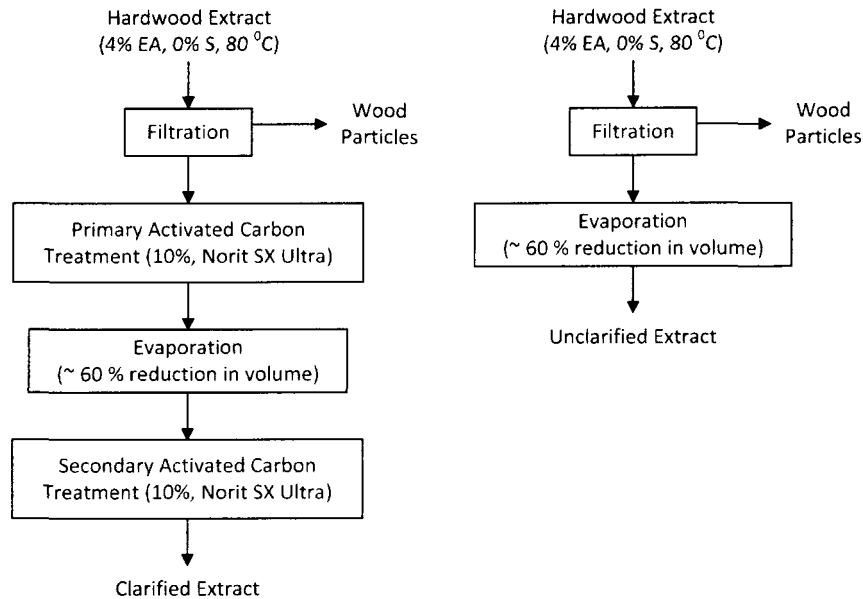


Figure 4.3 Pre-treatment of Hardwood Extract Prior to Use in the Electrodialysis Experiments

The concentration of sodium acetate in the pre-treated extracts following evaporation was maintained at 37 to 42 g/L so that these solutions could be processed at a middle-level current density of about 40 mA/cm². The use of the clarified solution allowed the understanding of the effect of different salts present in the extract on the selectivity of the process and protects ion exchange membranes from possible fouling due to the lignin. However, since the activated charcoal is not easily regenerated, such pre-treatment is expensive, and thus, would adversely affect the economic viability of the process. Therefore, an additional experiment was performed to demonstrate the processing of unclarified extract in ED. For practical applications,

the effect of lignin on ion exchange membranes could be determined by performing long term stability studies.

Table 4.4 summarizes the composition and volumes of the pre-treated (feed) solutions used in the current study. The concentration of the hardwood extract is also given in the table. A variety of sodium compounds were contained in the extract in addition to sodium acetate even at the low temperatures used in the extraction experiments (80 °C). Notably among these lesser compounds found in the raw extract are sodium formate, sodium lactate, sodium glycolate as well as lignin and component sugars. The formate, lactate and glycolate ions were thought to result as by-products in the extraction process resulting from alkaline peeling and stopping reactions which occur simultaneously with the alkaline cleavage of the acetyl groups from the xylan hemicellulose polymers [Rydholm, 1965]. Figure 4.4 shows the effect of the extraction temperature on the concentration of sodium formate in 8% EA white liquor extract [Patil, 2013]. A similar trend was shown for sodium lactate as well.

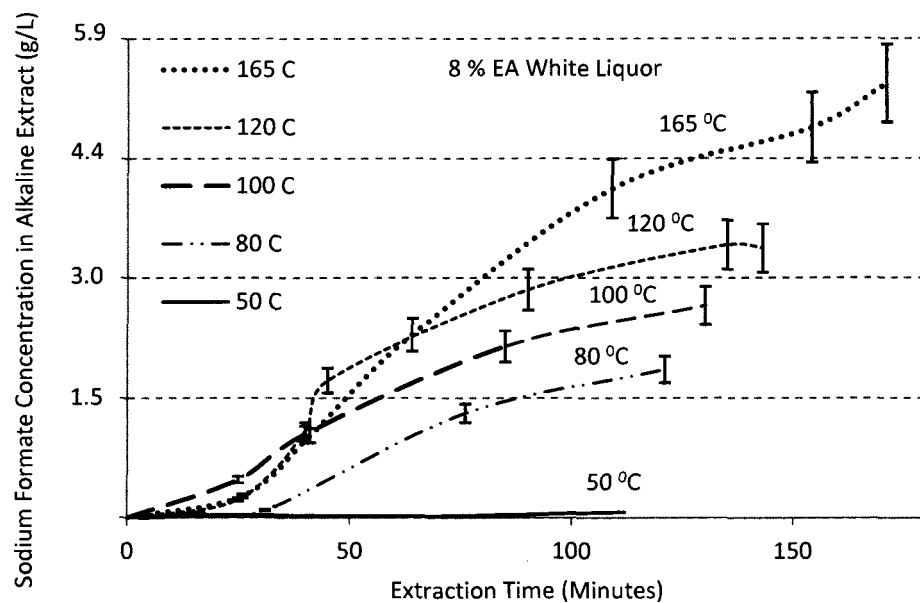


Figure 4.4 Effect of Extraction Temperature on Sodium Formate Concentration in Extract

In Table 4.4, the sugars are reported in the aggregate as “total sugars”. At the high pH values of the extracts, the lignin would most likely be partially ionized and exist as lignin phenolate ions.

Table 4.4 Composition of Pre-Treated Extracts (4% EA, 0% S, 80 C) used in Electrodialysis

	Concentration (g/L)						pH	Volume (L)
	Na-Acetate	Na-Formate	Na-Lactate	Na-Glycolate	Total Lignin	Total Sugars		
4% EA Caustic Extract (80 °C)	14.60	1.55	0.28	0.69	4.52	1.05	12.20	---
Unclarified extract	36.80	3.98	0.82	1.93	9.66	1.56	10.4	1.50
Clarified extract	42.20	3.90	0.89	1.09	0.40	0.20	10.5	1.65

The concentration of sodium acetate in the initial product and electrode rinse solutions was 17 and 45 g/L, respectively. The initial volume of each of these solutions was 1 L. Approximately the same amounts of electric energy and charge were applied in both of the ED experiments.

The total concentration of sodium ion in the feed and product solutions was separately determined using Inductively Coupled Plasma Optical Emission Spectrometry (ICP-OES). The total sodium ion content data was used to estimate the total amount of sodium salts transferred from the feed to the product solution. By using a mass balance, the data on the sodium ion concentration was used to check the results of the salt concentration measurements obtained from the HPLC analyses. This independent check was thought necessary since the HPLC measurements may not have identified all the component salts present in the feed and product solutions.

The concentrations of sodium acetate, sodium formate, sodium lactate and sodium glycolate were measured at the conclusion of each experiment following conversion to their

acid forms using high performance liquid chromatography. Sodium hydroxide and sodium carbonate were analyzed by titrating a sample of synthetic extract with 0.1 N hydrochloric acid [TAPPI Standard T625, 1984]. Sodium carbonate was acidified only up to a pH of 8.3 and was determined as bicarbonate to avoid the interference of the sodium acetate-acetic acid equilibrium during the analysis. Sodium sulfate was gravimetrically analyzed by using 20% barium chloride after the removal of sodium carbonate from the sample by adding 1 N hydrochloric acid to form carbon dioxide [TAPPI Standard T625, 1984].

4.3 Results and Discussion

This section contains detailed discussion about the results of the separation experiments.

4.3.1 Determination of Limiting Current Density

Figure 4.5 shows the limiting current density as a function of sodium acetate concentration in the feed for the Neosepta AMX/CMX membranes. The limiting current density increased linearly with the sodium acetate concentration.

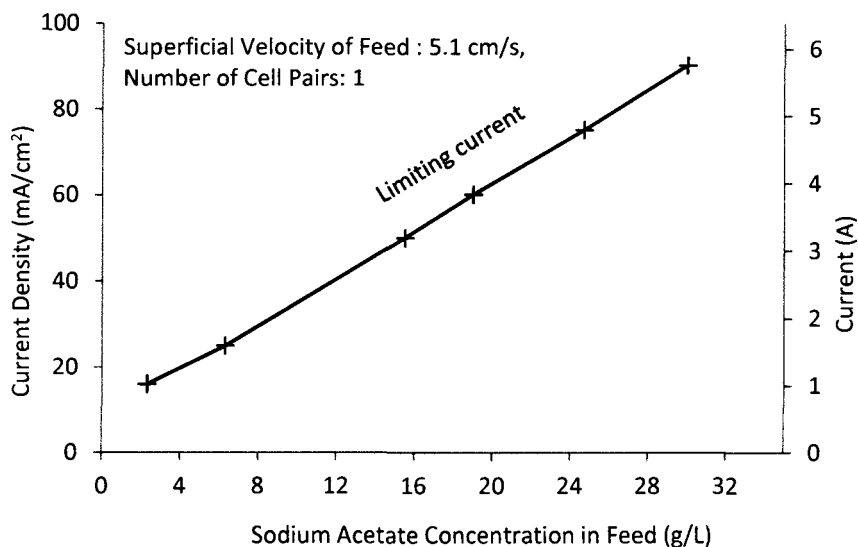


Figure 4.5 Limiting Current Density for Neosepta AMX/CMX Membranes

4.3.2 Separation of Sodium Acetate from Water

Figure 4.6 illustrates the variation in the feed and product concentrations and volumes for experiment C-3. It shows that the sodium acetate concentration in the feed solution decreased from 85 g/L to 3 g/L after 4.5 hours.

In aqueous solutions, ions are solvated by water molecules. Consequently, when a solvated ion migrates in an electric field, water molecules are also transferred along with the ionic species. This phenomenon is called electro-osmosis, and it results in a continuous transfer of water from feed to the product. Water transfer also occurs by osmosis either in the same or in the opposite direction depending upon the concentration gradient between the feed and product compartments. Hence, the volumes contained in both feed and product compartments change with time. In experiment C-3, approximately 700 mL of water was transferred along with the sodium and acetate ions (Figure 4.6).

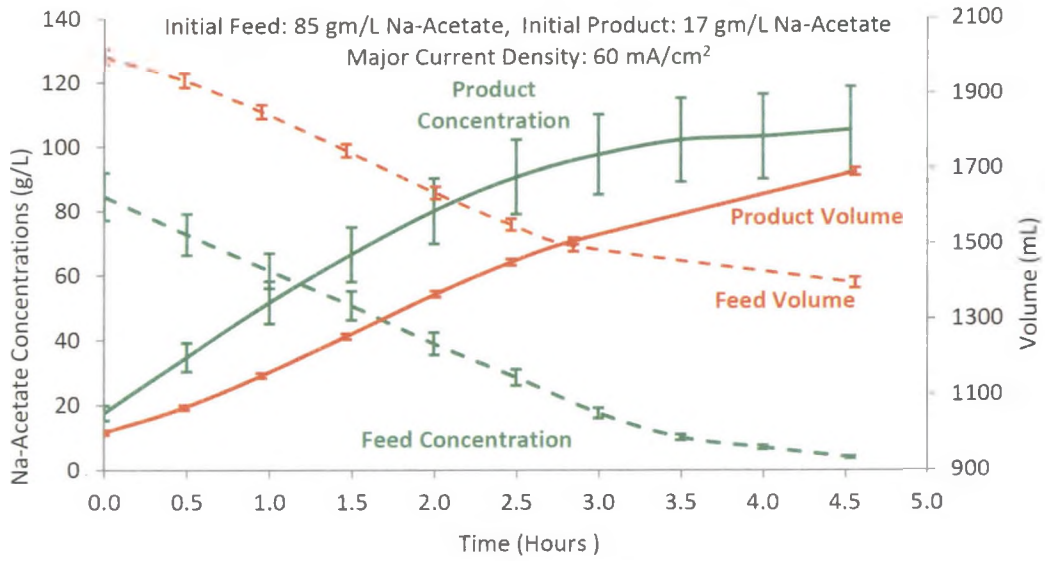


Figure 4.6 Concentrations and Volumes of Feed and Product Solutions for Experiment C-3

Figure 4.7 shows the variation in the current, voltage and cumulative energy for experiment C-3. The applied current was controlled in such a way that it was always less than the limiting current and the resulting voltage drop across the ED cell also remained less than the limiting voltage. The limiting current was estimated based on the feed conductivity (concentration). The limiting voltage drop was 10.4 V.

The voltage drop across the ED cell is the product of the current (I) and the sum of the resistances R_i (Equation 4.1),

$$V = I \times \sum_i R_i = I \times (R_F + R_P + R_{ER}) \dots \dots \dots \text{Equation 4.1}$$

where the total electrical resistance is sum of the resistances of the feed (R_F), product (R_P) and electrode rinse (R_{ER}) compartments.

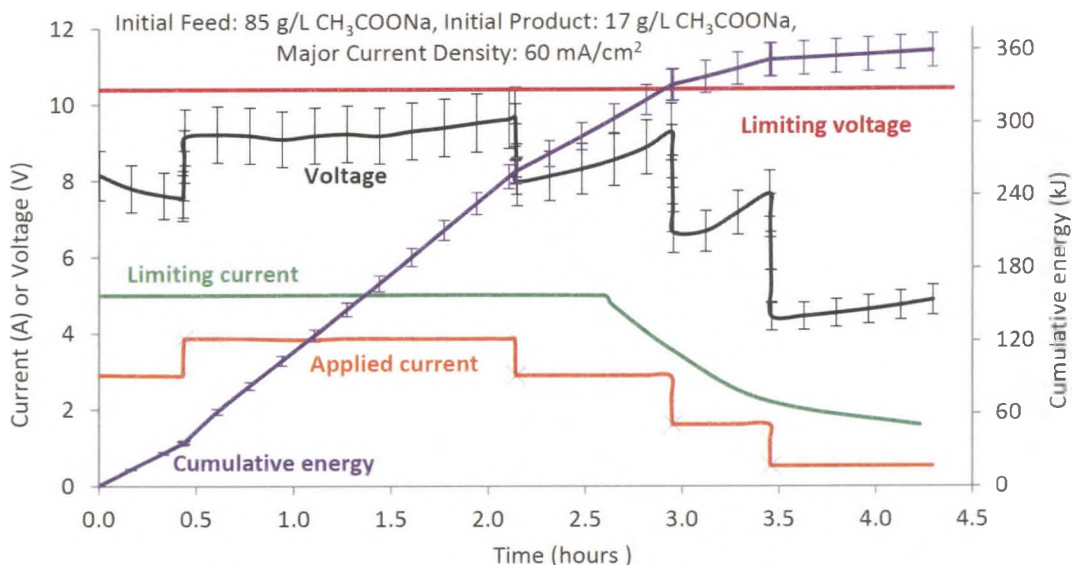


Figure 4.7 Current, Voltage and Cumulative Energy for Experiment C-3

The concentration of electrode rinse solution remains constant because it does not lose or gain ions. Therefore, at a fixed current, the voltage drop across the cell is proportional to the sum of the resistances of feed and product solutions (Equation 4.1). Since the resistance of a salt solution is inversely proportional to its concentration, the solution with the lowest concentration of salt has the highest resistance, and thus, it becomes the major factor in determining the voltage drop across the ED cell.

As shown in Figure 4.6, during the first hour of the running time of experiment C-3, the concentration of the product solution was lower than that of the feed solution. Therefore, the resistance of the product solution was the limiting resistance. Since the product concentration was continuously increasing during this period, the limiting resistance was decreasing, and thus, the overall voltage drop also decreased with time (Figure 4.7).

However, after two hours of running time of the experiment, the concentration of the feed solution was lower than the product concentration, and thus, the resistance of the feed

solution was the limiting resistance. As shown in Figure 4.6, the feed concentration was continuously decreasing after two hours. Hence, the limiting resistance increased during this period and the overall voltage drop also increased with time.

Table 4.5 summarizes the results of the experiments listed in Table 4.2. The overall sodium acetate mass balance in most of these experiments closed within 90 and 100%. All the experiments in Table 4.2, except D-2 and E-2, were terminated when approximately 80% of the initial mass of the sodium acetate in the feed solution was transferred into the product compartment.

Table 4.5 Results of ED Experiments for Separating Sodium Acetate from Water

Initial feed and product concentrations and volumes	Final feed and product concentrations, volumes, time and current efficiency as a function of the major current density		
	25 mA/cm ²	45 mA/cm ²	60 mA/cm ²
F: 17 g/L, 2 Liters P: 17 g/L, 1 Liter	Experiment A-1 F: 3 g/L, 1.94 L P: 38 g/L, 1.16 L Energy: 1581 kJ/kg Time: 1.8 Hours Current efficiency: 100 %	-----	-----
F: 34 g/L, 2 Liters P: 17 g/L, 1 Liter	Experiment B-1 F: 8 g/L, 1.8 L P: 57 g/L, 1.25 L Energy: 1656 kJ/kg Time: 2.7 Hours Current efficiency: 92%	Experiment B-2 F: 6.2 g/L, 1.87 L P: 52 g/L, 1.23 L Energy: 2127 kJ/kg Time: 2.1 Hours Current efficiency: 90%	-----
F: 85 g/L, 2 Liters P: 17 g/L, 1 Liter	Experiment C-1 F: 21.4 g/L, 1.6 L P: 101 g/L, 1.7 L Energy: 1428 kJ/kg Time: 6 Hours Current efficiency: 94%	Experiment C-2 F: 18 g/L, 1.6 L P: 100 g/L, 1.5 L Energy: 2021 kJ/kg Time: 3.4 Hours Current efficiency: 91%	Experiment C-3 F: 18 g/L, 1.6 L P: 102 g/L, 1.5 L Energy: 2281 kJ/kg Time: 2.9 Hours Current efficiency: 91%
F: 150 g/L, 2 Liters P: 17 g/L, 1 Liter	-----	Experiment D-2 F: 135 g/L, 1.9 L P: 48 g/L, 1.2 L Energy: 1767 kJ/kg Time: 1 Hour Current efficiency: 96 %	-----
F: 200 g/L, 2 Liters P: 17 g/L, 1 Liter	-----	Experiment E-2 F: 178 g/L, 2 L P: 49 g/L, 1.1 L Energy: 1520 kJ/kg Time: 0.9 Hour Current efficiency: 109 %	-----

4.3.2.1 Effect of Feed Concentration

Figure 4.8 shows the effect of feed concentration on the sodium acetate and water fluxes, and the specific energy consumption. Specific energy is defined as the amount of electric energy required for the separation of unit mass of sodium acetate. As the feed concentration increased, the resistance of the cell also decreased, which resulted in an increase in the electrical efficiency. Because of the increased electrical efficiency, the specific energy consumption decreased.

Figure 4.8 also illustrates that the water flux decreased with an increase in the feed concentration. The decrease in the transport of water molecules was thought to be due to the reduction in the availability of water molecules for the solvation of sodium acetate. As the concentration increases, a greater number of sodium acetate molecules compete for the available water molecules.

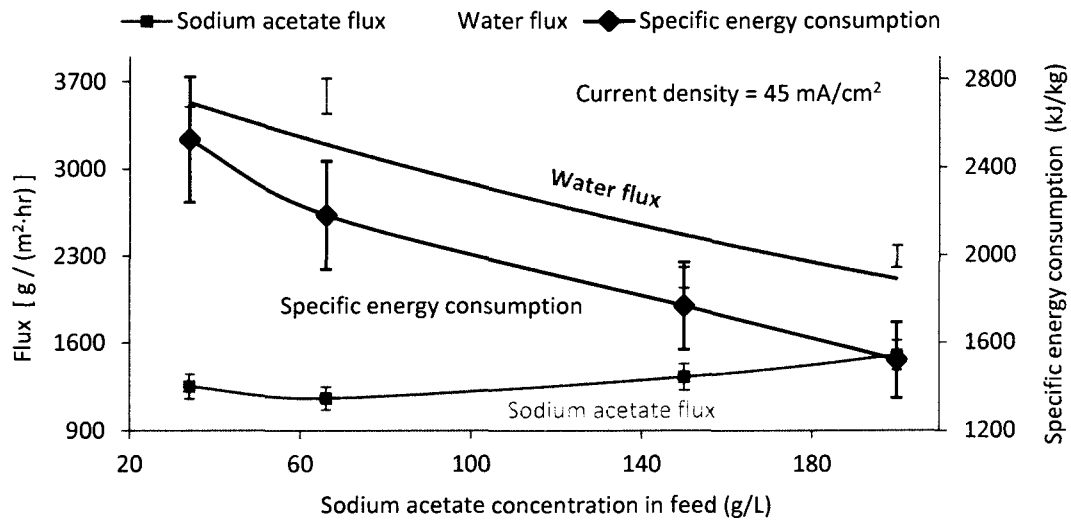


Figure 4.8 Effect of Feed Concentration on Sodium Acetate and Water Fluxes and Specific Energy

4.3.2.2 Effect of Current Density

Figure 4.9 shows the effect of current density on the sodium acetate and water fluxes, and the specific energy consumption. As the current density is increased, the driving force for the process increased leading to an increase in the rate of transfer of ions and water molecules from the feed to the product. Therefore, sodium acetate and water fluxes increased with an increase in the current density. Since the current density is the major driving force in ED, the thermodynamic irreversibility of the process increased with an increase in the current density. Hence, the specific energy consumption also increased with an increase in the current density.

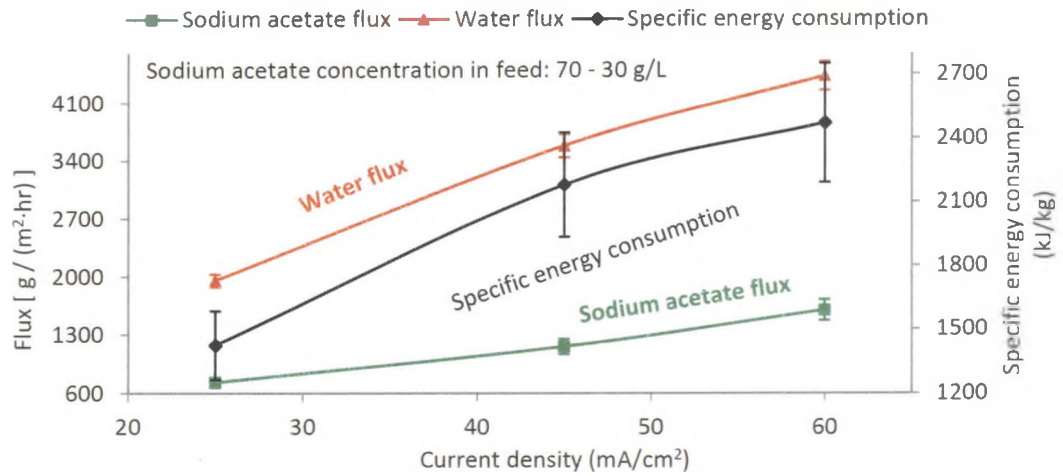


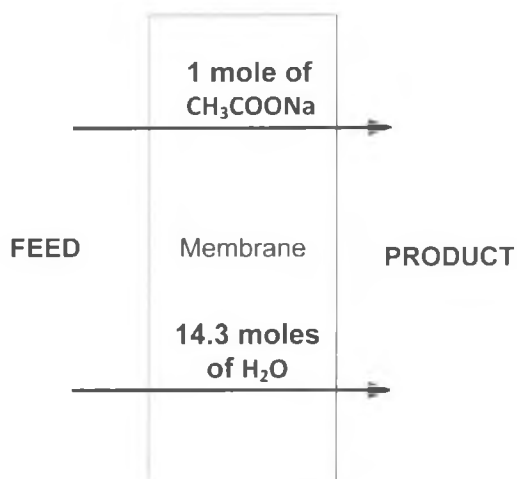
Figure 4.9 Effect of Current Density on Sodium Acetate and Water Fluxes and Specific Energy

4.3.2.3 Maximum Attainable Product Concentration

Electro-osmosis and osmosis result in the transfer of water molecules across the ion exchange membranes. The overall water transport index (OWTI) is defined as the moles of water transported from the feed to the product compartment per unit mole of sodium acetate transported in the same direction.

The OWTI was about 11 to 15 when the initial feed concentration was equal to or less than 85 g/L. For the experiments with initial feed concentrations of 150g/L and 200 g/L, the OWTI was about 7. The decrease in the OWTI was thought to result from a reduction in the solvation at the high concentrations of sodium acetate.

The OWTI dictates the theoretical limit for maximum attainable product concentration. For example, in the experiments with an OWTI of about 14.3, the theoretical maximum attainable product concentration was 1 mole of sodium acetate per 14.3 moles of water, which was equivalent to 273 g/L or about 24% by weight (Figure 4.10). Similarly, for an OWTI of 7, the theoretical limit on the product concentration was about 39% by weight.



$$\text{Overall Water Transport Index (OWTI)} = \frac{\text{moles of H}_2\text{O transported}}{\text{moles of CH}_3\text{COONa transported}}$$

$$\frac{82 \text{ gm CH}_3\text{COONa}}{82 \text{ gm CH}_3\text{COONa} + 257 \text{ gm H}_2\text{O}} \equiv 24 \% \text{ w/w} \equiv 273 \text{ g/L}$$

Theoretical maximum attainable concentration = 273 gm/L

Figure 4.10 Calculation of Overall Water Transport Index

4.3.3 Effect of Tramp Ions of Oxidized White Liquor Extract on Selectivity of Electrodialysis

Figure 4.11 illustrates the variation in the concentrations of feed and product solutions, current, and cell voltage for experiment F-1. In order to be able to compare the relative rate of transfer of the different ions, concentrations of all species are shown in equivalents/L. The concentration of feed was reduced from 0.38 eq/L to 0.1 eq/L during the course of the experiment. The electric energy input was 29.5 W-hours.

All experiments listed in Table 4.3 were performed by applying the same current-time profile as that of experiment F-1. In the cases where the cumulative energy consumption did not reach 29.5 W-hours in about 1.8-1.9 hours after starting the experiment, the experiment was allowed to continue at 0.51 A until the cumulative energy consumption reached the desired value.

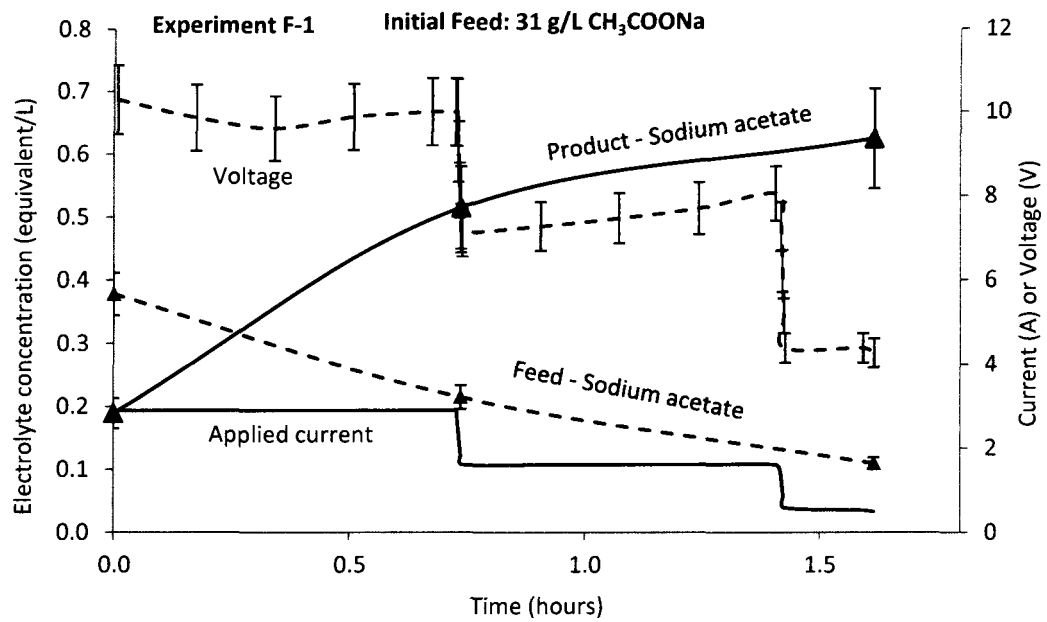


Figure 4.11 Concentrations of Feed and Product, Current and Voltage in Experiment F-1

Figure 4.12 illustrates the variation in the feed and product concentrations for experiment F-2. The final concentration of sodium acetate in the feed solution was slightly higher than that in experiment F-1. Thus, due to the presence of sodium sulfate, the efficiency of the separation process was slightly reduced and the sodium sulfate was also transferred in the product stream.

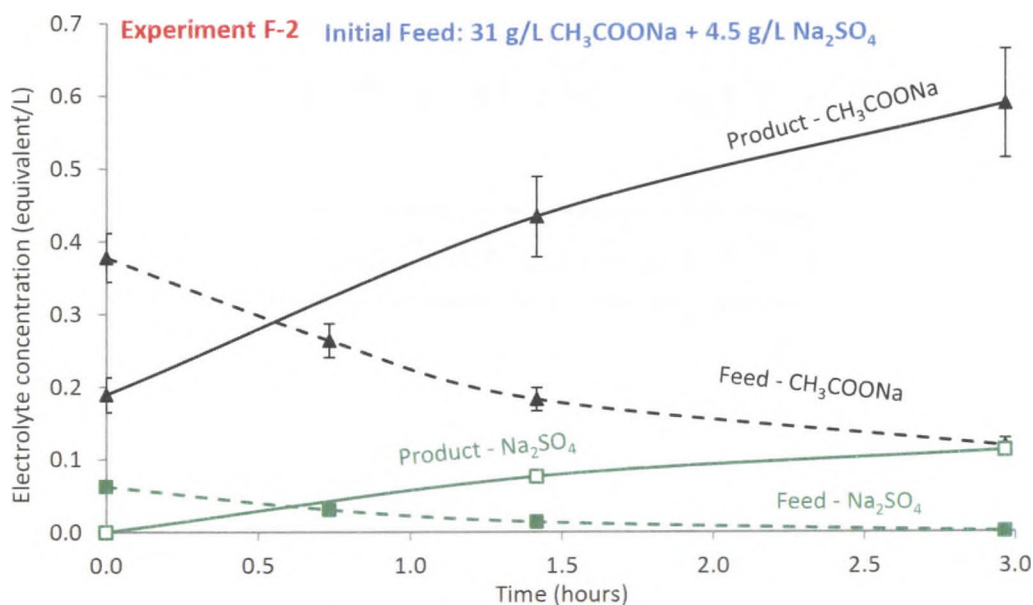


Figure 4.12 Concentrations of Feed and Product Solutions in Experiment F-2

Figure 4.12 also illustrates that the apparent rate of separation of sodium acetate was higher than that of sodium sulfate. The reason for the higher rate of separation can be explained by considering the expression for the electrochemical flux (Equation 2.5).

Table 4.6 lists the properties of the initial feed solutions used in experiments F-2 and F-4. In experiment F-2, the diffusion flux of sodium acetate was higher than that of sodium sulfate because of its high initial concentration and high diffusivity. As shown in Equation 2.5, the electric migration flux is proportional to the product of ionic mobility (u_i) and concentration (C_i) in the feed. Comparing the values of the product of u_i and C_i in Table 4.6, confirms that the electric migration flux was also higher for sodium acetate. Thus, the overall electrochemical flux was higher for sodium acetate compared to sodium sulfate in experiment F-2. The diffusivities of sodium acetate and sodium sulphate were obtained from the literature [Poling et al., 2001 & Rard, 1979].

Table 4.6 Properties of the Feed Solutions Used in Experiments F-2 and F-4

Property/Compound of the Feed Solution	Diffusivity (D_i) in water (m^2/s) [10, 11]	Ionic mobility (u_i)	Initial concentration in feed (equivalent/ m^3)	$U_i \cdot C_i$
CH ₃ COONa (F-2)	1.2×10^{-9}	4.7×10^{-8}	0.38×10^{-3}	1.80×10^{-11}
CH ₃ COONa (F-4)				
Na ₂ SO ₄ (F-2)	0.9×10^{-9}	7×10^{-8}	0.06×10^{-3}	0.44×10^{-11}
Na ₂ SO ₄ (F-4)			0.24×10^{-3}	1.72×10^{-11}

Figure 4.13 shows the variation in the feed and product concentrations for experiment F-3. The apparent rate of separation of sodium acetate was slightly higher than those of the rest of the components. The rates of separation of sodium sulphate and sodium carbonate were almost equal. The final concentration of sodium acetate in the feed solution was much higher than those in the previous experiments, and it showed a further decrease in the efficiency of the separation process.

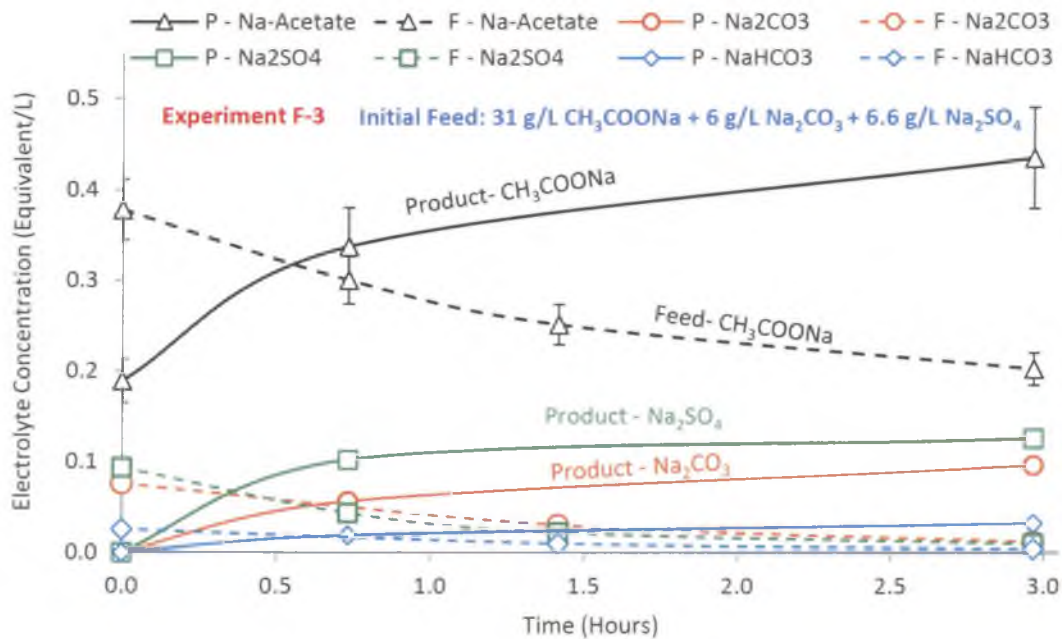


Figure 4.13 Concentrations of Feed and Product Solutions in Experiment F-3

Figure 4.14 shows the changes in the feed and product concentrations for experiment F-4. This experiment was performed in duplicate to check the repeatability of the experimental data. The final concentration of sodium acetate in the feed was about 0.3 eqv/L, much higher than that in experiment F-1 (0.11 eqv/L). In this experiment, the apparent rate of separation of sodium sulfate was higher than that of sodium acetate. However, the higher rate of separation of sodium sulfate could not be explained using Equation 2.5 because the product of ionic mobility (u_i) and initial feed concentration (C_i) was almost the same for sodium acetate and sodium sulfate (Table 4.6).

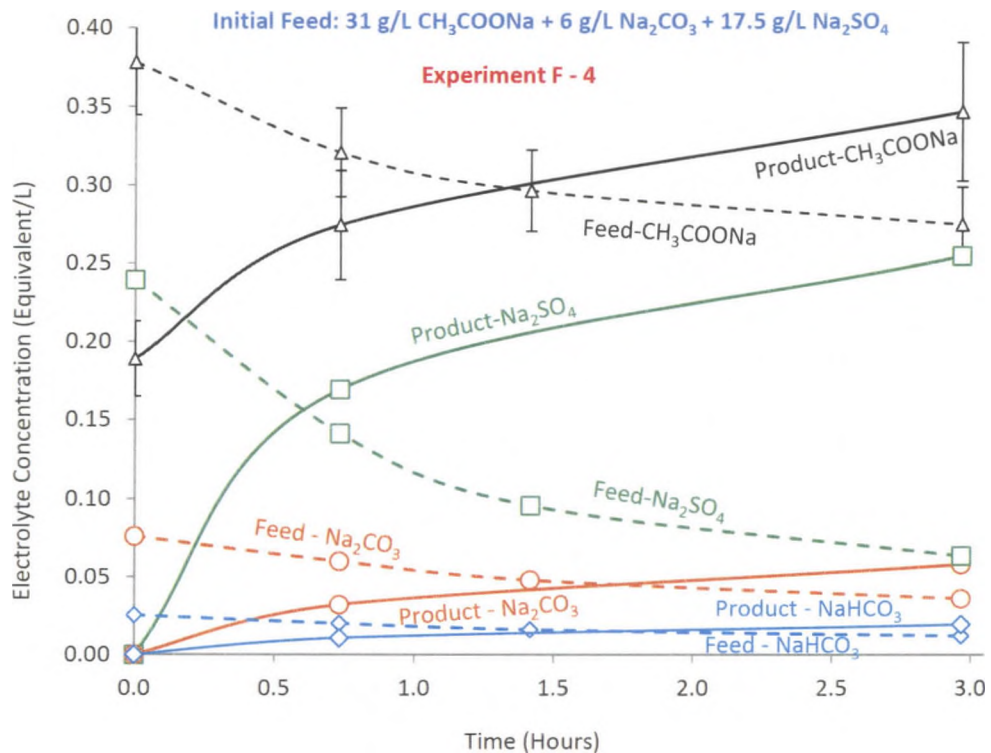


Figure 4.14 Concentrations of Feed and Product Solutions in Experiment F-4

Figure 4.15 shows the comparison of variation in feed concentration for all experiments and the effect of NaOH, Na₂CO₃ and Na₂SO₄ on the separation of sodium acetate from the synthetic extract.

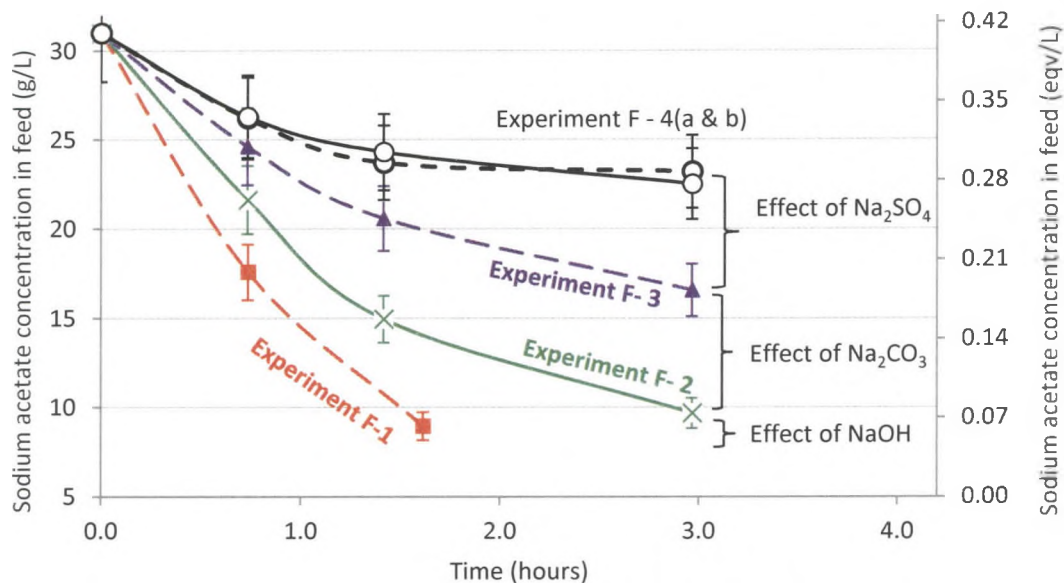


Figure 4.15 Variation in Feed Concentration for Separation Experiments

The separation factor for sodium acetate (SF_{NaAc}) is defined as the fractional amount of the sodium acetate in the feed solution that is transferred into the product compartment (Equation 2.16). The separation factor was corrected for the amount of sodium acetate that was lost when the samples were removed for analysis.

When comparing the results of experiments F-1 and F-4, the data showed that the separation factor for sodium acetate was reduced from 75% to 35% due to the presence of other components in the feed solution.

The sodium acetate and sodium carbonate mass balances closed between 90 to 100% for all experiments, whereas the sodium sulfate mass balance closed between 82 to 106%.

4.3.4 Electrodialysis Experiments Using Pre-Treated Extracts

Figure 4.16 shows the photos of pre-treated extracts. The clarified extract was clear and it did not contain much lignin.

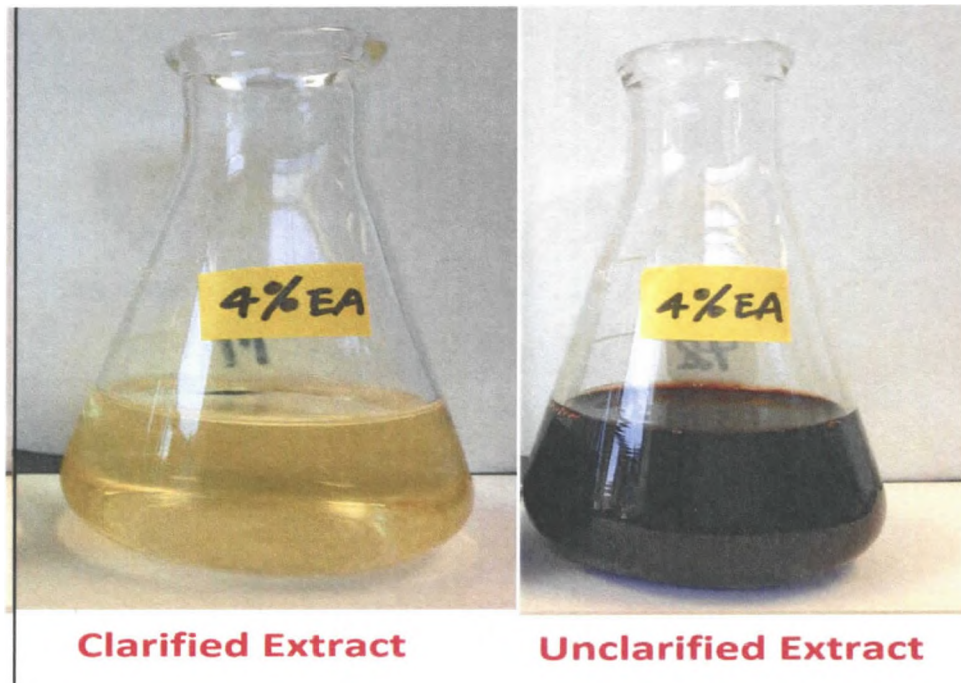


Figure 4.16 Photos of clarified and unclarified wood extracts

Figures 4.17 and 4.18 show the concentrations of the major components of the feed and product solutions in the ED experiments performed using pre-treated extracts. It can be seen that approximately the same amounts of sodium acetate and sodium formate were transferred from the feed solution to the product solution in the both experiments.

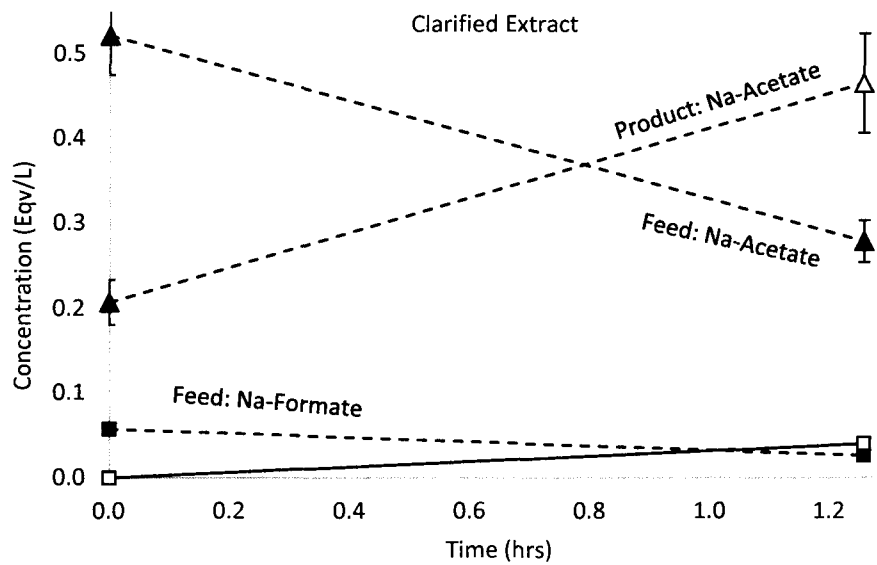


Figure 4.17 Concentration Profiles for ED Experiment Performed Using Clarified Extract

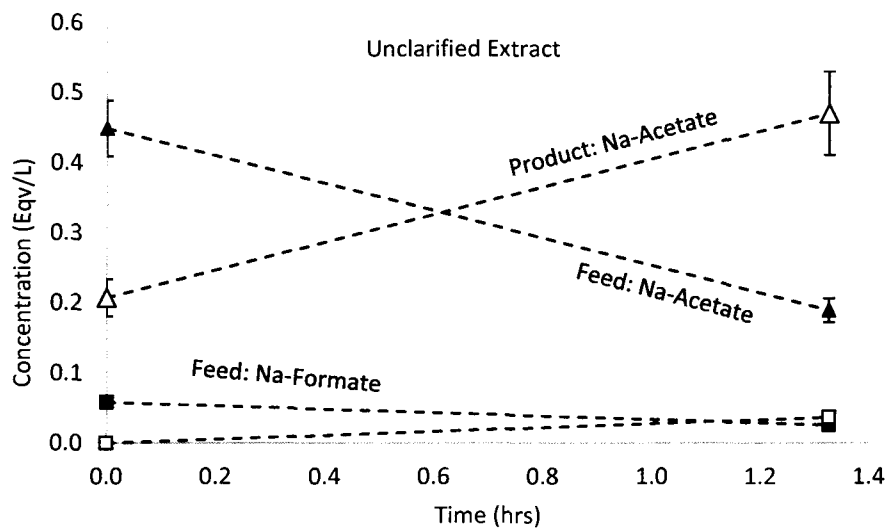


Figure 4.18 Concentration Profiles for ED Experiment Performed Using Unclarified Extract

Tables 4.7 and 4.8 summarize the concentrations of various components present in the feed and the product solutions from both ED experiments. Both the clarified and unclarified feed solutions also contained small amounts of sodium lactate and sodium glycolate, which were transferred into the product solutions. However, the total sugars and the lignin were

mostly retained in the feed solutions. The small amounts of sugars transferred from the feed to the product as shown in Tables 4.7 and 4.8 are thought to occur by *diffusion* since the component sugars are not charged. At pH 10, the lignin in solution would exist in ionic form as the phenolate ion. Under these conditions, the voltage drop across the membranes could electrochemically transfer some of the lignin across the membrane. These experiments suggest that ED can be used to obtain a clear solution of concentrated salts such as sodium acetate and sodium formate provided that the presence of lignin in the feed solution does not lead to appreciable fouling of the membranes in long run.

Table 4.7 Concentration of Feed and Product Solutions for the ED Experiment Performed using Clarified Extract

	Concentrations (Eqv/L)						Total Lignin (g/L)	Total Sugars (g/L)	pH	Vol. (L)
	Na-Acetate	Na-Formate	Na-Lactate	Na-Glycolate	Total Na Ion					
					By HPLC	By ICP				
Initial Feed	0.51	0.06	0.0079	0.0111	0.60	0.63	0.40	0.20	10.5	1.65
Final Feed	0.28	0.03	0.0038	0.0129	0.32	0.35	0.27	0.18	10.9	1.52
Initial Product	0.21	0.00	0.0000	0.0000	0.21	---	0.00	0.00	8.9	0.99
Final Product	0.46	0.04	0.0044	0.0068	0.51	0.51	0.21	0.03	10.1	1.15

Table 4.8 Concentration of Feed and Product Solutions for the ED Experiment Performed using Unclarified Extract

	Concentrations (Eqv/L)						Total Lignin (g/L)	Total Sugars (g/L)	pH	Vol. (L)
	Na-Acetate	Na-Formate	Na-Lactate	Na-Glycolate	Total Na Ion					
					By HPLC	By ICP				
Initial Feed	0.45	0.06	0.0073	0.0197	0.53	0.58	9.66	1.56	10.4	1.50
Final Feed	0.19	0.03	0.0023	0.0157	0.23	0.31	9.25	1.42	10.6	1.39
Initial Product	0.21	0.00	0.0000	0.0000	0.21	---	0.00	0.00	8.8	1.00
Final Product	0.47	0.04	0.0060	0.0038	0.52	0.47	0.30	0.02	9.9	1.27

For the ED experiment with clarified extract, the sodium ion concentration data obtained using ICP-OES was almost similar to the HPLC data. However, for the experiment with unclarified extract, the concentration of sodium ion in the feed solution was slightly higher when determined using ICP. This difference can be potentially attributed to the presence of sodium salts of lignin which were not identified in HPLC analysis.

Table 4.9 shows the current efficiency, the specific energy and the relative number of moles of each species transported for the ED experiments performed using pre-treated extracts. In Table 4.9, the relative number of moles of each species transported was estimated using equation 2.17 b. Current efficiencies in the experiments performed with the clarified and

unclarified extracts were similar to that of the experiments performed using synthetic sodium acetate. The experiment with pre-treated extracts required slightly higher energy than the experiment with synthetic sodium acetate; that is 195 to 207 kJ/equivalent of salt for the pre-treated extracts compared to 174 kJ/equivalent of salt for the synthetic solution.

The relative number of moles of each species transported during the process also indicates the fraction of the total useful electric energy spent for transporting the given salt molecule from feed to the product compartment. Since the synthetic sodium acetate solution contained only sodium acetate, all of the useful electric energy was spent for transporting only sodium acetate. The pre-treated extract contained additional tramp salts such as sodium formate, sodium lactate and sodium glycolate which were also transported along with sodium acetate. Hence, about 15 % of the useful electric energy was lost in transporting tramp salts.

Table 4.9 Comparisons of the ED Experiments Performed Using Pre-Treated Extracts

	Type of Feed Solution		
	Synthetic Sodium Acetate Solution	Clarified Extract	Unclarified Extract
Current Efficiency (%)	90 ± 2.5	90 ± 2.5	94 ± 2.6
Specific Energy (kJ/Equivalent of Salt Transported)	174 ± 14.6	195 ± 16.4	207 ± 17.4
Relative Number of Moles of Each Species Transported (%)			
Sodium Acetate	100	86.4	86.3
Sodium Formate	-----	11.4	10.6
Sodium Lactate	-----	1.4	1.6
Sodium Glycolate	-----	0.8	1.4

The mass balances for the major components of the extracts such as sodium acetate, sodium formate and lignin was estimated to close to between 90 and 100%. The color of the anion exchange membranes was slightly changed after processing the unclarified extract in the ED apparatus. However, no color change was observed after processing clarified extract. Most likely the color change in the anionic membrane after processing the unclarified extract was due to the presence of traces of lignin in the membrane.

CHAPTER 5

SPLITTING OF SODIUM ACETATE USING BI-POLAR MEMBRANE ELECTRODIALYSIS

5.1 Introduction

This chapter summarizes experimental data on the splitting of sodium acetate using bipolar membrane electrodialysis (BPMED). Experiments were performed using (1) dilute sodium acetate solutions and (2) pre-treated wood extracts. Regarding the pre-treated wood extracts, experiments were performed using clarified hardwood extract that had been pre-treated to *partially remove dissolved lignin, and also unclarified hardwood extract.*

Preliminary Scoping Experiments using Sodium Acetate: Initially, batch scale experiments were performed using dilute sodium acetate to gain an understanding of the effects of current density, feed-salt concentration and electro-osmosis, all of which are the major parameters that affect BPMED process. The secondary objective of these experiments was to determine the maximum achievable concentrations of acetic acid and sodium hydroxide in the BPMED process.

Study of Effect of Feed Concentration using Feed and Bleed Mode Experiments: Secondly, feed and bleed mode experiments were performed to simulate semi-batch processing using synthetic dilute sodium acetate solution. The purpose of these experiments was to determine the optimum concentration of sodium acetate in the inlet salt (feed) solution, and estimates for the current efficiencies, energy consumption and other system parameters important in salt splitting. In these experiments, the goal was to produce product solutions containing about 170 g/L of acetic acid and 30 g/L of sodium hydroxide solutions. These product concentrations were selected based on the results of the preliminary scoping experiments. The acetic acid product with 16-20 wt % concentration can be economically upgraded to glacial acetic acid if desired, and 3 wt% NaOH is about the concentration desired for use in the extraction experiments.

Experiments Using Pre-Treated Extracts: Pre-treated wood extract was processed through the BPMED apparatus to produce acetic acid and caustic and to estimate the electric energy consumption, current efficiency and selectivity of the process. The selectivity of the electrochemical reactions was estimated based on the amount of tramp salts of extract transported from feed to product solutions. Two types of pre-treated wood extracts, similar to those mentioned in Chapter 4, were evaluated as feed in the BPMED apparatus. These were again designated as (1) Clarified and (2) Unclarified wood extracts. As mentioned previously, these types of experiments are useful for obtaining data for the design and scale-up of BPMED systems.

5.2 Experimental Methods

This section contains information about the equipment used in this work and methodology used for the selection of experimental conditions.

5.2.1 Experimental Apparatus

The overall BPMED apparatus used for the splitting experiments was almost the same as the ED apparatus used in the separation experiments. The only difference was that different types of cationic and anionic membranes were used and their arrangement in the cell was modified. One additional electrolyte solution stream had to be added to the cell since the new configuration had two products. Since the splitting of sodium acetate using BPMED results in the production of caustic which can diffuse back into the salt and acid compartments, the BPMED cell was constructed using Neosepta AHA, CMB and BP-1 membranes (Tokuyama America; Arlington Heights, IL, USA) which are stable over the entire pH range expected in the process. Figure 5.1 shows the arrangement of membranes for the unit cell pair of a three-compartment

BPMED cell. The cell used in the present experiments contained five cell pairs. The surface area of each membrane was 64 cm².

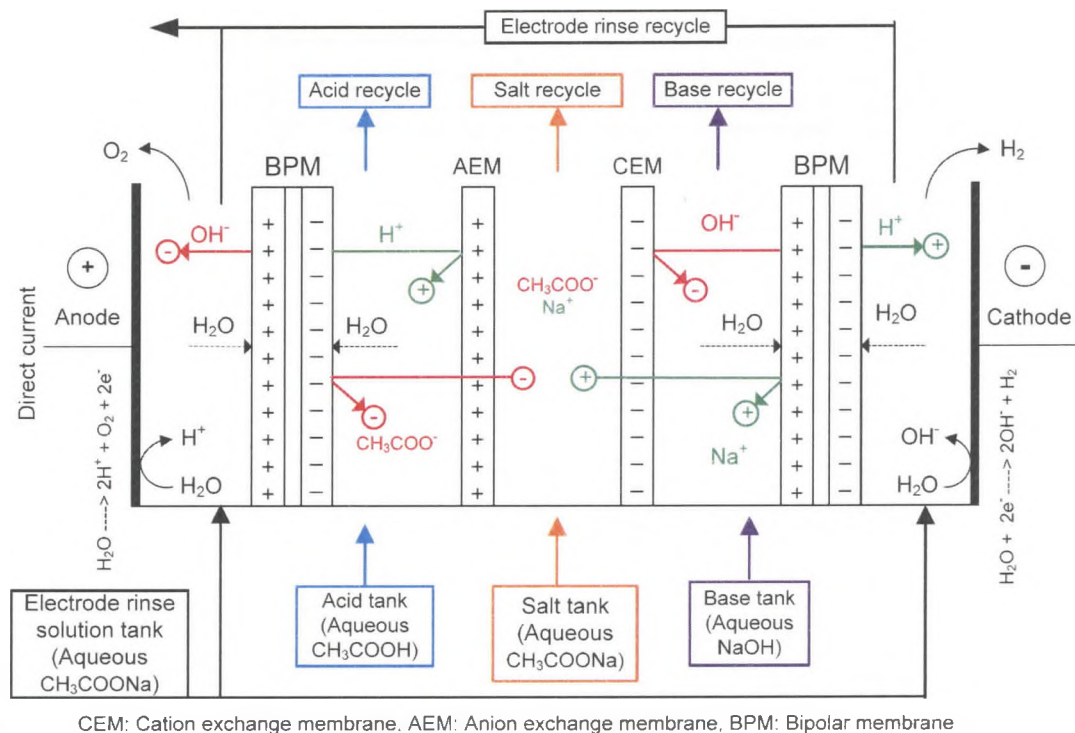


Figure 5.1 Configuration of a Three-Compartment Bi-Polar Membrane Electrodes Cell

The maximum allowed voltage drops for the different components of the BPMED cell are shown in Table 5.1. The maximum allowed voltage drop for the BPMED cell used in this study was 16.4 volts.

Table 5.1 Maximum Allowed Voltage Drop for Different Components of the BPMED Cell

Component	Maximum Voltage (V)	Quantity	Total Voltage
Cation Exchange Membrane	0.4	6	2.4
Anion Exchange Membrane	0.4	5	2
Bi-Polar Membrane	1.2	5	6
Electrodes (Anode and Cathode)	6	1	6
Maximum allowed voltage for the BPMED cell used in this work (V)			16.4

A schematic diagram of the BPMED apparatus being operated in the batch mode used in this study is illustrated in Figure 5.2 and shows the circulation of the acid, salt, base and electrode rinse flow streams. The equipment also had a heat exchanger (not shown).

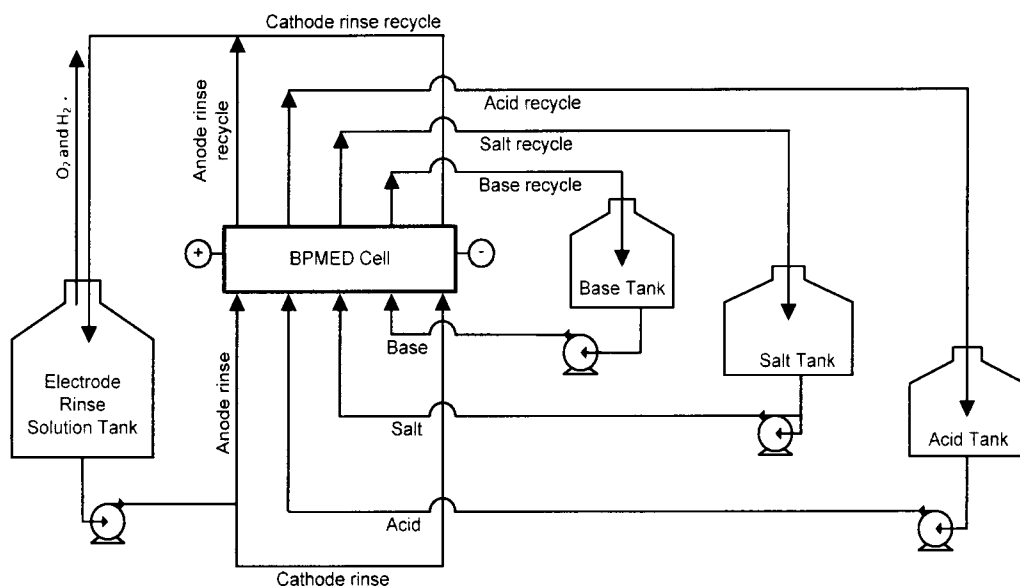


Figure 5.2 Schematic Diagram of BPMED Apparatus Operated in the Batch Mode

5.2.2 Experimental Procedure

The BPMED process was operated using constant current mode. The procedure for performing the BPMED experiments was the same as that of the ED experiments. All experiments were conducted in the recycle batch mode illustrated in Figure 5.2.

The salt solution was recirculated at a constant flow rate as shown in Table 5.2. The recirculation rates of the acid, base and the electrode rinse solutions were adjusted to maintain a constant pressure at the inlet to the BPMED cell.

Table 5.2 Circulation Rates of the Salt Solution

Experiment	Flow rate of salt solution (mL/min)	Superficial velocity (cm/sec)
Batch	550	5.1
Feed and Bleed Mode	410-510	3.8-4.7

5.2.3 Experimental Design

As previously discussed in Chapter 2, for electro dialysis, there is a trade-off between membrane cost and energy costs. The optimum current density is determined by plotting the cost for the electrical energy, the cost of the membranes and fixed charges associated with capital cost for the equipment as a function of current density. At the optimum current density, the yearly operating cost reaches a minimum (Figure 5.3).

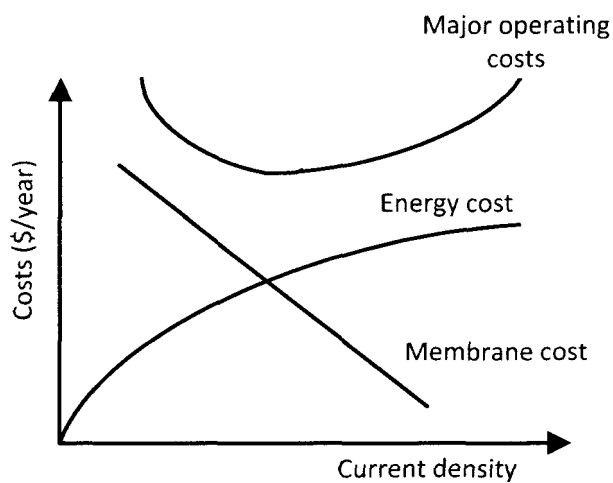


Figure 5.3 Costs in Electro dialysis as a Function of the Applied Current Density

According to published guidelines for BPMED, the current density should be 50 to 100 mA/cm² [Mani, 1991]. However, since sodium acetate is not a highly-conductive salt and acetic acid is a weak acid, the experiments in this work were performed at 60 and 40 mA/cm². Based on the limiting current density data shown in Figure 5.4, the alkaline hardwood extract must be concentrated to increase its sodium acetate concentration so that it can be practically processed at a current density higher than 15 mA/cm².

The published guidelines for BPMED also state that the initial conductivity of the salt solution used in the BPMED process must be higher than 35 mS/cm [Mani, 1991]. This value of conductivity corresponds to a sodium acetate concentration of 51 g/L which represents the minimum feed concentration required for application of BPMED. However, in order to study the effect of sodium acetate concentration in the feed-salt solution over a broader range, additional concentrations such as 85 g/L and 130 g/L were also used as the feed concentrations.

5.2.3.1 Determination of Limiting Current Density

As previously discussed in Chapter 4, the limiting current density was determined by following Cowan and Brown's procedure [1959].

5.2.3.2 Preliminary Scoping Experiments using Sodium Acetate

In these experiments, no material was added or removed from the system after the initial charge of the salt, base, acid and rinse solutions. The initial acid and base solutions contained some sodium acetate and sodium hydroxide, respectively, to maintain some minimum electrical conductivity in the acid and base compartments and to avoid high voltage drops across the BPMED cell. Table 5.3 provides operating parameters for the batch experiments.

Table 5.3 Batch Experiments using Bi-Polar Membrane Electrodialysis

Initial Concentration of Sodium Acetate in the Salt Solution and Volume of the Solution	Current Density	
	30 mA/cm ²	60 mA/cm ²
130 g/L, 2 Liters	----	Experiment - 1
85 g/L, 2 Liters	Experiment - 3	Experiment - 2
51 g/L, 2 Liters	Experiment - 4	----

The concentration of sodium acetate in the initial acid solution was varied between 42 to 70 g/L depending upon the experiment. The concentration of sodium hydroxide in the initial

base and rinse solutions was 6 g/L and 40 g/L, respectively. The initial volumes of acid, base and rinse solutions were one liter each.

5.2.3.3 Study of Effect of Feed Concentration using Feed and Bleed Mode Experiments

Feed and bleed experiments represent semi-batch operation of the BPMED system. These experiments were performed to determine the optimum concentration of sodium acetate in the inlet salt (feed) solution, the current efficiencies, the energy consumption and other system parameters required for the production of about 160 g/L of acetic acid and 30 g/L of sodium hydroxide solutions.

In electrodialysis, as the concentration of an ion or a molecule increases in the product compartment, the rate of back-diffusion of this ion or molecule also increases and the current efficiency is subsequently reduced. Therefore, current efficiency is a function of the product concentration. Consequently, it is necessary to experimentally achieve the desired product concentration to accurately determine the current efficiency for that concentration. In order to achieve such a high concentration of acetic acid (160 g/L) using laboratory scale equipment, long duration experiments termed "Feed and Bleed Mode" were performed.

In the feed and bleed experiments, when the concentration of sodium hydroxide in the base compartment reached about 30 g/L, most of the base solution was drained from the receiver and approximately the same quantity of water was added. This was done to restore the concentration of residual sodium hydroxide in the base solution to about 5 to 6 g/L. Furthermore, as the concentration of sodium acetate in the feed-salt solution reached the limiting concentration for the given current density, the residual salt solution was drained and a new batch of sodium acetate was charged. However, the volume of the acid solution was allowed to build up until the acid tank was completely filled. At this time, about 300 to 500 mL of solution was drained and no water was added into the acid compartment.

Table 5.4 lists the feed and bleed mode experiments performed using BPMED. These experiments were performed using dilute sodium acetate solution. In order to establish a baseline for comparing the results of these experiments, approximately the same quantity of salt was split in each experiment.

Table 5.4 Feed and Bleed Mode Experiments using Bi-Polar Membrane Electrodialysis

Experiment Number	Current Density (mA/cm ²)	Initial Concentration of Sodium Acetate in Salt Solution and Total Volume Processed	Concentration of Sodium Hydroxide in Initial Base Solution and Volume of the Solution
FB-1	60	130 g/L, 10.75 Liters	4.3 g/L, 2.3 Liters
FB-2	60	85 g/L, 20 Liters	3.8 g/L, 3.7 Liters
FB-3	40	50 g/L, 38.75 Liters	5.1 g/L, 5.6 Liters

Since acetic acid is a weak acid, the initial acid solution was made up of 1 Liter of 150 g/L sodium acetate to maintain some minimum conductivity in the acid compartment until the end of the experiment. There are two phenomena that decrease the conductivity of the acid solution as acid is produced. Firstly, when an anion and a proton are transferred into the acid compartment, some amount of water also gets transferred into the acid compartment and thus, the conductivity of the acid solution is lowered due to the dilution of the solution. Secondly, as more and more acetic acid molecules are formed in the acid solution, the conductivity of the acid solution decreases due to the increase in the collisions between the acid and salt molecules. The initial electrode rinse solution consisted of 1 Liter of 40 g/L sodium hydroxide solution, here again to achieve some minimal level of conductivity.

5.2.3.4 Experiments using Pre-Treated Extracts

The pre-treated extracts were prepared following the procedure shown in Figure 4.3. The concentration of sodium acetate in the pre-treated extracts used in the BPMED experiments was maintained at 55-45 g/L so that these solutions could be processed at a middle-level current density of 40 mA/cm². Table 5.5 summarizes the composition and volumes of the pre-treated

(feed) solutions used in the BPMED experiments. The concentration of the raw hardwood extract is also given.

Table 5.5 Composition of Pre-Treated Hardwood Extracts (4% EA, 0% S, and 80 °C)

	Concentration (g/L)						pH	Volume (L)
	Na-Acetate	Na-Formate	Na-Lactate	Na-Glycolate	Total Lignin	Total Sugars		
4% EA Caustic Extract (80 °C)	14.60	1.55	0.28	0	4.52	0.76	12.2	---
Unclassified extract	46.20	3.24	1.72	0	12.07	2.11	10.2	1.74
Clarified extract	56.50	3.28	1.18	0	0.62	0.25	10.5	1.64

In the BPMED experiments, the initial liquid placed in the acid receiving vessel was one liter of 17 g/L sodium acetate. The initial liquid placed in the base receiving vessel and the liquid used as the electrode rinse solutions consisted of one liter each of 6 g/L and 40 g/L of sodium hydroxide, respectively. Approximately the same amounts of electric energy and charge were applied in the BPMED experiments using pre-treated extracts.

The concentrations of sodium acetate, sodium formate and sodium lactate in the acid compartment were measured at the conclusion of each experiment following conversion to their corresponding acids using high performance liquid chromatography (HPLC). The concentration of sodium hydroxide in the base compartment was determined by titration.

Since sodium formate and sodium lactate were also present in the extracts, it was expected that smaller quantities of formic and lactic acids would be present in the acid compartment in addition to the desired acetic acid product. The total concentration of all acids present in the final acid solution was separately determined by titration with base. This independent check was thought necessary since it was felt that the HPLC measurements may not have identified all the component acids present in the acid solution.

5.3 Results and Discussion

This section contains detailed discussion about the results of the salt splitting experiments.

5.3.1 Determination of Limiting Current Density

Figure 5.4 shows the limiting current density as a function of the sodium acetate concentration in the salt compartment for the Neosepta AHA/CMB membranes. The limiting current density increased linearly with increasing sodium acetate concentration.

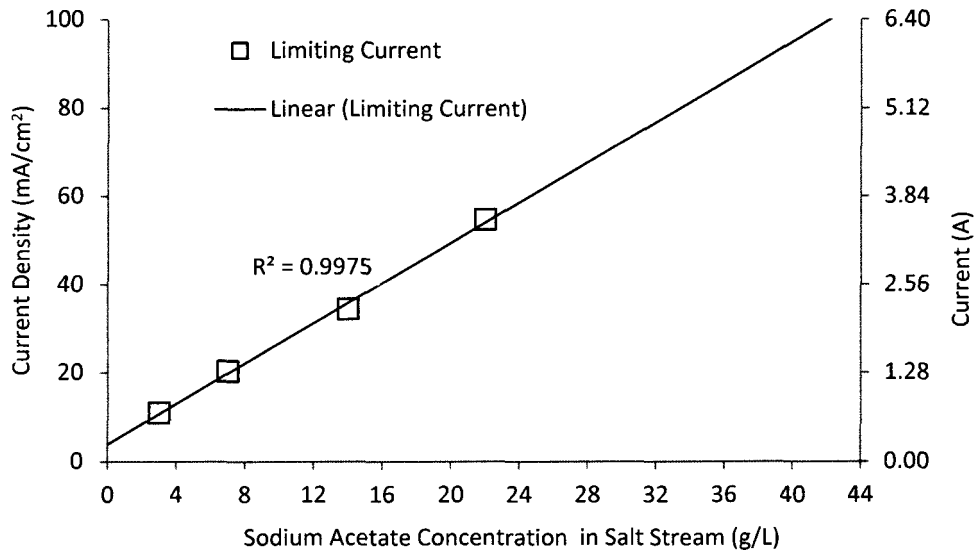


Figure 5.4 Limiting Current Density for Neosepta AHA/CMB Membranes

5.3.2 Preliminary Scoping Experiments using Sodium Acetate

Figure 5.5 shows the change in the concentration of sodium acetate in the salt solution over time for the batch experiments. All experiments were terminated when the applied current density became approximately equal to or slightly higher than the limiting current density for the given concentration of sodium acetate in the salt solution. For the applied current densities of 60 mA/cm² and 30 mA/cm², the limiting concentration of sodium acetate was about 30 g/L

and 20 g/L, respectively. For the experiments performed at the same current densities, the slopes of the salt concentration profiles (or the rate of decomposition of salt) were almost equal. This observation was interpreted to mean that the salt concentration did not have an appreciable effect on the BPMED process.

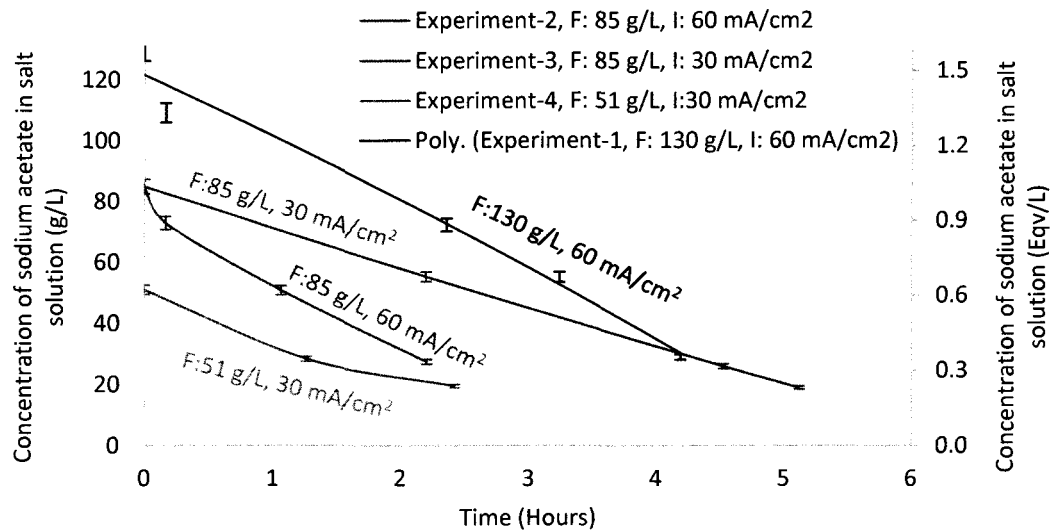


Figure 5.5 Concentration of Sodium Acetate in Salt Solution during Batch Experiments

The concentration profiles for acetic acid and sodium hydroxide in the acid and base solutions, respectively, are shown in Figures 5.6 and 5.7 respectively. In each experiment, approximately 0.5 to 2 equivalent/L of acid and base were formed depending upon the initial concentration of sodium acetate in the salt solution and the time that the BPMED apparatus was operated. Theoretically for each equivalent of acetic acid formed, one equivalent of sodium hydroxide should also be formed. The data shown in Figures 5.6 and 5.7 for the acetic acid and caustic formed are seen to overlap at the same current densities. These results confirm the well-known axiom that current density is the major variable governing the BPMED process.

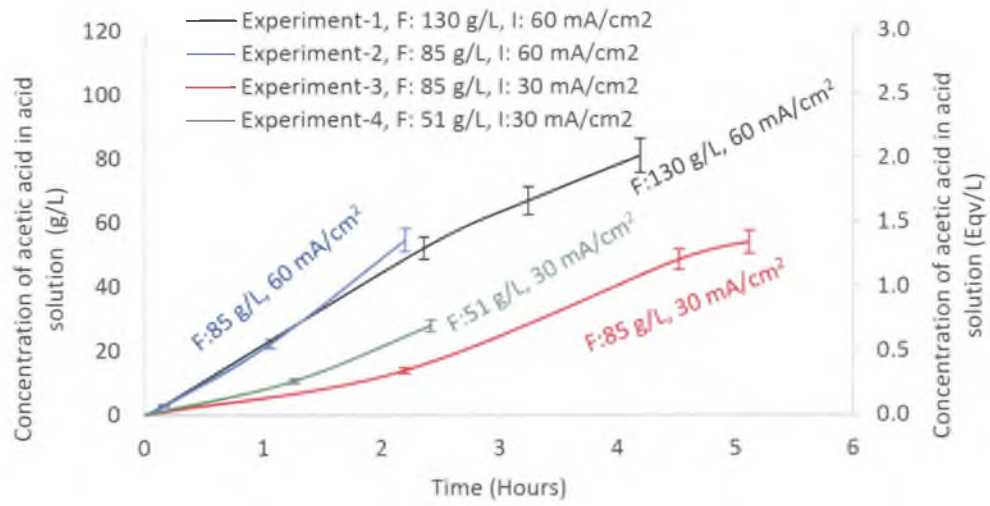


Figure 5.6 Concentration of Acetic Acid in Acid Solution during Batch Experiments

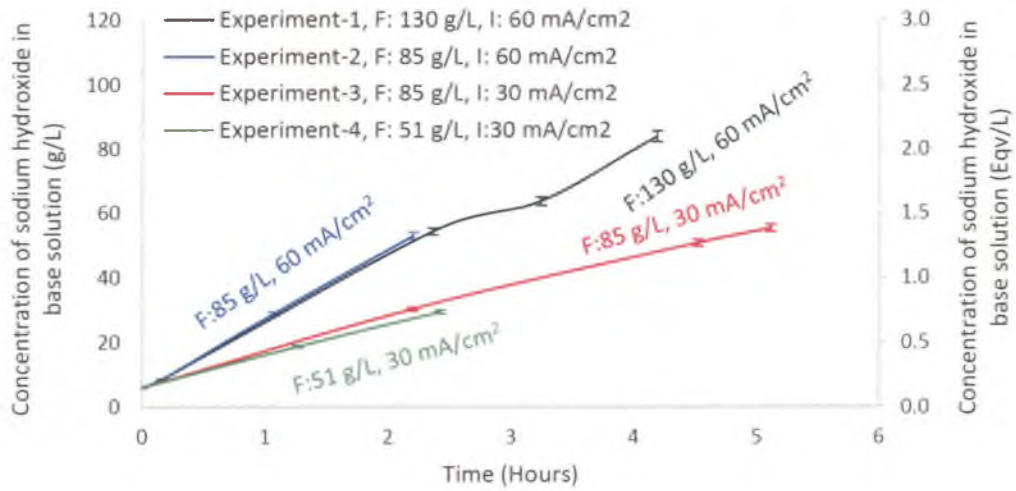


Figure 5.7 Concentration of Sodium Hydroxide in Base Solution during Batch Experiments

Figures 5.8, 5.9 & 5.10 show the variations in the volumes of solution as a function of time in the salt, acid and base compartments, respectively. As discussed previously, the volume of salt (feed) solution decreased with time due to electro-osmosis (transfer of water molecules

of hydration along with the ions) and osmosis. Concurrently, the volumes of acid and base solutions (products) increased with time.

The experiments performed at the same current densities had almost equal rates of transfer of water out of the feed compartment (Figure 5.8) and into the acid (Figure 5.9) and base (Figure 5.10) product compartments. Therefore, here again, current density was the major factor that affected the results.

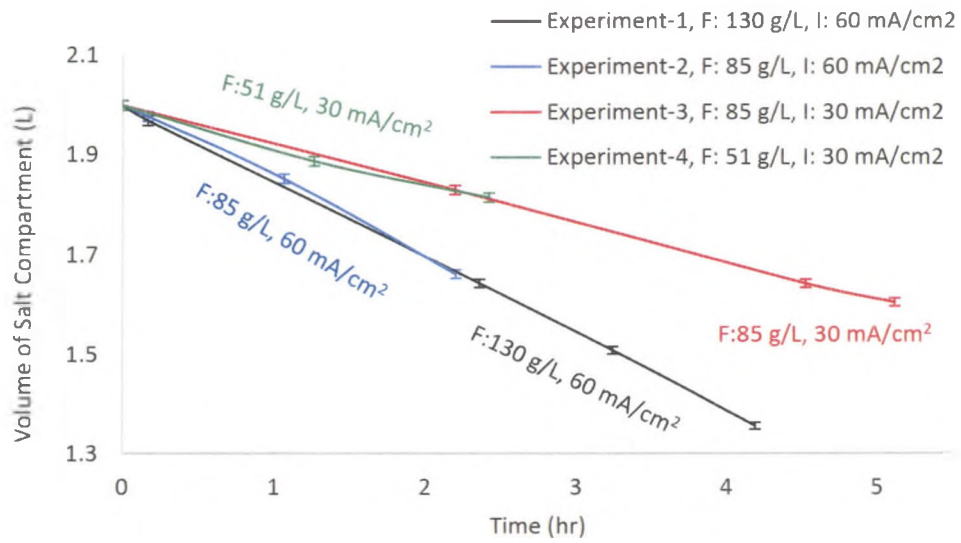


Figure 5.8 Volumes of Salt Solutions during Batch Experiments

The final volumes of all electrolyte solutions drained from their respective tanks were corrected for the amount (50 mL) that remained in the transfer lines of the equipment. This increase in the volumes of electrolyte solution is an artifact of the measurement techniques and not due to the electro dialysis process, and consequently is not shown on the graphs.

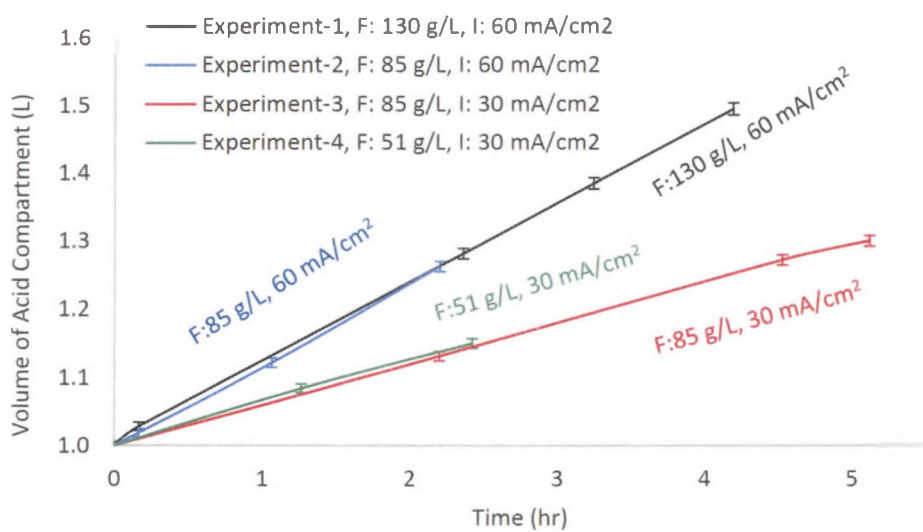


Figure 5.9 Volumes of Acid Solutions during Batch Experiments

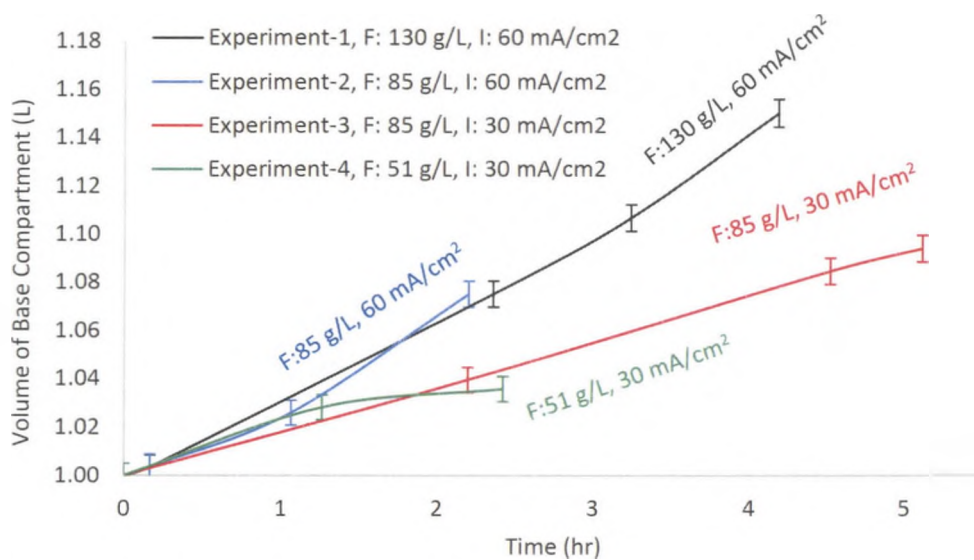
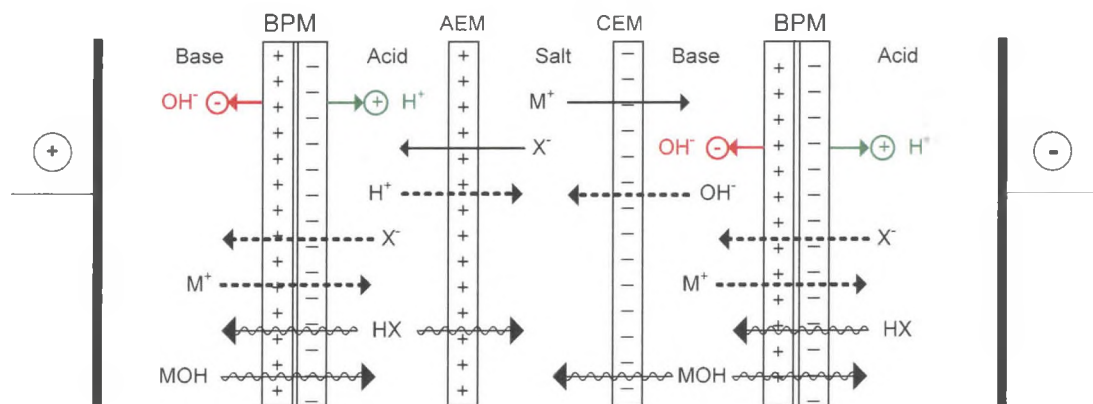


Figure 5.10 Volumes of Base Solutions during Batch Experiments

Theoretically, the base and salt solutions from the BPMED experiments should contain only sodium hydroxide and sodium acetate, respectively. However, the final base solution contained about 0.5 g/L of sodium acetate and the final salt solution contained 1.6 g/L of

sodium hydroxide. These contaminants result because of the back diffusion of ions/molecules across the different compartments (Figure 5.11). As explained in Section 2.7.2, back-diffusion reduces the current efficiencies of the BPMED process and thus, set an upper limit to the concentration of acids and bases that can be efficiently achieved using the BPMED process [Paleologou et al., 1992].



CEM: Cation exchange membrane, AEM: Anion exchange membrane, BPM: Bi-polar membrane

Figure 5.11 Pathways for Diffusion in Bi-Polar Membrane Electrodialysis Process

Table 5.6 shows the overall water transport indices (OWTI) and the maximum achievable product concentrations for the batch BPMED experiments. OWTI indicates the moles of water transported into a given compartment per unit mole of acid or base formed in the same compartment. It can be seen that, for the experiments performed at same current densities, the OWTI increased with a decrease in the feed-salt concentration. This trend is in agreement with the results discussed in Chapter 4 for the ED experiments, and is due to the decrease in the transport of water molecules of hydration at higher salt concentrations. Although the current density affects considerably the rate of water transport, it seems to have a marginal effect on the OWTI.

The amount water transported along with acetic acid is much higher than that for the sodium hydroxide and this difference can be attributed to the difference in their solvation

numbers. The sum of the solvation numbers of acetate (2.2) and H⁺ (12) ions is much higher than that of sodium (3.5) and hydroxide (2.7) ions [Marcus, 1991].

Table 5.6 Overall Water Transport Indices and Maximum Achievable Product Concentrations

Experiment No.	Experimental Conditions	Estimated Maximum Achievable Concentration (g/L)		Overall Water Transport Index (OWTI)	
		Acetic Acid in Acid Solution	Sodium Hydroxide in Base Solution	Acetic Acid	Sodium Hydroxide
Experiment-1	F: 130 g/L, Current: 60 mA/cm ²	255	635	10.1	1.3
Experiment-2	F: 85 g/L, Current: 60 mA/cm ²	285	723	8.7	0.9
Experiment-3	F: 85 g/L, Current: 30 mA/cm ²	245	609	10.4	1.4
Experiment-4	F: 51 g/L, Current: 30 mA/cm ²	227	754	11.8	0.7

The maximum achievable product concentrations shown in Table 5.6 were calculated using the OWTI listed in the same table. These concentrations are affected by the corresponding current efficiencies and overall water transport indices. Up to 220-280 g/L solution of acetic acid can be readily produced using BPMED and this concentration seems to be sufficient for upgrading the BPMED product to glacial acetic acid. Although about 600 to 700 g/L solution of sodium hydroxide can also be produced using BPMED, 30 g/L solution was felt sufficient for reuse in the extraction process. Using such a low concentration of caustic significantly reduces losses due to the back-diffusion of the product.

Figure 5.12 shows variation in the current and voltage for Experiment-2. Both of these parameters were always maintained below their limiting values. Approximately 140 Watt-Hours of electric energy was required to bring about the given changes in the concentrations of the salt, acid and base solutions in this particular experiment.

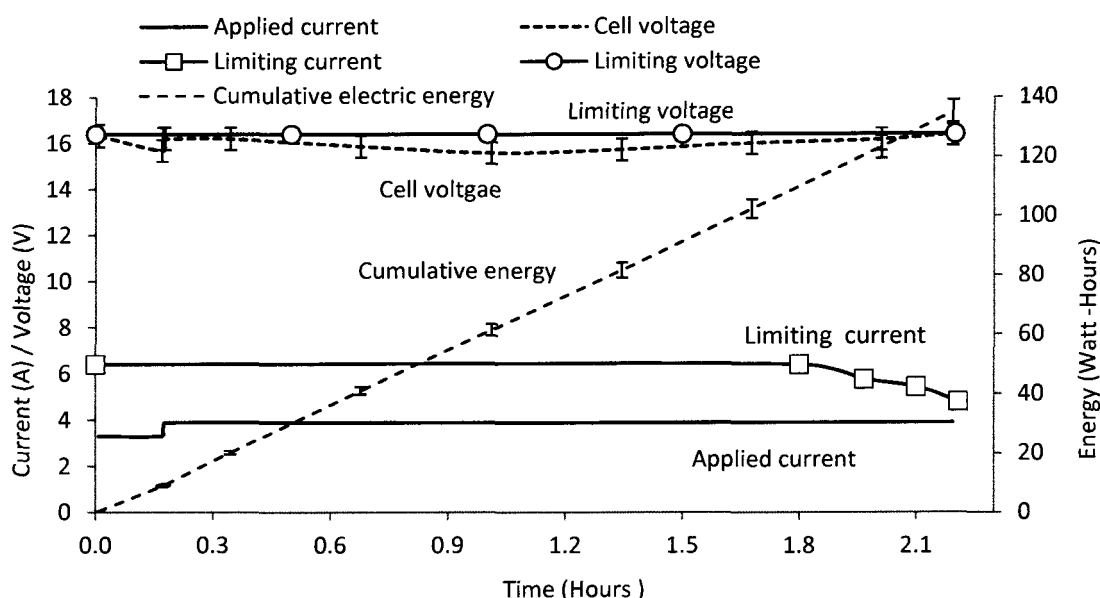


Figure 5.12 Current, Voltage and Energy Consumption for Batch Experiment No. 2

Table 5.7 and Figure 5.13 show the specific energy consumption and current efficiencies for the batch experiments, respectively. Since Experiment-1 was performed for a longer duration and had a higher level of concentrations of acid and base than that of experiment-2, the extent of back-diffusion of ions and molecules was higher in Experiment-1. Thus, the specific energy consumption was higher and the current efficiencies were lower for Experiment-1 as compared to Experiment-2. The initial salt concentration did not have much effect on the specific energy. Rather the main effect was related to the current density. The higher the current density, the higher the energy consumption.

Table 5.7 Specific Electric Energy Consumption for Batch Experiments Performed using BPMED

Experiment No.	Experimental Conditions	Specific Electric Energy (kWatt-Hrs/Kg of HAc formed)
Experiment-1	F: 130 g/L, Current: 60 mA/cm ²	1.98 ± 0.20
Experiment-2	F: 85 g/L, Current: 60 mA/cm ²	1.83 ± 0.19
Experiment-3	F: 85 g/L, Current: 30 mA/cm ²	1.52 ± 0.16
Experiment-4	F: 51 g/L, Current: 30 mA/cm ²	1.64 ± 0.17

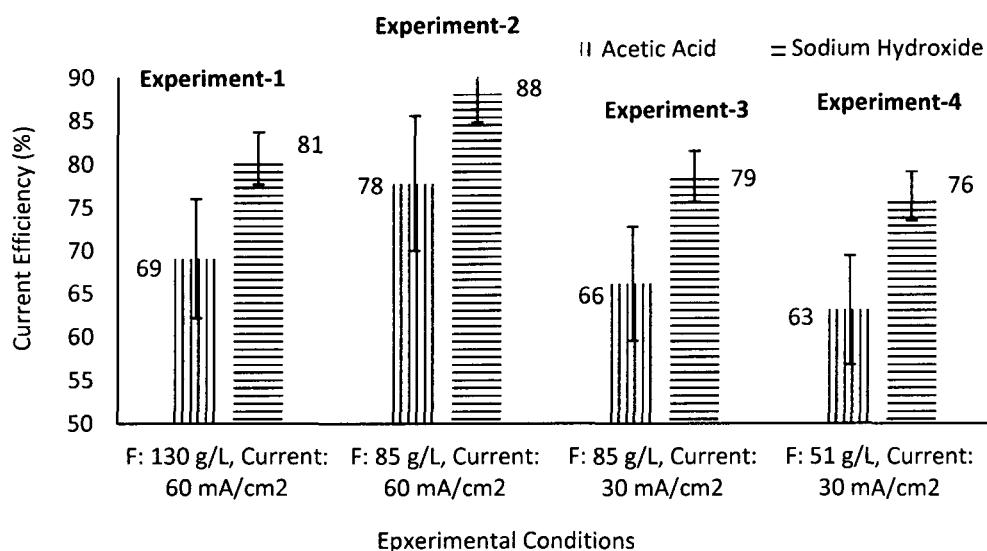


Figure 5.13 Current Efficiencies for Batch Experiments Performed using BPMED

Experiment-3 was performed at a lower current density and hence, the electrolyte solutions were in contact with each other for a longer period of time. The longer exposure time was thought to cause an increase in the amount of back diffusion of ions/molecules diffusing into the different compartments. Thus, the current efficiencies for Experiment-3 were lower than those for Experiment-2. Because of the low current density, the specific energy consumption was also lower for Experiment-3.

Based on the logic used to interpret the current efficiency data observed in Experiment-1 and Experiment-2, the current efficiencies and specific energy for Experiment-4 should be higher and lower, respectively, than the values observed for Experiment-3. Both the observed values for the specific energy and current efficiency data are not in agreement with this logic. This discrepancy could be due to the statistical error associated with the low amounts of acids and bases formed in Experiment-4.

The overall acetate mass balance closure varied between 84 to 89% for the batch experiments.

5.3.3 Study of Effect of Feed Concentration using Feed and Bleed Mode Experiments

The feed and bleed mode of operation represents semi-batch processing. In these experiments, the final concentration of acetic acid in the acid solution was approximately 150-170 g/L (Figure 5.14). The acetic acid concentration seems to be limited due to water transport into the acid compartment. Since both experiments FB-1 and FB-2 were performed at the same current density, the acetic acid concentration profile was similar for these experiments. Experiment FB-3 was performed at a lower current density and thus, it required additional time to achieve the same level of concentration of acetic acid as in experiments FB-1 and FB-2.

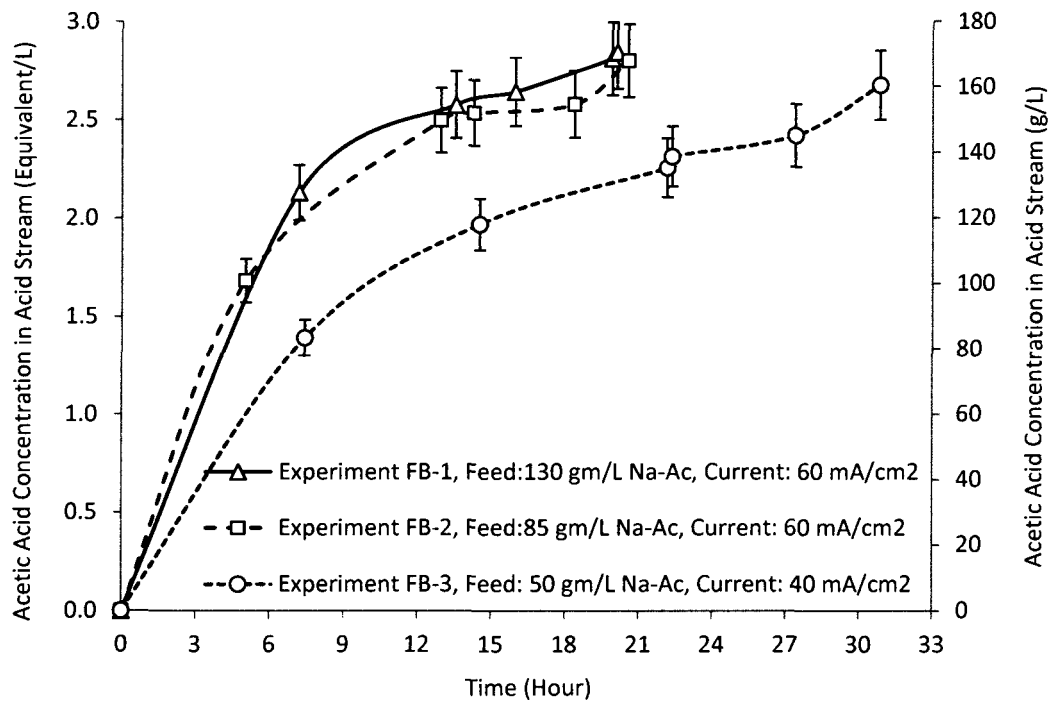


Figure 5.14 Concentration of Acetic Acid in the Acid Solution for Feed and Bleed Mode Experiments

Figure 5.15 shows the volumes of the acid solution as a function of time. The volumes increased with time due to the transfer of water along with the ions. In each experiment, a total of 550 to 900 mL of the acid solution was removed from the acid tank when it was completely filled (Figure 5.15). The capacity of the acid tank was about 3 liters. A total of 150 to 280 mL of the acid solution was withdrawn as samples. In addition, 50 mL of solution remained as the dead volume in the tubes of the equipment. Volumes of samples and dead solutions are not shown in Figure 5.15 to make the plot more legible. However, the data shown in Table 5.9 was calculated by considering the amount of acid lost in the samples and the tubes of the equipment.

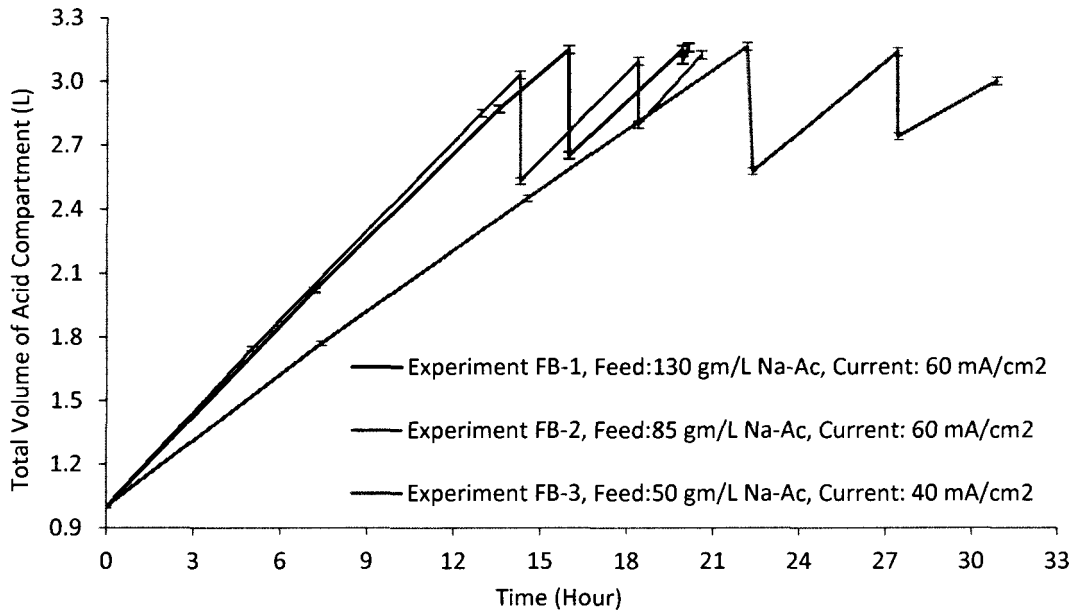


Figure 5.15 Volume of the Acid Solution for Feed and Bleed Mode Experiments

Figure 5.16 shows the concentration of sodium hydroxide and sodium acetate in the base and the feed-salt solutions, respectively, as a function of time for Experiment FB-1. As explained previously, once the concentration of sodium acetate in the salt solution dropped from the initial value of 130 g/L to about 30 g/L, a new batch of sodium acetate (volume: 1.25 or

1 L) was charged and the experiment was continued. Thus, the concentration of sodium acetate in the salt solution varied between these two values.

Similarly, as the concentration of sodium hydroxide in the base solution reached approximately 30 g/L, most of the solution was drained from the base compartment and a similar quantity of water was added. This was done to maintain the concentration of residual sodium hydroxide in the base compartment at about 3 to 5 g/L. Thus, the concentration of sodium hydroxide in the base solution oscillated between 30 and 3 to 5 g/L. The salt and base concentration profiles for the remaining experiments were similar to Figure 5.16.

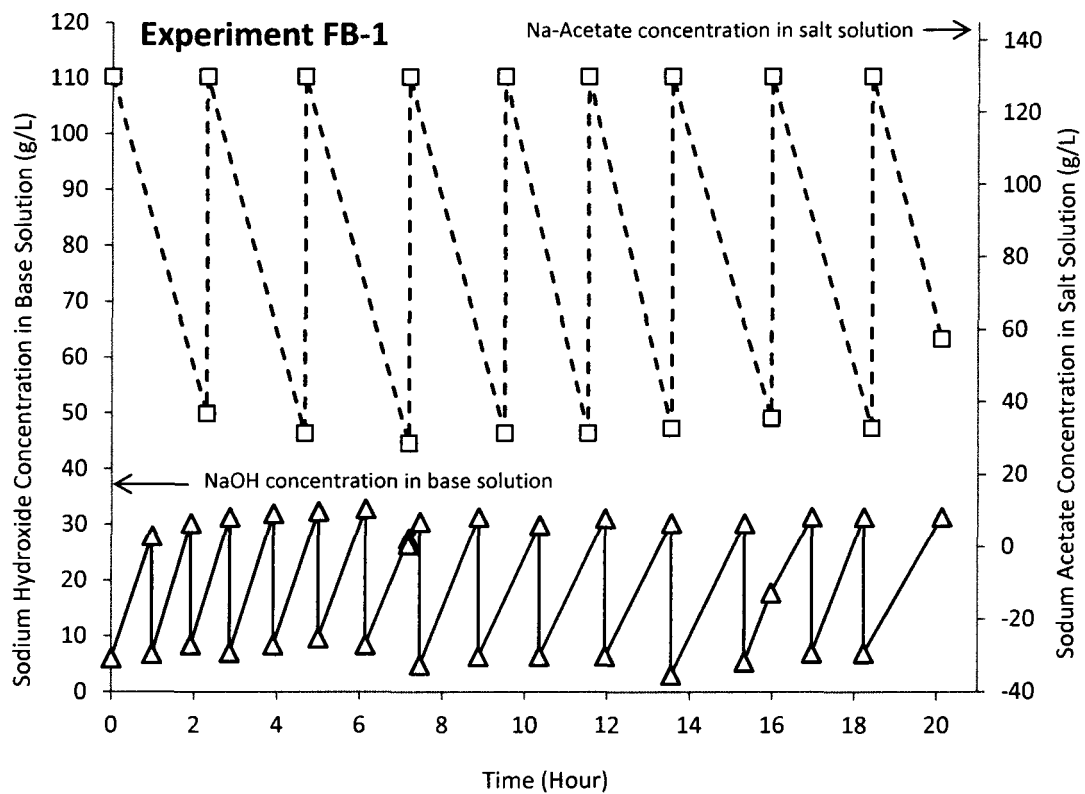


Figure 5.16 Sodium Hydroxide and Sodium Acetate Concentrations in Base and Salt Solutions (respectively) for Experiment FB-1

Figure 5.17 illustrates the variation in the volumes of the salt and base solutions for experiment FB-1. As explained previously, the volume of the base solution increased with time. After a certain amount of the base was withdrawn as product, a similar quantity of water was replenished. However, sometimes lesser amounts of water were replenished into the base tank; accordingly, there was an abrupt drop in the volume of the base solution and the curve does not appear cyclic.

As shown in Figure 5.17, the volume of the salt solution decreased with time in a cyclic manner. The initial volume of each batch of sodium acetate was either 1 or 1.25 L.

The salt and base concentration and volume profiles for the remaining experiments were similar to Figures 5.16 and 5.17.

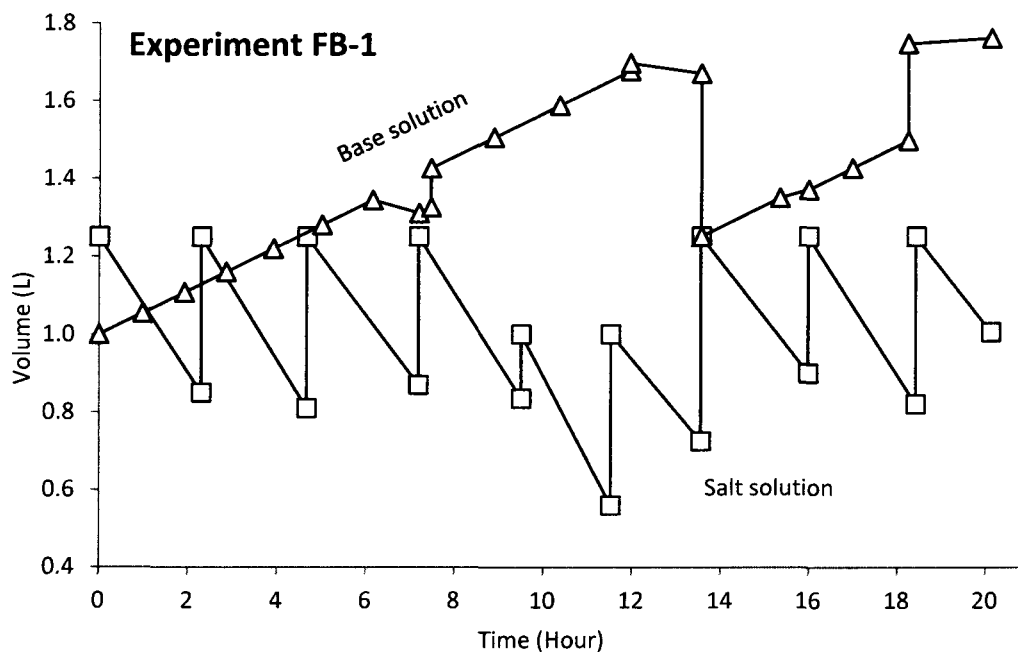


Figure 5.17 Variation in Volumes of Acid and Base Solutions for Experiment FB-1

Table 5.8 shows the total volume and the average concentration of the NaOH product and the residual salt solutions withdrawn in each experiment. The sum of the total amount of water added to the base tank and the water of hydration transported into the base compartment is equal to the difference between the final and the initial volumes of the base solutions. Table 5.8 also shows that for each feed-and-bleed experiment, there was about 1 to 1.3 L of residual salt solution with a sodium acetate concentration higher than the limiting value for the given current density. These solutions were from the last batch of these experiments which needed to be terminated at a certain concentration to maintain the amount of sodium acetate split in each experiment to about 14.1 gram moles.

Table 5.8 Average Concentrations of the Base Product and Residual Salt Solutions in Feed and Bleed Mode Experiments

	Base Solutions (Product)		Residual Salt Solutions	
	Total Volume (L)	Average Sodium Hydroxide Concentration (g/L)	Total Volume (L)	Average Sodium Acetate Concentration (g/L)
Experiment FB-1	16.9	31.0 ± 2.0	6.4	32.7 ± 4
			1	57.4
Experiment FB-2	18.9	27.8 ± 2.8	15.3	30.6 ± 1.5
			1.1	52.8
Experiment FB-3	21.4	26.4 ± 2.1	34	20.9 ± 3.3
			1.3	35.3

Figure 5.18 shows the variation in the concentrations of minor components in the major electrolyte streams for experiment FB-1. Similar plots were obtained for experiments FB-2 and FB-3 as well.

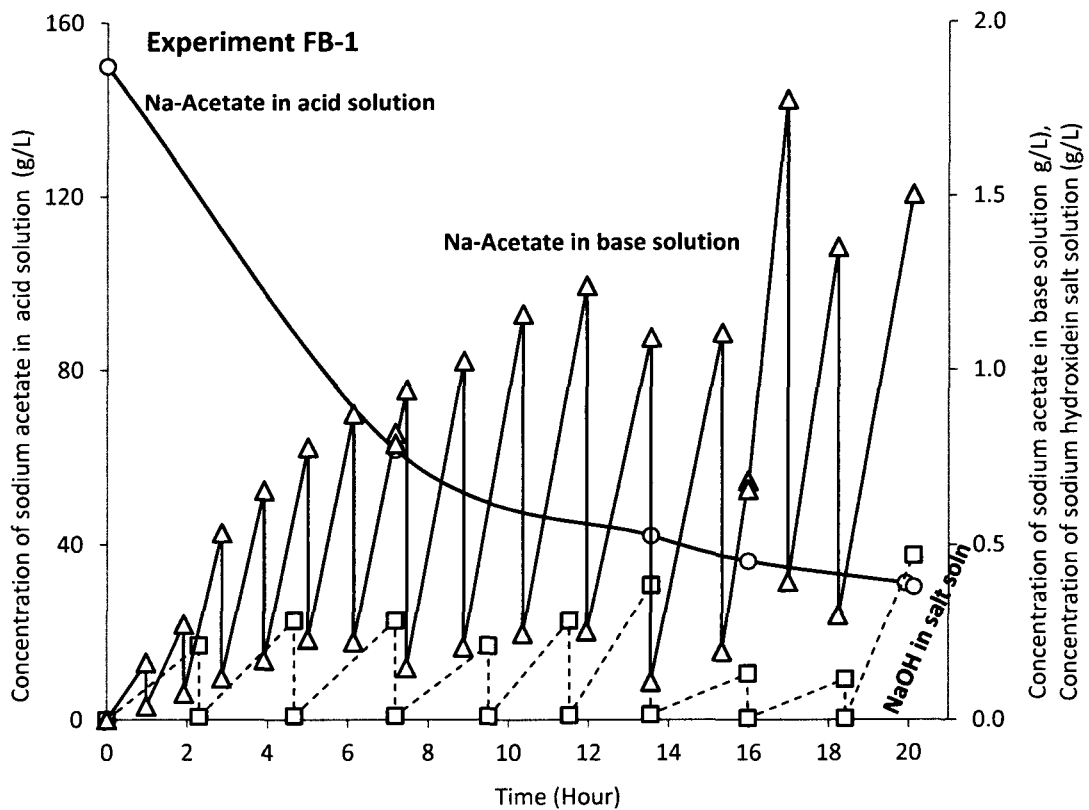


Figure 5.18 Concentrations of Minor Components in Salt, Acid and Base Solutions for Experiment FB-1

The base solutions were found to contain an increasing amount of sodium acetate (0.2 to 2 g/L) throughout all of the feed and bleed mode experiments. The diffusion of acetic acid from the acid compartment into the base compartment seemed to be the major pathway for the presence of sodium acetate in the base solution for the following reasons:

Referring to Figure 5.11, since the base solution was periodically refilled with pure water, the concentration of sodium acetate in it depended upon the rate of instantaneous diffusion of acetate rather than the accumulation over a long period of time. The acetate accumulation in the base came from two sources, the salt compartment and also from the acid compartment as illustrated in Figure 5.11. The concentration of acetic acid in the acid solution was increasing with time throughout the experiment and hence, an increasing amount of acetic

acid could be diffused into the base compartment over time. Whereas, the concentration of the sodium acetate in the acid solution decreased with time (see Figure 5.18) due to the increase in the volume of the acid solution from the solvated water. Thus, it was thought not to be the major pathway for the increase in acetate concentration in the base compartment. In addition, the concentration of sodium acetate in the salt compartment periodically varied between the fixed limits. Consequently, diffusion of sodium acetate from the salt compartment was not thought to be the major pathway for the presence of an increasing amount of sodium acetate in the base compartment.

Similarly, the salt solutions were also found to contain about 0.2 to 0.5 g/L of sodium hydroxide (Figure 5.18). The major reason for the presence of OH^- ions in the salt solutions was thought to be the diffusion of the sodium and hydroxyl ions from the base compartment into the salt compartment through the cation exchange membranes (See Figure 5.11).

Figure 5.19 shows the cumulative current efficiencies for the production of acetic acid as a function of time. Since the current efficiency was estimated after every 6-8 hours, there are no data about the current efficiency for the first 6-8 hours of all feed and bleed mode experiments. As shown in Figure 5.19, the current efficiencies for the Experiments FB-1 and FB-2 were almost similar because these experiments were performed at the same current density. Experiment FB-3 was performed at a lower current density. As discussed previously, the current efficiencies for this experiment were lower than those for the remaining experiments.

The current efficiencies of acetic acid for Experiments FB-1 and FB-2 gradually decreased with the time (Figure 5.19). One possible reason for this decrease is the increase in the rate of back-diffusion of acetic acid from the acid compartment into the base and salt compartments. The concentration of acetic acid in the acid solution increased with time and thus, it increased the driving force for the diffusion of acid into neighboring compartments. However, the current

efficiency for acetic acid in Experiment FB-3 remained almost constant throughout the experiment.

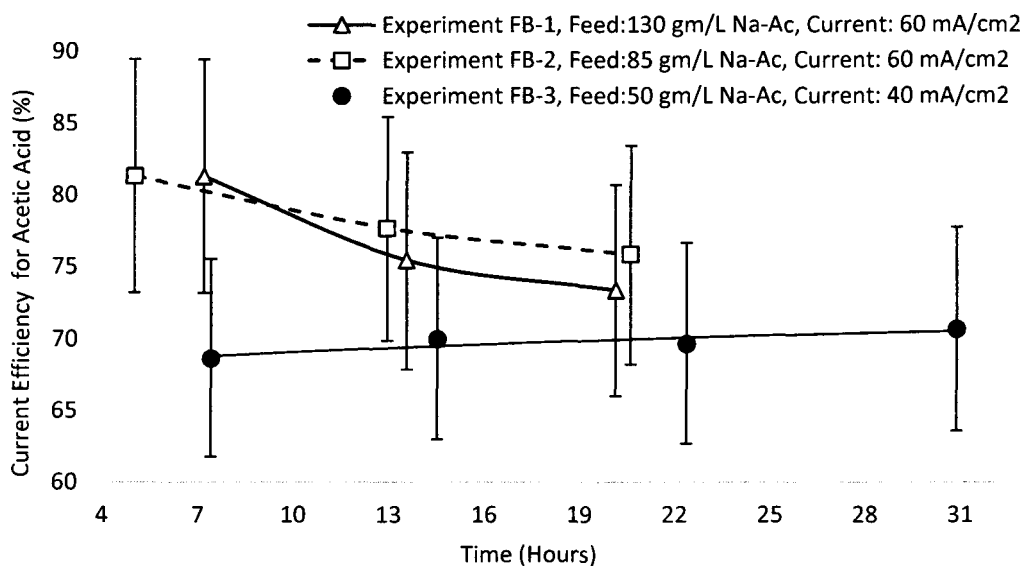


Figure 5.19 Cumulative Current Efficiencies for the Production of Acetic Acid in Feed and Bleed Mode Experiments

As shown in Figure 5.20, the cumulative current efficiencies for the production sodium hydroxide did not significantly change with time except for the Experiment FB-1 where it gradually decreased over the time. Also, the current efficiency for the production of sodium hydroxide was always higher than that of acetic acid. Theoretically, the current efficiencies for the acetic acid and the caustic should be the same since one mole of acetic acid and one mole of caustic are formed for every mole of sodium acetate that is decomposed. However, the diffusivity of H^+ ion ($9.3 \cdot 10^{-9} \text{ m}^2/\text{s}$) is higher than that of OH^- ion ($5.3 \cdot 10^{-9} \text{ m}^2/\text{s}$). Thus, the extent of back-diffusion of H^+ ions was much higher and it resulted in a low current efficiency for acetic acid.

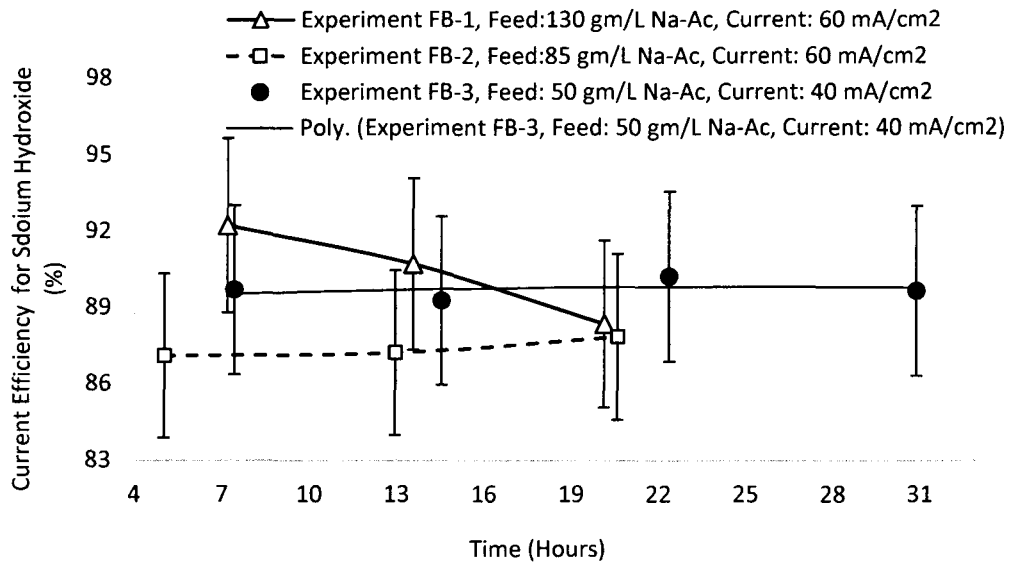


Figure 5.20 Cumulative Current Efficiencies for the Production of Sodium Hydroxide in Feed and Bleed Mode Experiments

Since both Experiments FB-1 and FB-2 were performed at the same current density, the energy consumption was similar for these experiments (Figure 5.21). Experiment FB-3 was performed at a lower current density and was thermodynamically more reversible than the other experiments because of the decrease in the current density, the major driving force. Hence, Experiment FB-3 required less energy to bring about the same effect.

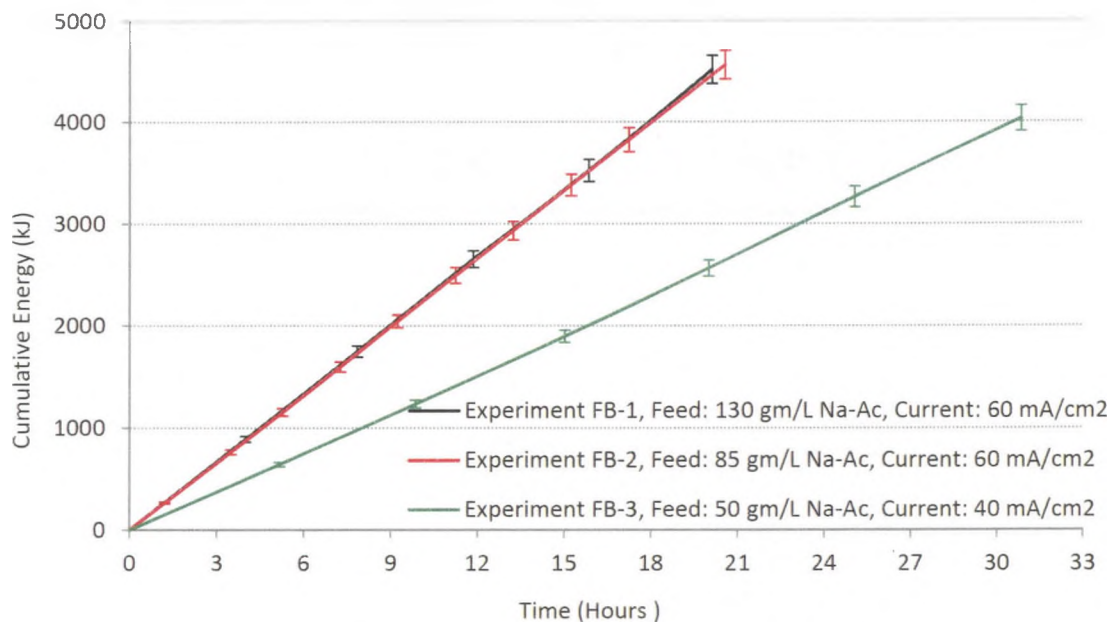


Figure 5.21 Energy Consumption for Feed and Bleed Mode Experiment

Figures 5.22 and 5.23 present the specific average energy consumption for the production of acetic acid and the normalized rate of production of acetic acid, respectively. The normalized rate of production was obtained by dividing the rate of production by the total membrane area. Since all feed and bleed mode experiments were performed in the intervals of 7 to 8 hours, the specific average energy consumption (Figure 5.22) and normalized rate of production of acetic acid (Figure 5.23) were calculated for each interval and plotted at the mean-time of the corresponding interval. In this calculation, the first point was established starting at zero time.

For Experiments FB-1 and FB-2, the specific energy consumption and the normalized rate of production increased and decreased, respectively, with time. Hence, it is evident that the efficiencies of these experiments decreased with the time. A possible reason for the decrease in efficiency was the back-diffusion of acetic acid into the salt and base compartments. Also, the

extent of back-diffusion increased with time because of the increase in the concentration of acetic acid in the acid solution. If superior membranes were used, perhaps the decrease in production could be avoided with less back-diffusion. For Experiment FB-3, the specific energy consumption and the normalized rate of production remained almost constant throughout the course of the experiment.

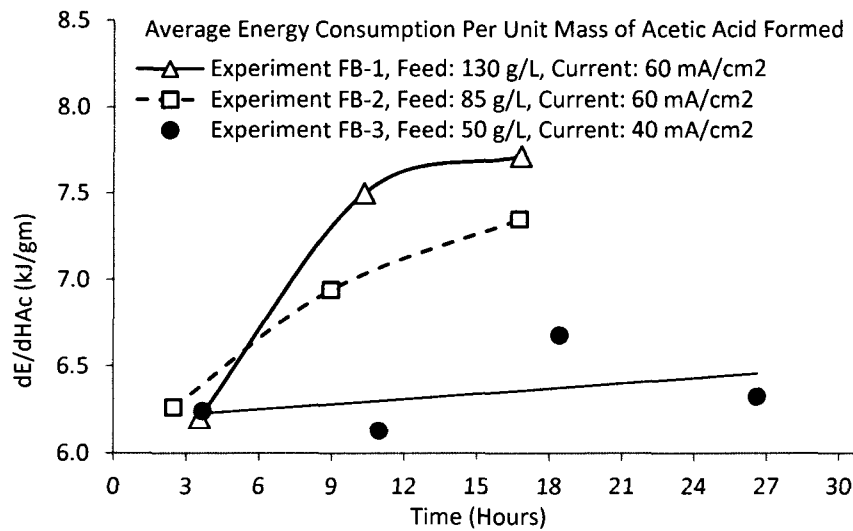


Figure 5.22 Specific Average Energy Consumption

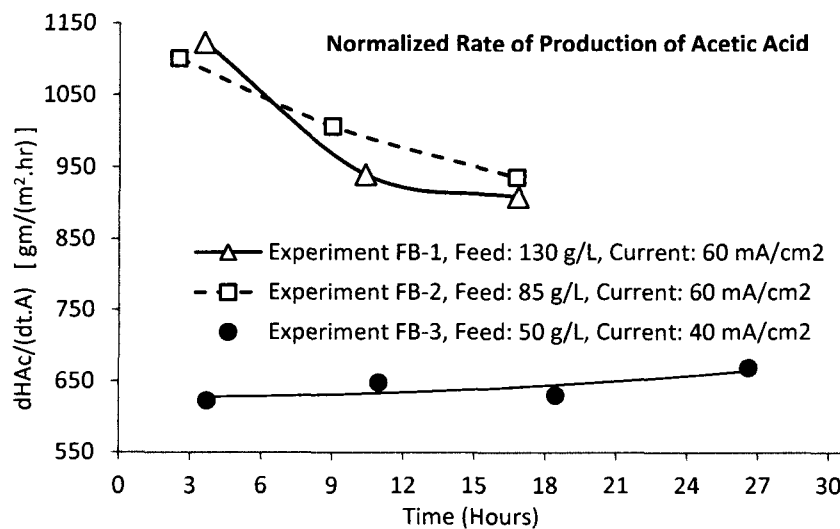


Figure 5.23 Normalized Rate of Production of Acetic Acid

Figure 5.24 presents a detailed comparison of the volumes and concentrations of acetic acid formed in each experiment. The small amounts of acid solution lost in the tubes of the equipment and withdrawn as samples were not included in this plot to make it more legible. However, the values shown in Table 5.9 were calculated by considering the above losses.

The height of each rectangle in Figure 5.24 represents the volume of an acid solution and the value shown inside a rectangle is the concentration of acetic acid in the corresponding acid solution. The rectangles adjacent to the x-axis represent the first withdrawal of the acid product in each experiment and are followed by the successive withdrawals. The total height of a column represents the total volume of the acid solutions for each experiment. As shown in the figure, each experiment mostly resulted in the production of acetic acid solution with a concentration of 160 to 170 g/L. The remaining solutions represent the amount of product withdrawn from the acid tank when it was completely filled during experiment.

The total volume of the acid solution slightly decreased with an increase in the initial concentration of sodium acetate in the feed-salt solution. This was thought to be due to the decrease in the transportation of water molecules of hydration into the acid compartment, which was in turn caused by a decrease in the availability of water molecules for hydration of sodium acetate in the concentrated salt solution. As the concentration of sodium acetate increases at a fixed temperature, a greater number of sodium acetate molecules compete for same number of water molecules and hence, the sodium (Na^+) and acetate (Ac^-) ions are hydrated to a lesser degree.

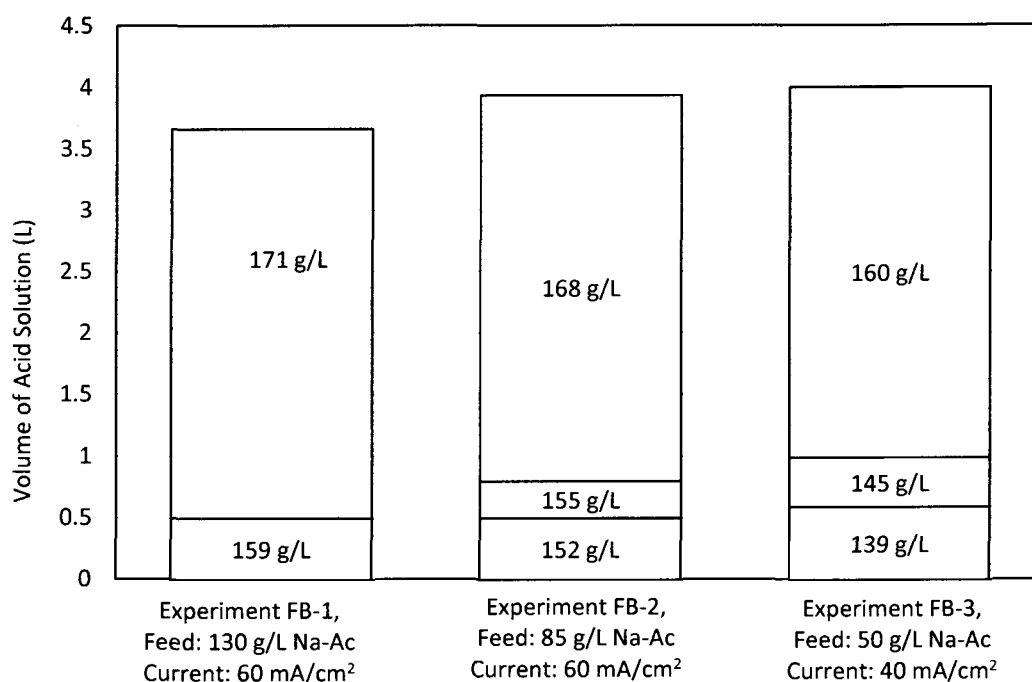


Figure 5.24 Volumes and Concentrations of Acids in Feed and Bleed Mode Experiments

Table 5.9 shows a detailed comparison of all feed and bleed mode experiments. A constant amount of sodium acetate was consumed in each of these experiments. The results of Experiments FB-1 and FB-2 were very similar because they were performed at the same current density. These two experiments also show that the salt concentration did not have an appreciable effect on the BPMED process for the current density of 60 mA/cm².

Although Experiment FB-3 was performed at a low current density, it resulted in the production of similar quantities of acids and bases as the other experiments. Due to the low current density, the time required for producing the same amount of acid and base was increased (30 hours vs 20 hours). Hence, the fluxes for the production of acetic acid and caustic were also lower. Also, the specific energy consumption and the acetic acid current efficiency were lower for Experiment FB-3. The current efficiency for sodium hydroxide was not affected by current density or salt concentration. The acetate mass balance closure was significantly

lower than the sodium mass balance closure. The rate of production of acetic acid was significantly lower than that of caustic. This is due to the higher rate of back-diffusion of acetic acid as compared to caustic and low mass balance closure of acetate ions.

Table 5.9 Summary of Results of Feed and Bleed Mode Experiments

		Experiment FB-1	Experiment FB-2	Experiment FB-3
Na-Acetate concentration in initial salt solution (g/L)		130	85	50
Current density (mA/cm ²)		60	60	40
Time (Hours)		20.1	20.6	30.9
Amount of Na-Acetate consumed	Moles	13.8	14.3	14.4
Amount of HAc formed	Moles	10.9	11.1	10.6
Amount of NaOH formed	Moles	12.9	12.8	13.4
Rate of production	Moles of HAc/Mole of Na-Ac	0.79	0.78	0.73
	Moles of NaOH/Mole of Na-Ac	0.93	0.90	0.93
Specific electric energy	W-Hours/kg of HAc formed	1912	1906	1764
Acetate mass balance closure (%)		84	85	86
Sodium mass balance closure (%)		95	93	99
Overall current efficiency	Acetic acid (%)	75	76	71
	Sodium hydroxide (%)	88	88	90

5.3.4 Experiments Using Pre-Treated Extracts

Figures 5.25 and 5.26 show the variation in the concentrations of the salt, acid and base solutions for the BPMED experiments performed using the clarified and unclarified extracts, respectively. Only the initial and final concentration points are illustrated on the graphs; since the experiments were rather short. Thus, straight lines are shown for concentration versus time in Figures 5.25 and 5.26. By comparing Figures 5.25 and 5.26, it can be seen that approximately the same amounts of salts were decomposed in both experiments. The total concentration of all acids present in the final acid solution from each experiment was about 0.36 to 0.38

equivalent/L. Similarly, the final base solutions contained about 0.56 to 0.58 equivalent/L of caustic.

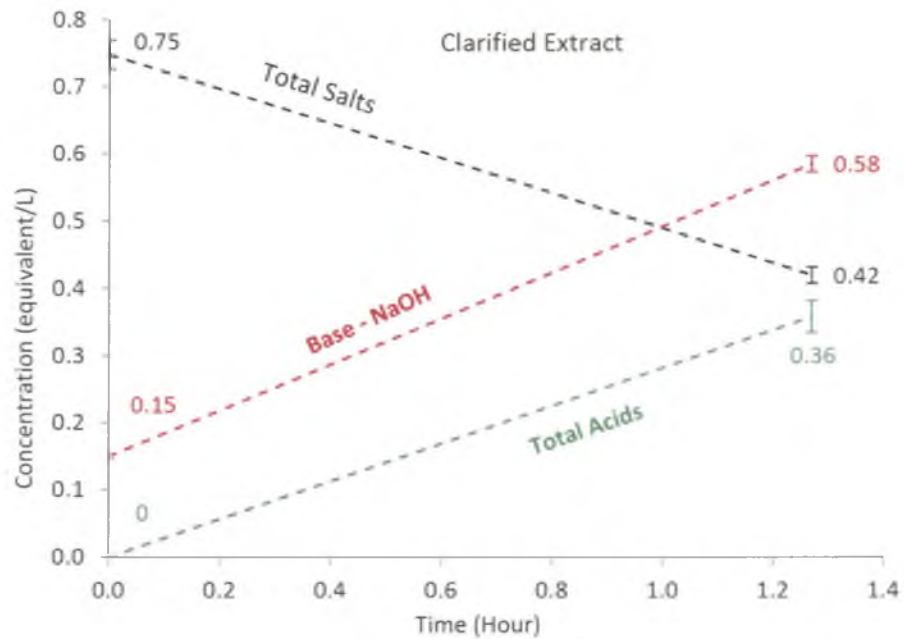


Figure 5.25 Concentration Profiles for the BPMED Experiment Performed using Clarified Extract

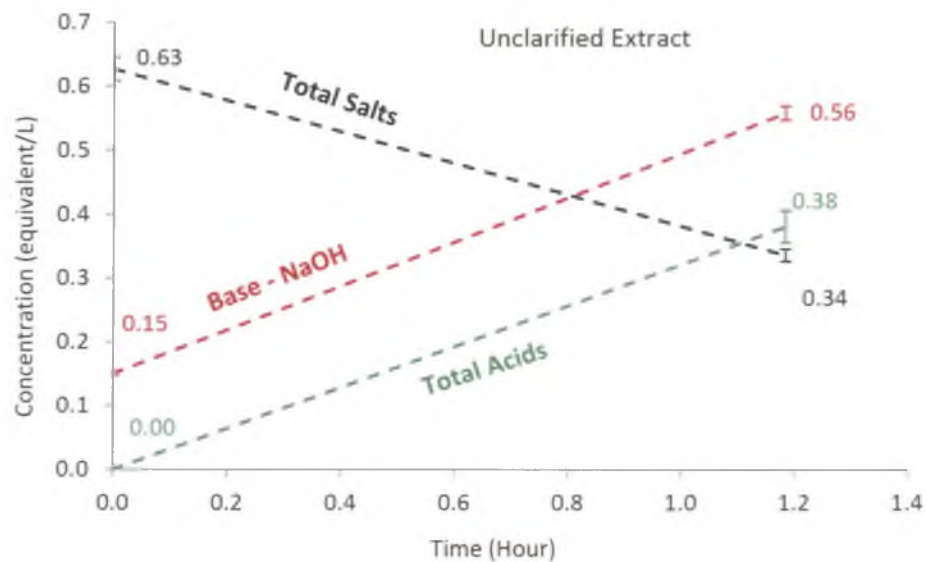


Figure 5.26 Concentration Profiles for the BPMED Experiment Performed using Unclarified Extract

Tables 5.10, 5.11, 5.12 and 5.13 summarize the concentrations of the various components present in the salt, acid and base solutions obtained in the BPMED experiments performed using the clarified and unclarified extract. Since both the clarified and unclarified feed-salt solutions contained small amounts of sodium formate and sodium lactate, these salts were subsequently split into the corresponding acids and sodium hydroxide in the BPMED electrochemical reactor. However, the total sugars and the lignin were predominately retained in the feed-salt solutions and did not penetrate the membranes.

Table 5.10 Concentration of Salt and Base Solutions for the BPMED Experiment Performed using Clarified Extract

	Concentrations (Eqv/L)				Total Lignin (g/L)	Total Sugars (g/L)	pH	Vol. (L)
	Na-Acetate	Na-Formate	Na-Lactate	NaOH				
Initial Salt	0.69	0.05	0.0105	0	0.62	0.25	10.5	1.64
Final Salt	0.40	0.01	0.0060	0	0.48	0.23	11.5	1.54
Initial Base	0	0	0	0.15	0	0	---	1.00
Final Base	0.0012	0	0	0.58	0.0036	0.0040	---	1.11

Table 5.11 Concentration of Acid Solution for the BPMED Experiment Performed using Clarified Extract

	Concentrations (Eqv/L)						Total Lignin (g/L)	Total Sugars (g/L)	Vol. (L)
	Na-Acetate	Formic Acid	Lactic Acid	Acetic Acid	Total Acids, by HPLC	Total Acids, by Titration			
Initial Acid	0.21	0	0	0	0	0	0	0	1.00
Final Acid	0.18	0.0450	0.0056	0.3075	0.3581	0.4040	0.26	0.043	1.16
Composition of Final Acid Solution (g/L)									
	Formic Acid		Lactic Acid		Acetic Acid				
Final Acid	2.1		0.5		18.5				

Table 5.12 Concentration of Salt and Base Solutions for the BPMED Experiment Performed using Unclarified Extract

	Concentrations (Eqv/L)				Total Lignin (g/L)	Total Sugars (g/L)	pH	Vol. (L)
	Na-Acetate	Na-Formate	Na-Lactate	NaOH				
Initial Salt	0.56	0.05	0.0154	0	12.07	2.11	10.2	1.74
Final Salt	0.32	0.01	0.0078	0	11.65	2.11	10.8	1.67
Initial Base	0	0	0	0.15	0	0	--	1.00
Final Base	0.0021	0	0	0.56	0.0034	0.004	--	1.11

Table 5.13 Concentration of Acid Solution for the BPMED Experiment Performed using Unclarified Extract

	Concentrations (Eqv/L)						Total Lignin (g/L)	Total Sugars (g/L)	Vol. (L)
	Na-Acetate	Formic Acid	Lactic Acid	Acetic Acid	Total Acids, by HPLC	Total Acids, by Titration			
Initial Acid	0.21	0	0	0	0	0	0	0	1.00
Final Acid	0.18	0.0537	0.0113	0.3150	0.3800	0.3860	0.24	0.03	1.16
Composition of Final Acid Solution (g/L)									
	Formic Acid		Lactic Acid		Acetic Acid				
Final Acid	2.5		1.0		18.9				

For the BPMED experiment performed using the clarified extract, the total acid concentration determined using titration was about 10% higher than the HPLC measurement. Whereas, for the experiment with the unclarified extract, both values were found to be almost equal.

Table 5.14 shows the current efficiencies, the specific electric energy, the selectivity and the relative number of moles of each species split for the BPMED experiments performed using the pre-treated extracts. The current efficiencies and specific energies for the experiments performed with the pre-treated extracts were similar to those of the experiments performed using synthetic sodium acetate.

As discussed in Chapter 4, the presence of tramp salts in the pre-treated extract leads to the loss of useful electric energy. Accordingly, about 13 to 15% of the total useful electric energy was lost in splitting tramp salts such as sodium formate and sodium lactate.

Selectivity values shown in Table 5.14 were calculated using Equation 2.17 a. Selectivity data shows that about 5 to 6 moles of desired product, acetic acid, were formed for every mole of undesired product.

Table 5.14 Summary of the BPMED Experiments Performed Using Pre-Treated Extracts

	Type of Feed Solution		
	Synthetic Sodium Acetate Solution	Clarified Extract	Unclarified Extract
Current Efficiency for Total Acids (Based on HPLC data, %)	76 ± 7.6	68 ± 6.8	76 ± 7.6
Current Efficiency for Base (%)	80 ± 3.0	81 ± 3.0	81 ± 3.0
Specific Electric Energy (kJ/Equivalent of Acid Formed)	382 ± 39.3	424 ± 43.7	411 ± 42.3
Relative Number of Moles of Each Species Split (%)			
Sodium Acetate	100	87.4	84.3
Sodium Formate	-----	11.1	12.9
Sodium Lactate	-----	1.5	2.8
Selectivity (Moles of Each Acid Formed Per Unit Mole of Formic Acid Formed)			
Acetic Acid	-----	5.87	6.83
Formic Acid	-----	1.00	1.00
Lactic Acid	-----	0.21	0.12

These experiments suggest that BPMED can be used to obtain a clear solution of concentrated acetic acid together with smaller quantities of formic acid and lactic acid provided that the presence of lignin in the feed-salt solution does not lead to appreciable fouling of the membranes over extended run periods.

The mass balances for the major components of the extracts such as sodium acetate, sodium formate and lignin was estimated to close to between 89 and 100%. Similar to the ED experiment performed with unclarified extract, the color of the anion exchange membranes was slightly changed after processing the unclarified extract in the BPMED apparatus.

CHAPTER 6

CONCLUSIONS AND RECOMMENDATIONS FOR FUTURE WORK

6.1 Conclusions

This section contains the conclusions for the experiments listed in Chapters 3, 4 and 5.

6.1.1 Low Temperature Extraction and Two-Stage Pulping Experiments

The extent of cleavage of acetyl groups from industrial hardwood chips depended upon the caustic charge, extraction time and the extraction temperature. The acetyl groups are readily cleaved from the hemicellulose polymers by using sodium hydroxide as the reactant. In a Kraft mill, there are three practical sources of concentrated sodium hydroxide that can be used. These are: (1) white liquor, (2) makeup caustic and (3) oxidized white liquor. Although the application of white liquor (6% EA at 50 °C and 4% EA at 80 °C) resulted in the almost complete extraction of acetyl groups with minimal residual sodium hydroxide concentration in the extract, use of makeup caustic is the preferred reagent for the extraction process.

The composition of the sodium acetate in the extract was similar when either caustic or white liquor was used as the reactant for cleavage of the acetyl groups provided the initial effective alkali charge (4% EA) was the same in both cases. In the white liquor case, there was residual sodium sulfide and sodium carbonate present in the extract. No extraction experiments were performed using oxidized white liquor.

The properties of the kraft brownstock pulp did not change appreciably when the acetyl groups were removed using 6% EA white liquor when compared to the control pulp. This conclusion was predicated on handsheet data obtained on brown stock pulp for the control pulp and for pulp produced using the two-stage pulping process. Properties evaluated were opacity,

brightness, caliper, bulk, tensile strength, tear strength, scott internal bond and wet zero-span breaking length.

6.1.2 Separation and Concentration of Sodium Acetate Using Electrodialysis

The primary conclusion drawn from these experiments is that electrodialysis is suitable for concentrating sodium acetate when it is present alone in an extract; but less so for separating and concentrating sodium acetate when other ions are present in the extract. The presence of tramp ions in the extract solution reduces the efficiency of the ED since additional energy is expended in pushing the tramp ions across the membrane.

An increase in the current density increased the rate of separation of sodium acetate, the specific energy consumption and the associated solvated water moving with the ions. An increase in the feed concentration increased the rate of separation of sodium acetate from water and decreased both the specific energy consumption and the water flux. The overall water transport index (OWTI) or moles of water transported per mole of sodium acetate limited the maximum attainable product concentration to about 273 g/L when starting with about 17 g/L sodium acetate in the feed.

Based on the separation factor (SF_{NaAc}) data for sodium acetate illustrated in Experiments F-1 and F-4, the use of oxidized white liquor for the extraction of acetyl groups from wood significantly reduced the separation efficiency of the ED process. The presence of sulfate and carbonate ions which were transported across the membranes resulted in the loss of efficiency. Using white liquor to cleave the acetyl groups during extraction would be expected to increase the operating cost of the separation process. Therefore, based upon separation considerations, it was concluded that dilute NaOH rather than white liquor should be used in the extraction process if possible economically. Secondly, it was concluded that the final pH of the

extract be limited to a value of 11 or lower to prevent damage to the membranes and avoid high maintenance cost associated with replacing membranes.

The results of the ED experiments performed using pre-treated extracts were similar to those of the synthetic sodium acetate solution except for the loss of about 15% of the useful electric energy. The loss was due to the transport of tramp salts present in the extract such as sodium formate, sodium lactate and sodium glycolate. Lignin and sugars were mostly retained in the feed solution. Hence, it was concluded that ED can be used to obtain a clear solution of concentrated sodium acetate provided the presence of lignin in the feed solution does not lead to membrane fouling when the apparatus is operated over extended periods of time. If fouling occurs, then membrane life would be shortened and operating cost would be increased.

6.1.3 Splitting of Sodium Acetate using Bi-Polar Membrane Electrodialysis

Sodium acetate is readily split into sodium hydroxide and acetic acid in both batch and feed-and-bleed mode experiments. It was concluded from the batch experiments that the current density was the major driving force for the BPMED process. The feed concentration did not have an appreciable effect on the BPMED process. Based on the overall water transport indices, up to 220-280 g/L of acetic acid and 600-700 g/L of sodium hydroxide can be produced using the BPMED process. Acetic acid solution with a concentration of 220-280 g/L is sufficient for upgrading to glacial acetic acid. It was concluded that about 30 g/L sodium hydroxide concentration was sufficient for reuse in the extraction process and thus, producing high concentrations of NaOH was unnecessary although clearly possible using the BPMED process. Producing a lower concentration of sodium hydroxide has the advantage that loss of sodium hydroxide due to back-diffusion through the BPMED membranes is reduced compared to production of higher concentrations.

The feed-and-bleed mode experiments performed at a current density of 60 mA/cm² using 130 and 85 g/L sodium acetate as feed solutions resulted in the production of similar amounts of acetic acid and sodium hydroxide. The only difference between these two experiments was the small change in the amount of water transported into the acid and base compartments.

The feed-and-bleed mode experiment conducted at a feed concentration of 50 g/L sodium acetate and current density of 40 mA/cm² resulted in the production of similar quantities of acetic acid and sodium hydroxide as in the other feed-and-bleed mode experiments. However, the time required was longer and the energy consumption and acetic acid current efficiency were lower at 40 mA/cm² than those at 60 mA/cm².

Due to back-diffusion, the current efficiency for the production of acetic acid in the feed and bleed mode experiments decreased as the concentration of acetic acid in the acid solution increased. The current efficiency for sodium hydroxide remained almost constant in all feed and bleed mode experiments. These results implied that there was less back diffusion of NaOH through the membranes into salt and acid compartments. Sodium hydroxide produced in the salt splitting process would be recycled back to the extraction step for cleavage of acetyl groups off the xylan polymers in the wood.

The results of the BPMED experiments performed using pre-treated extracts were similar to those of the synthetic sodium acetate except for a loss of about 15% of the total useful electric energy. This loss was again due to the transport of tramp salts present in the extract such as sodium formate and sodium lactate. Lignin and sugars were mostly retained in the feed solution. Hence, it was concluded that BPMED can be used to obtain a clear solution of concentrated acetic acid but will contain small quantities of formic and lactic acid. The formic and lactic acids can be separated from the acetic acid and possibly sold as additional by-

products. But, their concentration in the acid solution is low and thus, it may not be practical to separate and recover them.

6.2 Recommendations for Future Work

Two-Stage Pulping Experiments To Increase Pulp Yield: Using caustic followed by using white liquor to produce brown-stock pulp in a two-stage pulping process has the potential of increasing the pulp yield in the pulping process. Consequently, it is recommended that additional two-stage pulping experiments be performed with commercial hardwood chips using 6% effective alkali (at 50 °C) in the extraction step and white liquor in the second stage pulping step. In these experiments, the total alkali charge would be kept equal to that used in the conventional single stage kraft pulping.

Techno-Economic Analysis: It is recommended that a techno-economic analysis be performed in a manner similar to the study described by Mao and co-workers (2010). The primary objective of this work would be to determine the economic feasibility of recovering acetic acid from hardwood by alkali extraction. In addition, an economic comparison should be made by comparing electrodialysis and evaporation to determine the more appropriate method for concentrating aqueous solution of sodium acetate prior to the BPMED process.

Membrane Stability Study: It is recommended that long-term BPMED/ED experiments be performed using unclarified extract to determine the operational life of the ion exchange membranes. Replacement cost for the membranes will be high if membrane life is short.

Alternative Membranes: It is recommended that a search be conducted for an alternate membrane that would limit the back diffusion of acetic acid and thus, increase the efficiency of the process.

Chip Washing Study: Approximately 1/3rd of the total acetyl groups originally present in the raw wood remain in the wet macerated wood chips as sodium acetate following the extraction

process. This occurs because in the extraction experiments performed in the present study, the extraction liquor was simply drained from the extraction vessel without washing additional sodium acetate from the chips. Much of the sodium acetate present in the macerated wood would eventually be washed from the brown stock pulp and sent to the recovery process. Consequently, in an effort to increase the amount of acetic acid and caustic produced in the BPMED process, it is recommended that chip washing experiments be performed to determine the feasibility of recovery of additional sodium acetate which is otherwise lost with the chips in the second stage of pulping.

Minimization of Concentration of Sodium Formate and Sodium Lactate in Alkaline Extract: It is recommended that additional extraction experiment be performed at a low temperature such as 50 °C to evaluate the possibility of reducing the concentration of sodium formate and sodium lactate in the alkaline extract by limiting the alkaline peeling reactions. A reduction in the concentration of tramp salts in the feed solution would increase the efficiency of the BPMED/ED process. Extraction conditions of 5 to 5.5% EA, 0% S at 50 °C should be evaluated. In these experiments, it is desired to maintain the concentration of residual sodium hydroxide below about 2 g/L so that it does not lead to an appreciable loss of useful electric energy.

Modelling of Alkali Induced Deacetylation Reaction: It is further recommended that the experiments be performed to evaluate the applicability of the shrinking core model to the deacetylation of alkali in mixed hardwoods. In these experiments, milled wood would be used to eliminate diffusion effects. This would permit a kinetic expression to be developed for the true reaction rate of mixed hardwood, much like what was done by Zanuttini and co-workers (1997). Using the reaction rate determined in the wood meal experiments, a diffusion model could then be developed to more accurately predict the deacetylation process in commercial wood chips; which is thought to be controlled by diffusion of caustic into the chips.

REFERENCES

- Bar, D., (2006) The 'Eurodia Industry' bipolar membrane electro dialysis unit for the conversion of sodium acetate into reusable acetic acid and caustic acid: More than five years of successful operation, Membrane and Separation Technology News: March
- Chukwu, U. N., and Cheryan, M., (1996) Concentration of vinegar by electro dialysis, Journal of food science, 61(6): 1223-1226
- Chukwu, U. N., and Cheryan, M., (1999) Electro dialysis of acetate fermentation broths, Applied Biochemistry and Biotechnology, 77-79: 485-599
- Cowan, D. A., and Brown, J. H., (1959) "Effects of turbulence on limiting current in electro dialysis cells," Industrial Engineering and Chemistry, 51(12): 1445-1448
- Eurodia (2013) <http://www.eurodia.com/html/elep.html>, Accessed on September 13th, 2013
- Fidaleo, M., Moresi, M. (2005) Modeling of sodium acetate recovery from aqueous solutions by electro dialysis and comparison with experimental data. Biotechnology and Bioengineering, 91(September 5th), 556-568
- Huang, C., and Xu, T. (2006) "Electro dialysis with bipolar membranes for sustainable development, Environmental science & technology", 40(17), 5233-5243
- Kassotis, J., and Harry, P., and Chlanda, F. P., (1984) Electro dialytic water splitting – Conversion of dilute sodium acetate or acetic acid into concentrated acid. Journal of electrochemical society, 131(12): 2810-2814
- Krol, J. J., (1997) Monopolar and bipolar ion exchange membranes - Mass Transport Limitations. PhD Dissertation, University of Twente, Netherlands
- Li, Jian. "Two-stage kraft cooking." U.S. Patent No. 5,522,958. 4 Jun. 1996
- Luo, G. S. Shan, X. Y., Qi, X., Lu, Y. C., (2004) Two-phase electro-electro dialysis for recovery and concentration of citric acid, Separation and purification technology, 38(3): 265-271
- Luo, J., Genco, J., and Zou, H. (2012) Extraction of hardwood biomass using dilute alkali. TAPPI Journal, 11(6): (19-27)
- Magnotta, V. L., Ayala, V., and Cirucci, J. F. (1996) "Method for producing fully oxidized white liquor," US Patent 5,500,085
- Mani, K. N. (1991). "Electro dialysis water splitting technology", Journal of membrane science, 58(2), 117-138
- Mao, H., Genco, J. M., van Heiningen, A., and Pendse, H. (2010) Kraft mill biorefinery to produce acetic acid and ethanol: technical economic analysis. BioResources, 5(2): 525-54

- Marcus, Y. (1991) Thermodynamics of solvation of ions. Part 5.—Gibbs free energy of hydration at 298.15 K. *Journal of the Chemical Society, Faraday Transactions*, 87(18), 2995-2999
- Mitchell, J. (2006) Production of ethanol from Hardwood. M.S. Thesis, University of Maine, Orono, ME, USA
- Narebska, A. N., Kurantowicz, M. and Staniszewski, M. (2001) Separation of fermentation products by membrane techniques- IV: Electrodialytic conversion of caboxylates to carboxylic acids, *Separation science and technology*, 36(3): 443-455
- Neosepta (2013) <http://www.astom-corp.jp/en/en-main2-neosepta.html>, Accessed on September 13th, 2013
- Nomura, Y., Iwahara, M., and Hongo, M., (1988) Acetic acid production by an electrodialysis fermentation method with a computerized control system, *Applied and environmental microbiology*, 54(1): 137-142
- Nomura, Y., Iwahara, M., and Hongo, M., (1989) Continuous production of acetic acid by electrodialysis bioprocess with a computerized control of fed batch culture, *Journal of Biotechnology*, 12:317-326
- Olah, R., and Vadasdi, K. (1987) Investigation of cation transport through cation permselective membranes from solutions of salts composed of strong bases and weak acids. *Desalination*, 67: 547-557
- Paleologou, M., (1992) Solution to Caustic/Chlorine Imbalance: Bipolar Membrane Electrodialysis”, *Journal of Pulp and Paper Science*, 18(4): 138-145
- Patil, R. (2012) Cleavage of acetyl groups for acetic acid production in Kraft pulp mills. MS Thesis, University of Maine, Orono, ME, USA
- Patil, R., Genco, J. M., Pendse, H., and Van Heiningen, A. (2013) Cleavage of acetyl groups from northeast hardwood for acetic acid production in kraft pulp mills. *TAPPI JOURNAL*, 12(2), 57-67
- Patil, R., Truong, C., Genco, J. M., Pendse, H., and van Heiningen, A. (2015) “Applicability of electrodialysis to the separation of sodium acetate from synthetic alkaline hardwood extract”, *TAPPI JOURNAL*, 14(11), 695-708
- Poling, E. B., Prausnitz, J. M. and O’Connell J. P. (2001), “The properties of gases and liquids”, 5th ed., McGraw-Hill, New York, USA
- Rard, A. R., Miller, D. G. (1979), “The mutual diffusion coefficients of Na₂SO₄-H₂O and MgSO₄-H₂O at 25°C from Rayleigh interferometry”, *Journal of Solution Chemistry*, 8(10):755- 766
- Rydholm, S. (1965) *Pulping Processes*, Interscience Publishers, New York, USA
- Sjöström, E. (1993) *Wood chemistry*, Academic Press Inc, California, USA

Smook, G. A. (2002). Handbook for pulp & and paper technologists. Angus Wilde Publication, Canada

Strathmann, H., (2000) Bipolar Membrane and Membrane Processes, in Encyclopedia of Separation Science (Editor: Wilson, I.D., Publisher: Academic Press, United Kingdom); 1667-1676

Strathmann, H., (2003) Membranes and Membrane Separation Process, Ullmann's Encyclopedia of Industrial Chemistry (Publisher: Wiley-VCH, Weinheim) Volume 21:243-322

H. Strathmann (2004), Assessment of electrodialysis water desalination process costs, in: Proceedings of the International Conference on Desalination Costing, Limassol, Cyprus, 2004, pp. 32–54

Strathmann, H., (2010) Electromembrane Processes: Basic Aspects and Applications, in Comprehensive Membrane Science and Engineering (Editors: Driol, E., Giorno, L. Publisher: Elsevier, United Kingdom) Volume 2- Membrane Operations in Molecular Separations: 391-427

Tanaka, Y., (2010) Ion exchange membrane electrodialysis, Nova science publishers, New York, USA

TAPPI Standard T 205 sp-12 (2012) Forming handsheets for physical tests of pulp

TAPPI Standard T 227 om-09 (2009) Freeness of pulp (Canadian standard method)

TAPPI Standard T 236 cm-85 (1993) Kappa number of pulp

TAPPI Standard T 248 sp-08 (2008) Laboratory beating of pulp (PFI mill method)

TAPPI Standard T 273 pm-95 (1995) Wet zero-span tensile strength of pulp

TAPPI standard T 411 om-10 (2010) Thickness (caliper) of paper, paperboard, and combined board

TAPPI standard T 414 om-12 (2012) Internal tearing resistance of paper (Elmendorf-type method)

TAPPI Standard T 452 om-98 (1998) Brightness of pulp, paper and paperboard (directional reflectance at 457 nm)

TAPPI Standard T 494 om-01 (2006) Tensile properties of paper and paperboard (using constant rate of elongation apparatus)

TAPPI Standard T 569 om-09 (2009) Internal bond strength (Scott type)

TAPPI Standard T 625cm-85 (1985) Analysis of soda and sulfate black liquors

- Trivedi, G. S., Shah, B. G., Adhikary, S. K., Indusekhar, V. K., Rangarajan, R., (1997) Studies on bipolar membranes, Part II — Conversion of sodium acetate to acetic acid and sodium hydroxide, *Reactive and Functional Polymers*, 32(2):209-215
- van Heiningen, A. (2006) Converting a kraft pulp mill into an integrated forest biorefinery, *Pulp and Paper Canada*, 107(6): 38-43
- Walker, W. S., (2010) Improving recovery in reverse osmosis desalination of inland brackish groundwaters via electrodialysis, PhD Dissertation, University of Texas at Austin
- Wooley, R., Ruth, M., Sheehan, J., and Ibsen, K. (1999) Lignocellulosic biomass to ethanol process design and economics utilizing co-current enzymatic hydrolysis- current and futuristic scenarios. National Renewable Energy Laboratory (NREL) Report No: TP-580-26157 (July 1999)
- Xu, T., (2005) Ion exchange membranes: State of their development and perspective, *Journal of Membrane Science*, 263: 1-29
- Zanuttini, M., Marzocchi, V., (1997) Kinetics of alkaline deacetylation of poplar wood, *Holzforschung*, 51(3):251-256
- Zhang, S., and Toda, K. (1994) Kinetic study of electrodialysis of acetic acid and phosphate in fermentation broth, *Journal of fermentation and bioengineering*, 77(3): 288-292

APPENDIX A: ESTIMATION OF THE ERRORS ASSOCIATED WITH THE ELECTRODIALYSIS

EXPERIMENTS

A batch scale separation experiment was repeated three times in an effort to estimate the reproducibility of the electro dialysis experiments. Table A.1 summarizes the experimental conditions for this batch scale experiment.

Table A.1 Experimental Conditions for Error Analysis Experiments for Electrodialysis

Parameter	Description
Initial Feed Solution	2 Liters of 85 g/L sodium acetate
Initial Product Solution	1 Liter of 17 g/L sodium acetate
Initial Rinse Solution	1 Liter of 85 g/L sodium acetate

The results of the experiments to estimate the reproducibility of the ED experiments are shown in Figures A.1 to A.3. Error bars are illustrated on the figures.

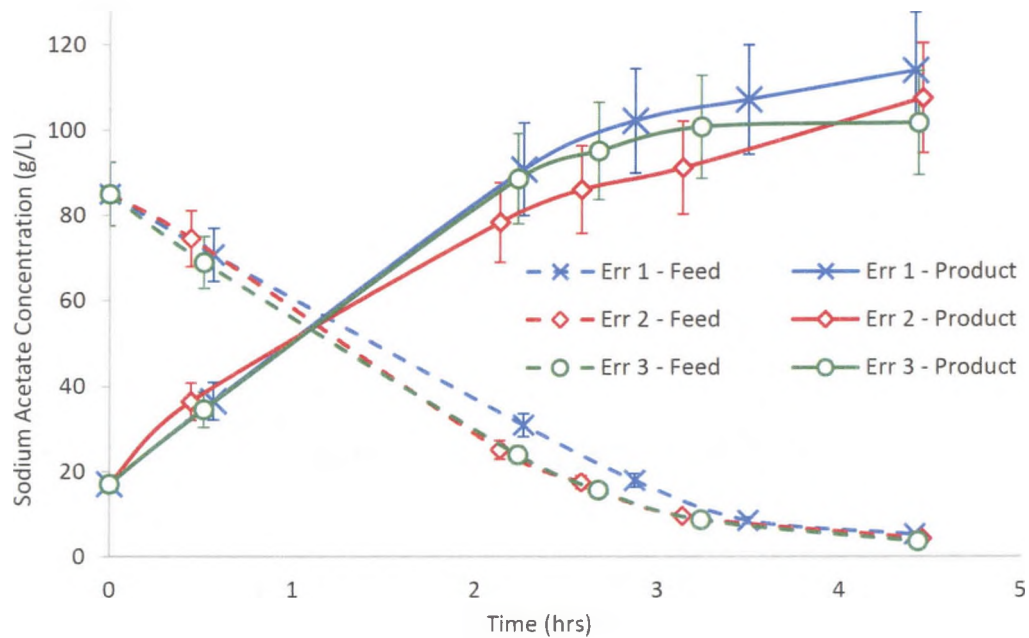


Figure A.1 Reproducibility of the sodium acetate concentration measurement for Electrodialysis

No statistical error analysis was performed for current because it was an input parameter.

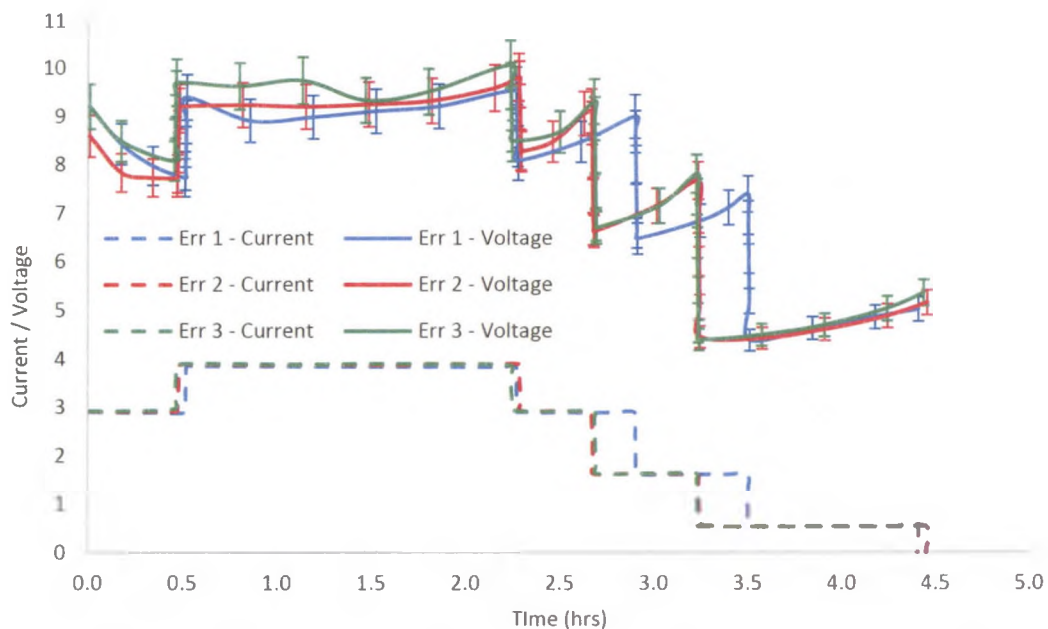


Figure A.2 Reproducibility of the cell voltage measurement for Electrodialysis

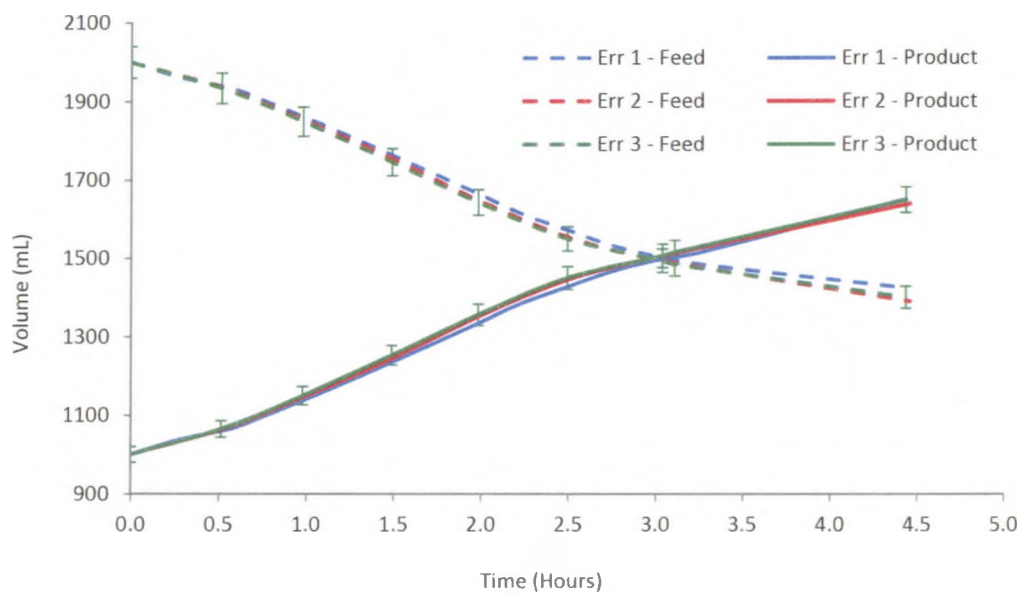


Figure A.3 Reproducibility of the volume measurement for Electrodialysis

Owing to the small sample size (3 to 4), the student's t-distribution was used to calculate the confidence interval for the mean value of a normal random variable. The method outlined by Mendenhall and Sincich (1995) was used to estimate the 95% confidence limits on the data as defined using equation A.1. This was done using the measured mean value (X), the standard deviation (s), the number of data points (n) and the t-statistic ($t_{\alpha/2, (n-1)}$) for a confidence limit of α . By using the $t_{\alpha/2, (n-1)}$ statistic, the total error α , represents a two-tail test with an $\alpha/2$ error on each side of the mean in the distribution.

$$X - t_{\alpha/2, n-1} \frac{s}{\sqrt{n}} < \mu < X + t_{\alpha/2, n-1} \frac{s}{\sqrt{n}} \dots \dots \dots \text{Equation (A.1)}$$

The percent error was calculated by dividing the absolute value of the error limit by the absolute value of mean as shown in equation A.2.

$$\text{Percent error (\%)} = \frac{t_{\alpha/2, n-1} \frac{s}{\sqrt{n}}}{X} 100 \dots \dots \dots \text{Equation (A.2)}$$

Table A.2 shows the results of the statistical error analysis. The average error for the feed and product concentrations measurements was estimated to be $\pm 8.7\%$ and $\pm 12.7\%$, respectively, as shown in Table A.2.

Table A.2 Error Analysis Data for Electrodialysis Experiments

Type of Measurement	Time (hr)	Experiment No.			Mean	Standard deviation (S)	Absolute error from mean	% Error from mean
		Err - 1	Err - 2	Err - 3			t·SD/√n	
Feed Concentration	4.5	4.5	4.3	4.2	4.3	5.51	13.7	8.8
Product Concentration	4.5	113	107	102	107	0.15	0.4	12.7
Energy (W-Hrs)		98.2	96.1	98.9	97.7	1.5	3.8	3.9
Specific Energy (W-Hrs/kg of Na-Ac Separated)		48	48.9	51	49.6	1.7	4.2	8.4
OWTI - Based on Sodium Acetate		14.4	15.2	15.8	15.2	0.7	1.7	11.5
Current Efficiency (%)		95	94	93	93.9	1.1	2.6	2.8
Cell voltage (V)		----						8.0
Feed volume (mL)		----						1.0
Product volume (mL)		----						0.6
t-Statistic used in above calculations was: n = 3, t (0.95, 2) = 4.303								

REFERENCE

Mendenhall, William; Sincich, Terry (1995) *Statistics for engineering and the sciences*; Prentice - Hall: New Jersey, USA

APPENDIX B: ESTIMATION OF THE ERRORS ASSOCIATED WITH THE BI-POLAR MEMBRANE

ELECTRODIALYSIS EXPERIMENTS

Similar to the error analysis performed for the ED experiments, a batch scale salt-splitting experiment was repeated four times to confirm the reproducibility of the bi-polar electro dialysis experiments. Table B.1 summarizes the conditions used in the standard salt-splitting experiment. The results of this quadruple experiment are shown plotted in Figures B.1 to B.3.

Table B.1 Experimental Conditions for Error Analysis Experiments for BPMED

Parameter	Description
Initial Salt Solution	2 Liters of 85 g/L sodium acetate
Initial Acid Solution	1 Liter of 17 g/L sodium acetate
Initial Base Solution	1 Liter of 3 g/L sodium hydroxide
Initial Rinse Solution	1 Liter of 85 g/L sodium acetate
Current Density	45 mA/cm ²

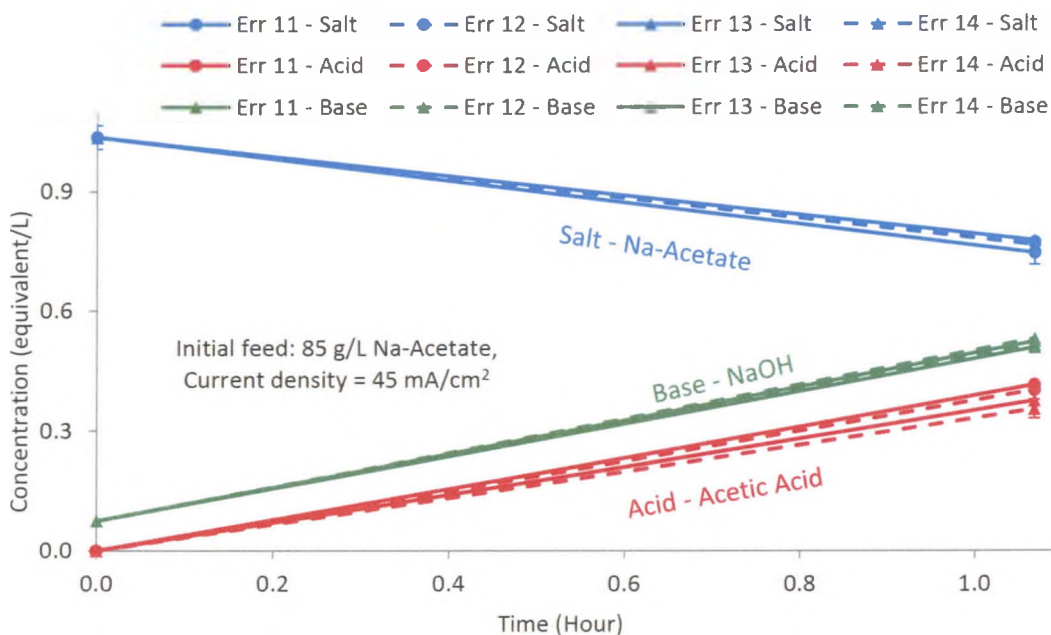


Figure B.1 Reproducibility of the concentration measurements for Bi-Polar Electro dialysis

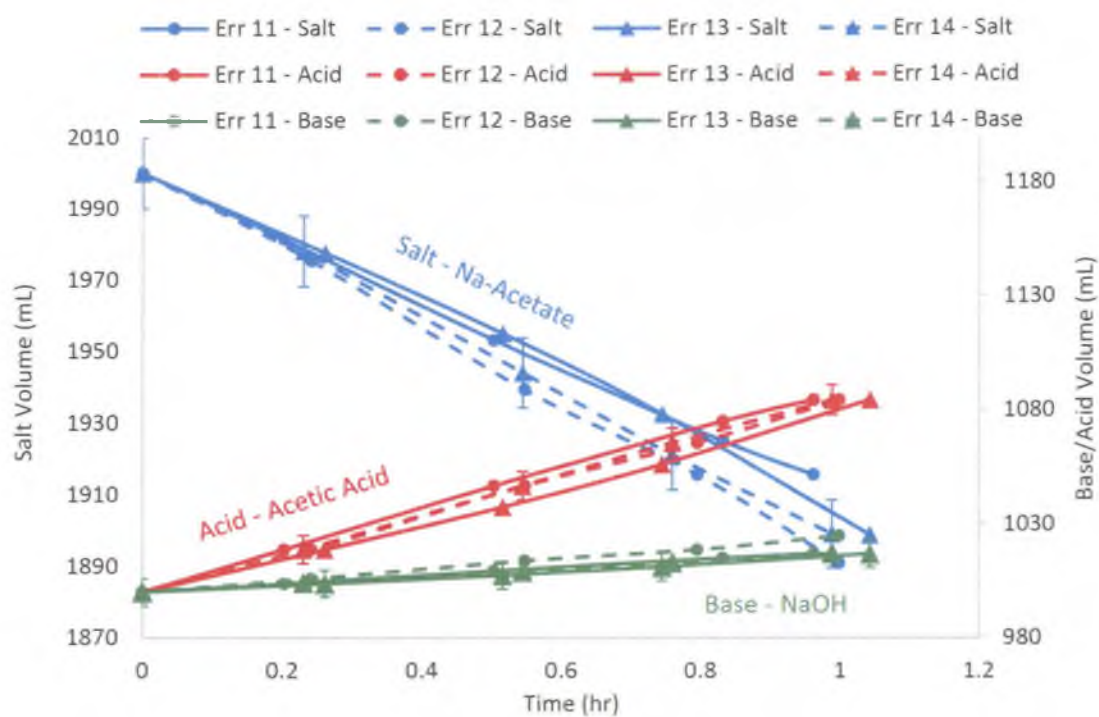


Figure B.2 Reproducibility of the volume measurements for Bi-Polar Electrodes

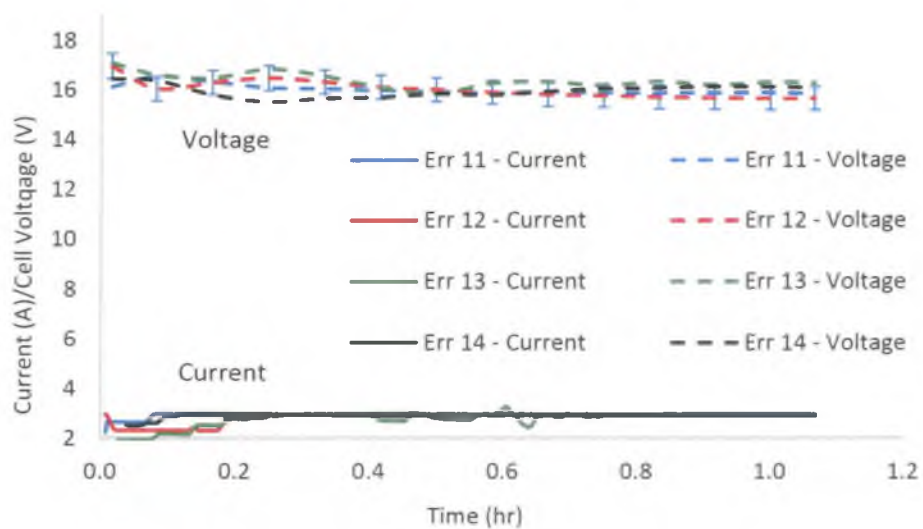


Figure B.3 Reproducibility of the voltage measurements for Bi-Polar Electrodes

Table B.2 shows the results of the statistical error analysis. The percentage error relative to the mean value varied from $\pm 3.1\%$ for the energy consumption to $\pm 10.3\%$ for the specific energy based on the production of acetic acid. Likewise, the current efficiency based on the production of acetic acid was $\pm 10\%$ while that for sodium hydroxide (NaOH) production was $\pm 3.7\%$. From these data, it was concluded that the experiments results of the salt-splitting experiment are reproducible.

Table B.2 Error Analysis Data for Bi-Polar Membrane Electrodialysis

Time (hr)	Type of Measurement	Experiment No.				Mean	Standard Deviation (S)	Absolute error from mean	% Error from mean
		Err - 11	Err - 12	Err - 13	Err - 14			t·SD/vn	
0	Salt - 1 [Na-Ac, g/L]	1.04	1.04	1.04	1.04	-	-	-	
1.07	Salt - 2 [Na-Ac, g/L]	0.74	0.77	0.78	0.76	0.76	0.01	0.02	2.9
0	Acid - 1 [HAc, g/L]	0.00	0.00	0.00	0.00	-	-	-	
1.07	Acid - 2 [HAc, g/L]	0.41	0.40	0.37	0.35	0.39	0.03	0.04	6.6
0	Base - 1 [NaOH, g/L]	0.08	0.08	0.08	0.08	-	-	-	-
1.07	Base - 2 [NaOH, g/L]	0.52	0.51	0.51	0.53	0.52	0.01	0.02	2.0
	Energy (W-Hrs)	50.4	48.7	48.2	49.5	49.2	0.96	1.54	3.1
	Charge (A·Minutes)	189	182	178	186	184	4.92	7.83	4.3
	Specific Energy (W-Hrs/kg of HAc formed)	1763	1743	1840	2004	1838	118.55	188.62	10.3
	Acetic Acid Current Efficiency (%)	81	82	79	71	78	4.91	7.81	10.0
	Sodium Hydroxide Current Efficiency (%)	85	89	86	87	87	2.00	3.17	3.7
	Cell Voltage (V)								3.0
	Salt Volume (mL)								0.5
	Acid Volume (mL)								0.6
	Base Volume (mL)								0.5
Coefficients used in above calculations: n = 4, t (0.95, 3) = 3.182									

APPENDIX C: STANDARD METHODS FOR EVALUATING PULP PROPERTIES

Kappa number

Kappa number is used to characterize residual lignin content in pulp samples. This test is based on the oxidation of residual lignin in the pulp samples by using potassium permanganate. The kappa number is the volume (in milliliters) of 0.1N KMnO_4 solution, consumed by one gram of moisture-free pulp under the conditions specified in the test method [TAPPI Standard T-236, 1993]. The kappa number increases linearly with an increase in the lignin content in the pulp sample.

Laboratory Processing of pulp (PFI mill method)

The performance of a given pulp sample when converted to paper can be obtained by physical testing of laboratory-beaten pulp samples [TAPPI Standard T-248, 2008]. Beating is a mechanical action that is applied to pulp sample held between two parallel surfaces, under constant loading, moving at different angular velocities relative to one another. In a PFI mill, this mechanical action is achieved by having the inner roll and outer casing rotate under constant load, in the same direction, but with different peripheral speeds.

Although no laboratory method can simulate the industrial refining process, the PFI mill method is accepted for small amount of pulps. Refining physically modifies the pulp fibers to form fibrillates and to increase its flexibility by forcing water into the structure of the pulp. Consequently, the bonding between fibers increases, as does its ability to hold water and its surface area. Hence there is an increase in the tensile and burst strength but a decrease in tear strength, porosity and drainage or rate at which the pulp can be filtered. A series of samples are refined at different levels and used to make different handsheets. A plot of physical properties as a function of degree of refining is called a beater or refining curve. Often the physical properties are plotted as a function of the drainage rate when measured by an empirical drainage rate test called the Canadian Standard Freeness.

Canadian Standard Freeness (CSF)

The freeness of pulp is an empirical test designed to give a measure of the rate at which a dilute suspension of pulp may be drained [TAPPI Standard T-227, 2009]. It can also give an indication of: 1) fiber Length of pulp, as long fiber pulps have more freeness compared to short fiber pulps, 2) damage to fiber during pulping, as short fibers or fines produced during the operation reduces pulp freeness, 3) refining energy required to achieve certain slowness during stock preparation. The freeness has been shown to be related to the amount of fines in the pulp, the swelling of the fibers as when measured by the water retention value (gm water/gm pulp), and their surface conditions. The freeness of pulp is modified to achieve desired properties in the paper. Besides these factors, the result is dependent also on conditions under which the test is carried out, such as stock preparation, temperature and water quality. This test is used to follow changes in drainage rate of various chemical pulps during beating and refining.

Preparation of Standard TAPPI Handsheets

Handsheets used in pulp testing are prepared at an oven dry weight of 60 gram/m² and are used for determining the physical and optical properties of pulp in both the unrefined and refined conditions [TAPPI Standard T-205, 2012]. Non-directional handsheets of the pulp being tested are prepared in a TAPPI test mold, and subjected to standard pressing and drying conditions. Handsheets made with the standard procedure are often used to describe properties of market pulps.

Thickness (caliper)

Since paper is compressible, the thickness of paper will depend upon the load applied. In the standard method, the thickness of paper is measured by using a micrometer when a specified load is applied for a minimum specified time on both surfaces of the paper [TAPPI Standard T-411, 2010]. However, the thickness measured using the standard TAPPI

method is different from apparent thickness determined by using calipers which put different amount of loads on the surfaces.

Specific volume (bulk)

Bulk indicates the volume of test sheet of pulp in relation to its weight and is often measured volume per unit mass. It is the reciprocal of density (mass per unit volume). It is calculated using basis weight (BW) and caliper (t) ($\text{Bulk} = t/\text{BW}$). The bulk that the pulp exhibits will depend upon the species of wood and the process by which it has been converted into pulp. A decrease in the bulk, or alternatively an increase in density of test sheets, of a pulp results from increased processing (refining), increased pressing and generally indicates increased fiber-to-fiber bonding which changes the physical and optical properties of the pulp. High bulk is required in absorbent papers, whereas lower bulk is desired for printing papers.

Tensile index

The tensile index of a pulp (N m/gram) is the tensile strength (N/m) divided by basis weight of the sample (grams/m^2) [TAPPI Standard T-494, 2006]. Tensile strength is the maximum tensile force developed in a test specimen before rupture on a tensile test carried to rupture under prescribed test conditions. Tensile strength (as used here) is the force per unit width of test specimen. The test procedure consists of using constant-rate of elongation equipment, for determining tensile strength. Tensile strength is indicative of the strength derived from factors such as strength, fiber length and fiber-to-fiber-bonding.

Tear Strength

The tear strength of paper is often measured on an Elmendorf-type tearing tester machine [TAPPI Standard T-414, 2012]. This method measures the shear force applied perpendicular to the plane of the paper required to tear multiple plies of the paper when acting through a specific distance after the tear has been started. A schematic diagram of the tear test is illustrated in Figure C.1 which shows the mechanism of this method. It does

not measure edge-tear resistance. Fiber length and fiber bonding are important factors in tearing strength. Longer fibers improve tear strength because they tend to distribute the stress over more fibers and more bond; whereas short fibers allow the stress to be concentrated in a smaller area. The tear strength of paper usually decreases with increased pulp processing and greater fiber-to-fiber bonding which leads to the concentration of stress.

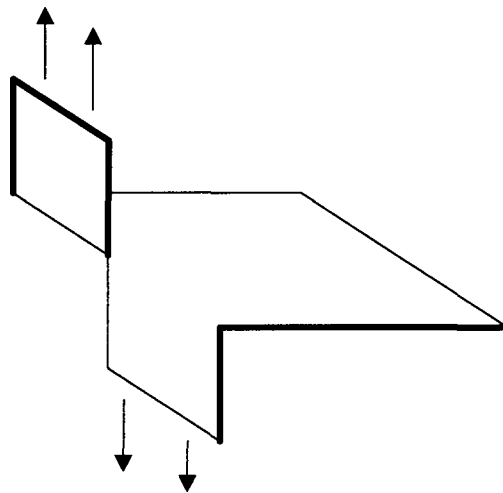


Figure C.1 Mechanism of Tear Testing

Wet Zero Span Breaking Length

During the papermaking process, the paper must have sufficient strength when wet to move through the various parts of the paper machine; especially across open draws or regions where the wet paper must support its own weight.

Some types of papers such as toweling, coffee filter paper and other grades come in contact with water while in use. So, these papers need to be strong enough to withstand tear or rupture when saturated with water. The wet zero span breaking length is the limiting length of a wet strip of paper having uniform width, beyond which, if such a strip were suspended by one end, it would break of its own weight [TAPPI Standard T-273, 1995].

Brightness

The brightness of paper provides an indication of the “whiteness” of paper and is indicative of the amount of bleaching that has been performed on the paper sample [TAPPI Standard T-452, 1998]. Since brightness is an aesthetic parameter and can change when viewed under different lightening conditions, its measurement has been carefully standardized. Brightness is the reflectance factor of a sample with respect to blue light of a specific spectral wave length (457 nm) under standardized geometric characteristics. The brightness can be indicated using either TAPPI brightness index or international standard (ISO) relative to a value of 100 which is the brightness of an MgO crystal. The values for the brightness are shown in Table C.1.

Table C.1 Typical Brightness Values for Different Grades of Paper

Paper Grade	Typical Brightness Values (% ISO)
Newsprint	62-65
Office/Business paper	80-95

Scott Internal Bond Test

The internal bond strength of paper or paperboard, also known as Scott type internal bond Strength or Z directional strength, is the ability of the paper to resist splitting when a tensile load is applied through the paper’s thickness i.e. in the Z direction of the sheet [TAPPI Standard T-569, 2009]. In this method a sheet of a paper is sandwiched between two double-coated tapes and the sandwich is then pressed between a flat metal anvil and an aluminum platen as shown in Figure C.2. A pendulum impacts the top inside surface of the platen, causing it to rotate and splits the paper specimen in the “Z” direction. The energy absorbed in rupturing the sample is computed by measuring the energy associated with the peak excess swing of the pendulum (Joules/m²).

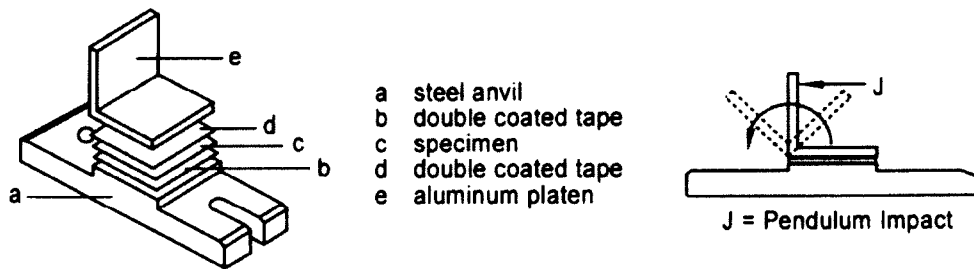


Figure C.2 Experimental Set-up for Measuring Internal Bond Strength

Screened yield

The screened yield is the amount of pulp obtained from a given mass of wood in a pulping process. It is measured after the pulp has been screened using a standard hole size in the screening process. It is expressed on dry basis as a percentage of wood fed during the pulping process.

Shives

The shives in pulp are the amount of rejects, or uncooked wood chips, dirt, large particles and foreign particles collected in the screening process. It is again expressed on a dry weight basis as a percentage of wood fed during the process.

REFERENCES

- TAPPI Standard T 236 cm-85 (1993) Kappa number of pulp
- TAPPI Standard T 248 sp-08 (2008) Laboratory beating of pulp (PFI mill method)
- TAPPI Standard T 227 om-09 (2009) Freeness of pulp (Canadian standard method)
- TAPPI Standard T 205 sp-12 (2012) Forming handsheets for physical tests of pulp
- TAPPI standard T 411 om-10 (2010) Thickness (caliper) of paper, paperboard, and combined board
- TAPPI Standard T 494 om-01 (2006) Tensile properties of paper and paperboard (using constant rate of elongation apparatus)
- TAPPI standard T 414 om-12 (2012) Internal tearing resistance of paper (Elmendorf-type method)
- TAPPI Standard T 273 pm-95 (1995) Wet zero-span tensile strength of pulp

TAPPI Standard T 452 om-98 (1998) Brightness of pulp, paper and paperboard (directional reflectance at 457 nm)

TAPPI Standard T 569 om-09 (2009) Internal bond strength (Scott type)

APPENDIX D: OPERATING PROCEDURE FOR ELECTRODIALYSIS EQUIPMENT

Figure D.1 shows a photo of the ED/BPMED cell used in this work.

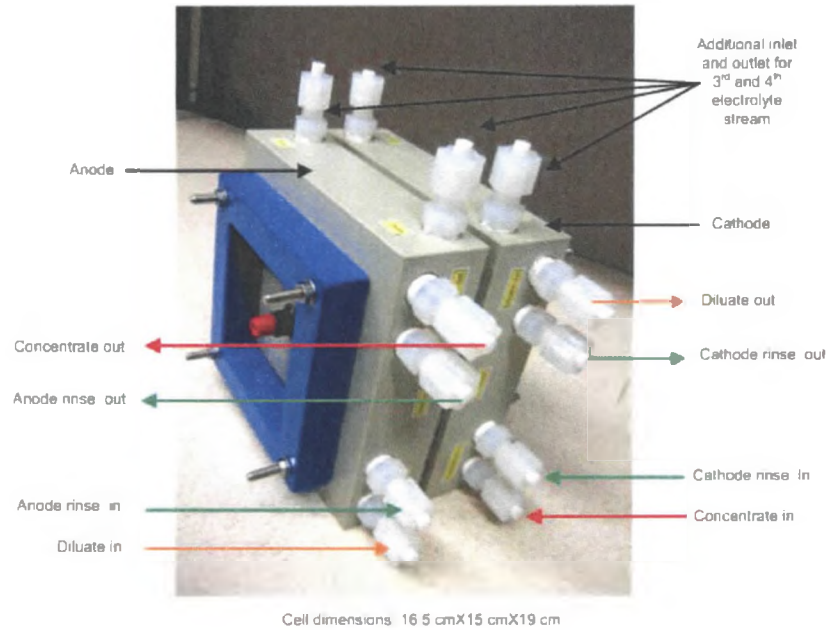


Figure D.1 Photo of PCCell ED 64-004 Electrodesis cell

Figure D.2 shows the detailed flow patterns within two-compartment ED cell. It shows circulations of diluate, concentrate and electrode rinse solutions. In order to simplify the understanding of flow patterns, the spacers and membranes are shown to be apart from each other. However, in practice, membranes, spacers and electrodes are tightened together to form a leak free cell.

Figure D.3 shows a detailed schematic diagram of the ED equipment used in this study. The flow pattern for a four-compartment ED cell is similar to that of the two-compartment ED system.

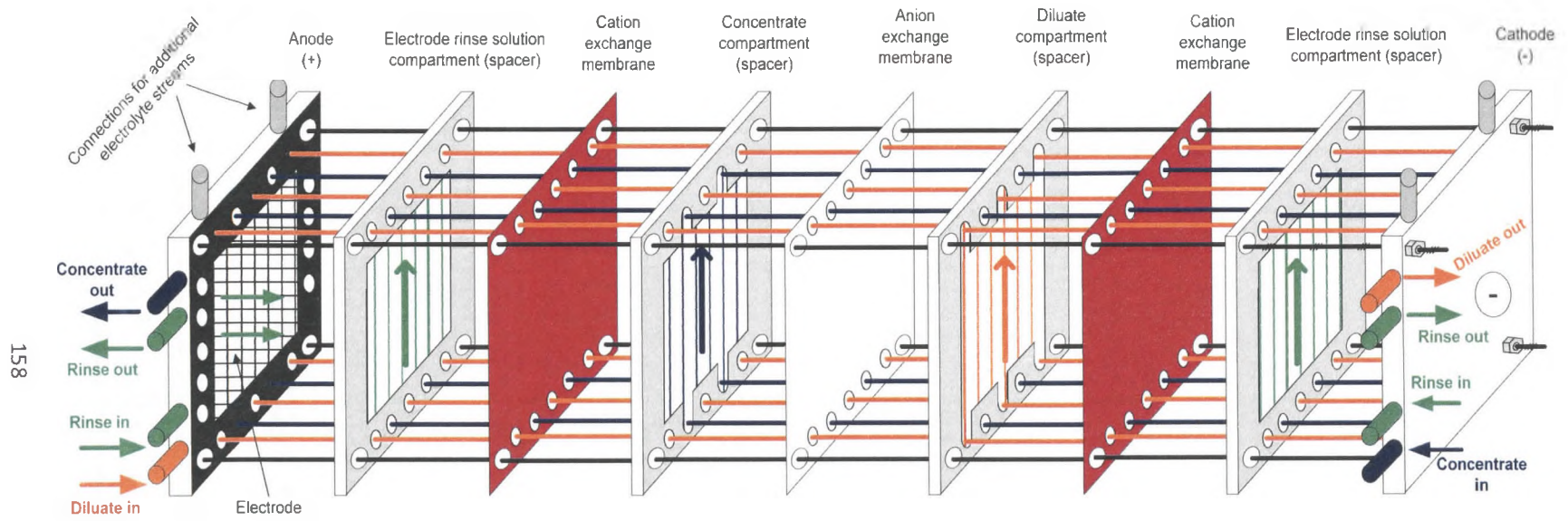
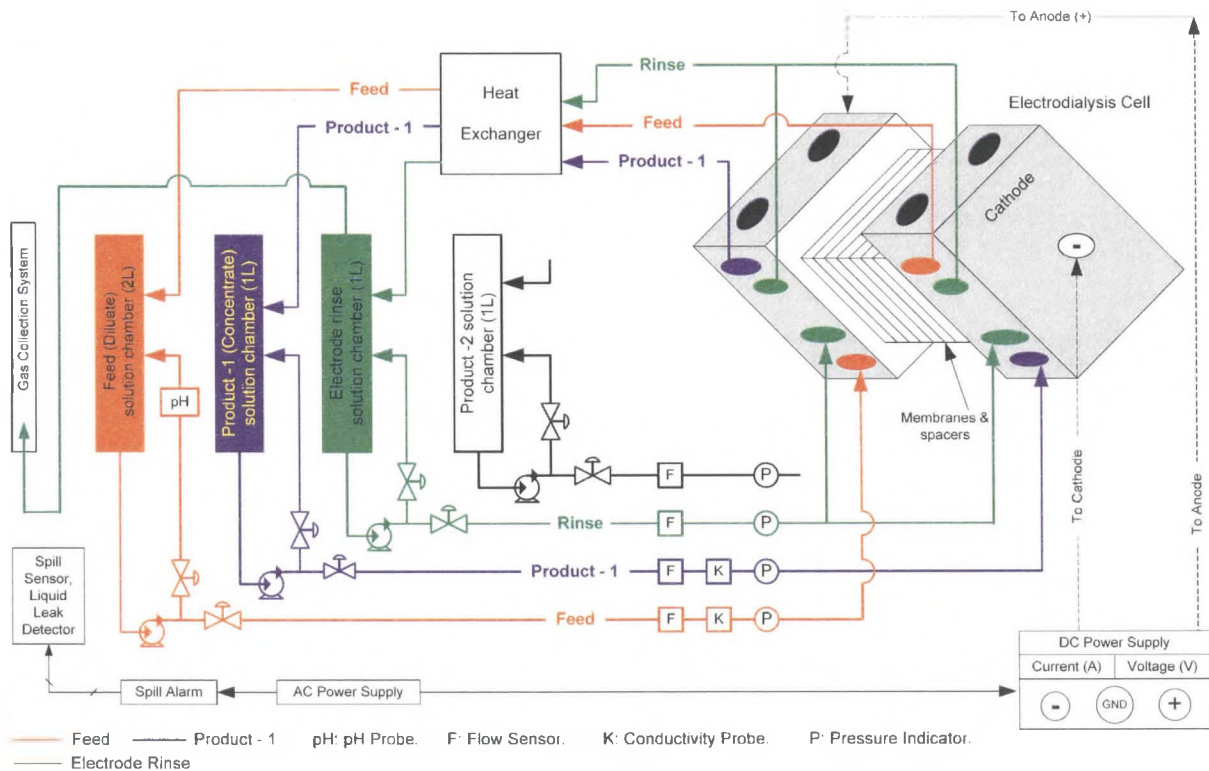


Figure D.2 Detailed Flow Patterns within Electrodiagnosis Cell

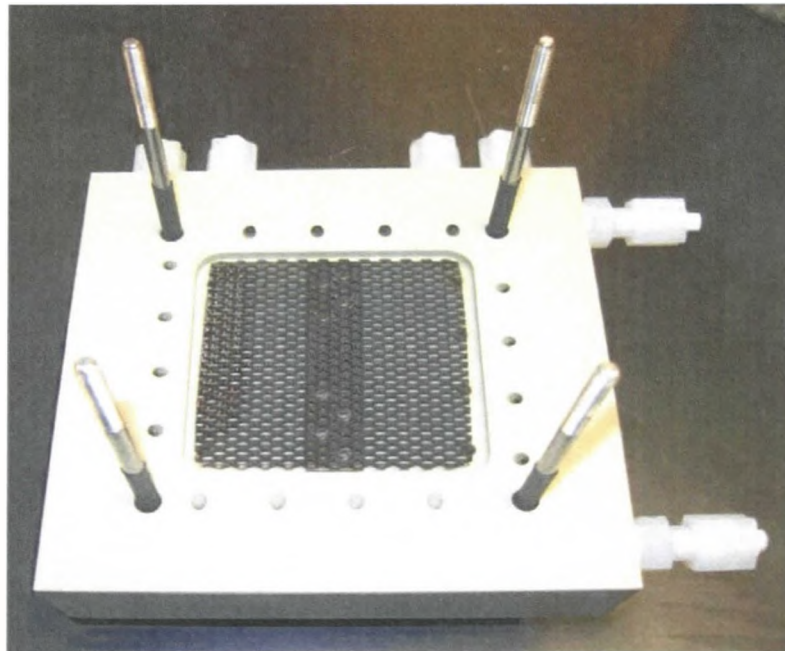


Laboratory Scale Electrodialysis Equipment (PCCell ED 64-004)

Figure D.3 Detailed Schematic of Laboratory Scale Electrodialysis Equipment

Procedure for Stacking the Electrodialysis Cell

The anode is put on a metal frame as shown in Figure D.4. An electrode rinse spacer is then placed on the anode. Membranes and spacers are stacked in a sequence (right to left) as shown in Figure D.5 for the ED cell and in Figure D.6 for the bipolar membrane electro dialysis apparatus (BPMED).



Top view

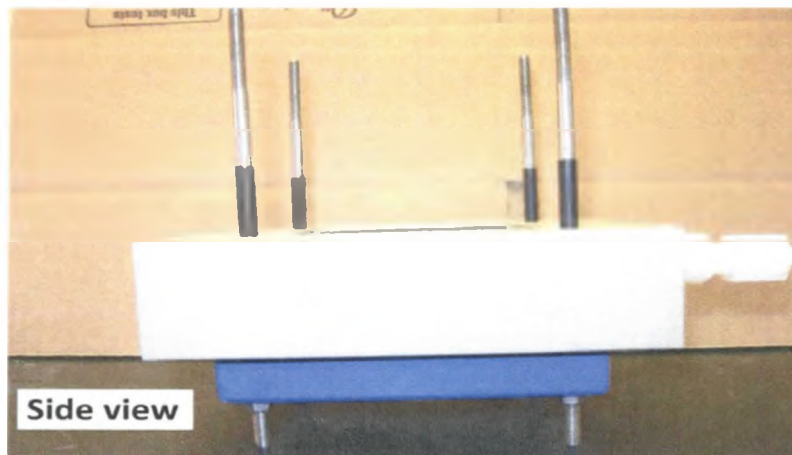


Figure D.4 Arrangement of Anode for Stacking the Cell

The anionic side of a Bi-Polar membrane should be placed facing towards the anode to avoid damaging the membrane. The anionic side of the membrane should be stamped appropriately. If the anionic side of Bi-Polar membrane is not stamped "Anion", then Methylene Blue (100 ppm) solution should be applied (dyed) to the both sides of the membrane. After few seconds, the dye is wiped off of the surfaces using a soft cloth. The side that turns blue is called the cationic side. Also, the cationic side is rough with ridges while the anionic side is smooth.

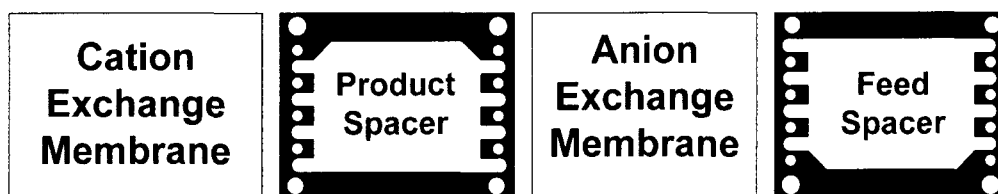


Figure D.5 Arrangement of Membranes and Spacers for Two-Compartment Electro dialysis Cell

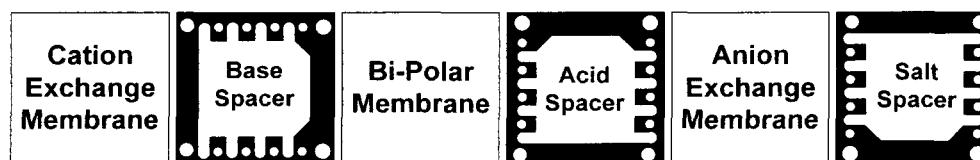


Figure D.6 Arrangement of Membranes and Spacers for Three-Compartment Bi-Polar Membrane Electro dialysis cell

Once all membranes and spacers are stacked on the surface of the anode, an electrode rinse spacer and a cathode are placed on them. The stack is then tightened by applying a torque of 6 Newton-meter irrespective of the number of cell pairs. The cell is then tested for leaks. The procedure for leak test is given in the next session. A leak free cell can be used until no leaks or deviations are observed during the operation of the cell. When not in use, the cell should be filled with water or appropriate electrolyte solution to avoid drying of the membranes.

Procedure for Leak Test

After each assembly of the ED cell, it must be tested for leaks within the membranes. Figure D.7 shows the experimental setup for leak testing. A water tank and the ED cell are arranged as shown in Figure D.7. Water coming out of the cell during the first two minutes should be discarded to evacuate air from the cell. The amount of water

coming out in the intervals of five minutes is noted down. A leakage rate of less than 0.5 mL per minute per cell pair is acceptable. However, a leakage rate of less than 0.05 ml per minute can be achieved with a properly build-up cell. Figure D.7 illustrates how the rate of leakage from the ED apparatus should be measured. Two arrangements are illustrated; one each for the (A) concentrate to diluate and (B) diluate to concentrate flow schemes respectively.

For a BPMED cell, the following leakage rates should be determined for the following conditions: 1] Salt to acid and base compartments, 2] Acid to salt and base compartments and 3] Base to acid and salt compartments.

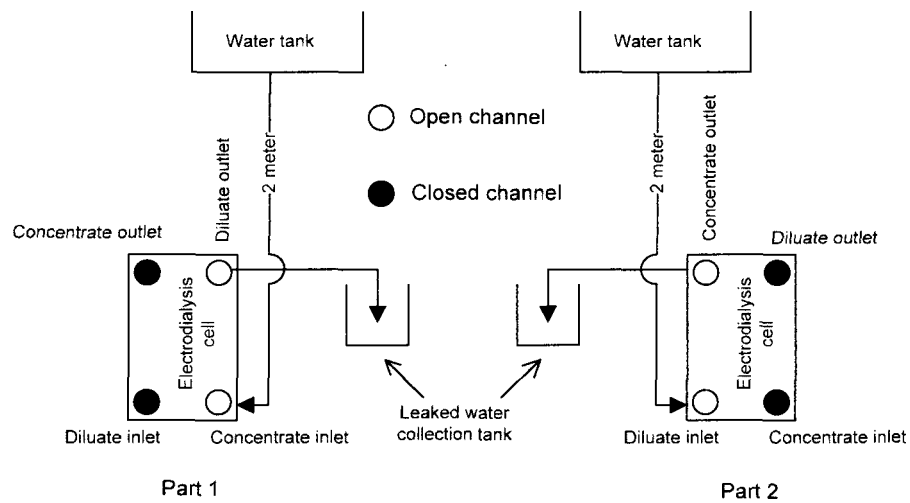


Figure D.7 Experimental Setup for Leak Test for Electrodesialysis Cell

Determination of Limiting Current Density

Limiting current is determined by measuring the current as a function of the applied voltage across one cell pair for different diluate (salt) concentrations (Figure D.8).

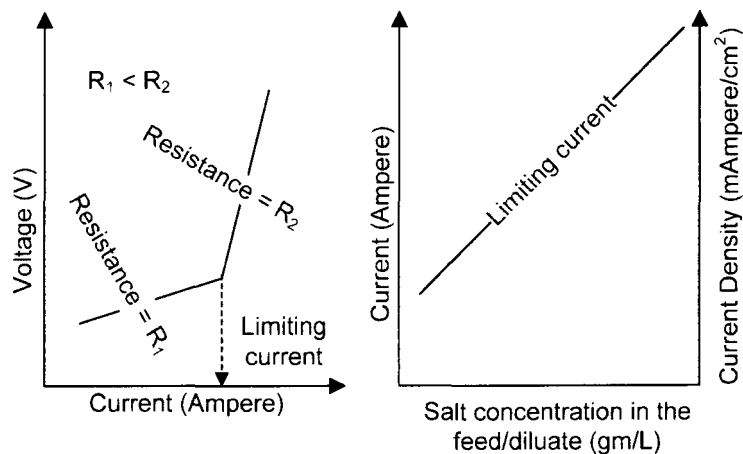


Figure D.8 Limiting Current

Measurements made with multi stack usually do not show a clear change in the resistance when the limiting current is reached. Therefore, Cowan and Brown (1959) determined the limiting current density by plotting the overall resistance versus the reciprocal of the current density [Strathmann, 2004].

Procedure for Operating Electrodialysis Equipment

- Prior to charging the electrolyte solutions, water is circulated through the equipment for cleaning purpose and to identify leaks. It also prevents the loss of electrolyte solutions due to leaks in the equipment.
- Initially, the flow rate for the feed compartment is selected. Accordingly, the flow rates of the other compartments are adjusted so that the trans-membrane pressure is zero.
- If there are bubbles in the electrolyte solutions, the recirculation pumps are turned off for few minutes until all bubbles are vanished.
- Water supply to the heat exchanger is turned on.
- The electrolyte solutions are then charged into individual reservoirs.
- A tube is attached to the outlet of the electrode rinse reservoir to vent H_2 and O_2 generated near the electrodes.
- The Vis-Sim software is turned on to record the experimental data.
- Once the desired flow rate and inlet pressure are achieved, and all air bubbles within the pump and tubing are removed, the current can be turned on.

- The current and voltage are always maintained below their limiting values. Information about the limiting voltage is given in later in this appendix. The instantaneous concentration of a salt present in the feed/diluate compartment can be approximately determined through its conductivity. The concentration data can then be used to ensure that the applied current is below its limiting value. However, this approach is applicable only for the aqueous solutions of pure salts.
- As the concentration of salt present in feed/diluate compartment decreases during the course of an experiment, the applied current density approaches the limiting current density.
- At the end of an experimental run, the current was first turned off and circulation of the solutions was stopped.
- Since bi-polar membranes must be stored at neutral pH, the pH of all electrolyte solutions should be adjusted to neutral, at end of BPMED experiments, to avoid possible damage to the bi-polar membranes. Although the salt compartment is not in direct contact with bi-polar membranes, it is important to adjust the pH of salt solution because residual acid/base present in the salt compartment can slowly diffuse into other compartments which are in contact with bi-polar membranes.
- To avoid large consumption of acid/base during the pH adjustment of electrolyte solutions, all compartments can be flushed with fresh water few times so that the amount of residual acids/bases present in the BPMED cell is reduced.
- Once the pH of all solutions is adjusted to neutral, all compartments of the cell should be filled with deionized water. The pH of all electrolyte solutions should be routinely checked during the storage.

Technical data (For PCCell ED 64-4 Electrodialysis Cell)

- Membrane Size: 110 mm X 110 mm
- Active Membrane Area: 64 cm²
- Maximum number of cell pairs: 25
- Current Connectors: 4 mm banana plugs
- Membrane Spacing: Electrode-Membrane: 1 mm, Membrane-Membrane: 0.5 mm
- Thickness of Spacer: 0.45 mm
- Flow through diluate/concentrate: 4-8 liter per hour per compartment
- Flow through electrode rinse: 150 liter/hour
- Maximum Amperage: 6.4 Ampere (equivalent to 100 mA/cm²)

- Maximum voltage drop is calculated based upon the sum of the maximum allowed voltage drops for each mono-polar membrane and two electrodes
 - A. Maximum allowed voltage drop for one mono-polar membrane is 0.4 volt
 - B. Maximum allowed voltage drop for one bi-polar membrane is 1.2 volt
 - C. Maximum allowed voltage drop for one electrode (cathode/anode) is 3 volts
- Maximum voltage drop across voltage: 30 volts per cell
- Materials of construction
 - A. Cell Frame: Polypropylene,
 - B. Tubes: Polyethylene,
 - C. Electrodes: Titanium, Pt/Ir coating

Precautions

- All electrolyte solutions must be filtered using 1 micrometer qualitative filter paper to avoid plugging of membranes by small particles and the loss of electricity.
- The electro dialysis cell must be placed in a diagonal position, wherein the inlet of each stream is located at the lowest place and the outlet at the highest place. This prevents the formation of static air bubbles inside electrolyte cell.
- All circulations pumps must be turned on together. This avoids build up of excessive pressure drop across membranes. Never circulate liquid only through one compartment. It increases the trans-membrane pressure drop excessively.
- The cell should be prevented from freezing conditions; direct sunlight should be avoided as well.
- All membranes must be stored in wet conditions. Some membranes, i.e. Neosepta AMX/CMX/ACS/CMX-s, are stored in 3% NaCl.
- The Neosepta BP- 1 membrane is stored in deionized water. If pure water is used, then pH is adjusted to neutral. The membranes are deteriorated due to the use of oxidative, reductive or detergent solutions.
- In order to avoid build-up of air bubbles inside the electrolyte reservoirs, the recycle solution was injected below the liquid level within the reservoir.
- A sparger can be put at the end of electrode rinse recycle tube to remove insoluble gases trapped within the solution. No sparger was used in the present study.
- The iridium coating on the anode must not be touched with hands or any other tools to prevent any damage to it.

- Anode and cathode must be connected properly. Wrong connections may not damage the ED cell permanently, as both electrodes are exactly identical; but, can damage the bipolar membranes.
- The temperature of all electrolyte solutions must be maintained below the limit (40 °C in most cases) specified by manufacturer of ion exchange membrane. A heat exchanger was used in the apparatus to maintain the temperature of the solutions below 40 °C.
- It is more accurate to use the difference in the height of the product compartment to estimate the amount of water transported across the membranes. The difference between the volumes of the solution charged and drained does not give an accurate estimate of the water because some amount of liquid remains in the circulation tubes and the cell.

Table D.1 summarizes the properties of the membranes used in this study [Astom Corporation, 2015].

Table D.1 Properties of Ion Exchange Membranes used in this Study

Title		Cation Exchange Membrane		Anion Exchange Membrane	
		Standard Grade	Special Grade	Standard Grade	Special Grade
		CMX	CMB	AMX	AHA
Characteristics	Type	Strong Acid (Na Type)		Strong Base (Cl Type)	
	Characteristics	High Mechanical Strength	High Mechanical Strength, Alkali Resistance	High Mechanical Strength	High Mechanical Strength, Alkali Resistance
	Electric Resistance ($\Omega \cdot \text{cm}^2$)	3.0	4.5	2.4	4.1
	Burst Strength (MPa)	≥ 0.40	≥ 0.40	≥ 0.25	≥ 0.90
	Thickness (mm)	0.17	0.21	0.14	0.22
	Application	Desalination of food Desalination and concentration of inorganic salts Removal of hardness and nitrogen from underground water	Alkali recovery Alkali production (Bi-Polar Membrane ED) Diaphragm	Desalination of foods Desalination and Concentration of Inorganic salts Removal of hardness and from underground water	Acid/Alkali recovery Acid/Alkali production (Bi-Polar Membrane ED) Diaphragm
Recommended field of application	Temperature ($^{\circ}\text{C}$)	≤ 40	≤ 60	≤ 40	≤ 60
	pH	0-10	0-14	0-8	0-14

REFERENCES

- Astom Corporation (2015), http://www.astom-corp.jp/en/product/images/astom_hyo.pdf
- Cowan, D. A., and Brown, J. H. (1959), "Effects of turbulence on limiting current in electro dialysis cells," *Industrial Engineering and Chemistry*, 51(12): 1445-1448
- H. Strathmann (2004), Assessment of electro dialysis water desalination process costs, in: Proceedings of the International Conference on Desalination Costing, Limassol, Cyprus, 2004, pp. 32–54

BIOGRAPHY OF THE AUTHOR

Ravikant Amogisidha Patil was born in Solapur, Maharashtra, India. He was raised in Mumbai, India where he completed his elementary and high school education. He graduated with a Bachelor of Chemical Technology degree from the Institute of Chemical Technology, Mumbai in 2007. After graduation, he worked as a process engineer at the Paxchem Ltd, Mumbai for one year. Then, he moved to the Indian Institute of Technology, Kharagpur, where he earned his Master of Technology degree in Chemical Engineering in May 2010. He enrolled into Chemical Engineering graduate program at the University of Maine in Fall 2010 and earned his Master of Science degree in Chemical Engineering in December 2012. He continued the same project to his PhD degree. Ravikant is a candidate for the Doctor of Philosophy degree in Chemical Engineering from The University of Maine in August 2016.